

Thermal Conductivity of Carbon Nanotubes and their Polymer Nanocomposites: A Review.

*Original*

Thermal Conductivity of Carbon Nanotubes and their Polymer Nanocomposites: A Review / Han, Zhidong; Fina, Alberto.  
- In: PROGRESS IN POLYMER SCIENCE. - ISSN 0079-6700. - STAMPA. - 36:7(2011), pp. 914-944.  
[10.1016/j.progpolymsci.2010.11.004]

*Availability:*

This version is available at: 11583/2381233 since: 2016-02-19T14:30:45Z

*Publisher:*

Elsevier

*Published*

DOI:10.1016/j.progpolymsci.2010.11.004

*Terms of use:*

This article is made available under terms and conditions as specified in the corresponding bibliographic description in the repository

*Publisher copyright*

(Article begins on next page)

**Author's version**

Published in

*Progress in Polymer Science* 36(7), pp 914/944

DOI: 10.1016/j.progpolymsci.2010.11.004

<http://dx.doi.org/10.1016/j.progpolymsci.2010.11.004>

# **Thermal Conductivity of Carbon Nanotubes and their Polymer Nanocomposites: A Review**

**Zhidong Han<sup>1</sup>, Alberto Fina<sup>2</sup>**

**1- School of Materials Science and Engineering, Harbin University of Science and Technology**

**Linyuan Road 4, Dongli District, 150040, Harbin, China**

**2- Department of Materials Science and Chemical Engineering, Politecnico di Torino**

**V.le Teresa Michel, 5, 15121, Alessandria, Italy**

## **Abstract**

Thermally conductive polymer composites offer new possibilities for replacing metal parts in several applications, including power electronics, electric motors and generators, heat exchangers etc., thanks to the polymer advantages such as light weight, corrosion resistance and ease of processing. Current interest to improve the thermal conductivity of polymers is focused on the selective addition of nanofillers with high thermal conductivity. Unusually high thermal conductivity makes carbon nanotube (CNT) the best promising candidate material for thermally conductive composites. However, the thermal conductivities of polymer/CNT nanocomposites are relatively low compared with expectations from the intrinsic thermal conductivity of CNTs. The

challenge primarily comes from the large interfacial thermal resistance between the CNT and the surrounding polymer matrix, which hinders the transfer of phonon dominating heat conduction in polymer and CNT.

This article reviews the status of worldwide research in the thermal conductivity of CNTs and their polymer nanocomposites. The dependence of thermal conductivity of nanotubes on the atomic structure, the tube size, the morphology, the defect and the purification is reviewed. The roles of particle/polymer and particle/particle interfaces on the thermal conductivity of polymer/CNT nanocomposites are discussed in detail, as well as the relationship between the thermal conductivity and the micro- and nano-structure of the composites.

## **Keywords**

Carbon nanotube, nanocomposites, thermal conductivity

\* Visiting Researcher at Politecnico di Torino.

Permanent email address: [harbinzhidonghan@yahoo.com.cn](mailto:harbinzhidonghan@yahoo.com.cn)

† Corresponding author. Email address: [alberto.fina@polito.it](mailto:alberto.fina@polito.it)

# Contents

## 1 Introduction

- 1.1 Limitation of Thermal Conductivity of Polymers
  - 1.1.1 Low Thermal Conductivity
  - 1.1.2 Crystallinity and Temperature Dependence
- 1.2 Fillers for Thermally Conductive Composites
  - 1.2.1 Carbon-Based Fillers
  - 1.2.2 Metallic Fillers
  - 1.2.3 Ceramic Fillers
- 1.3 Thermal conductivity - Measurement and Modelling
  - 1.3.1 Methods for thermal conductivity measurements
  - 1.3.2 Modelling of thermal conductivity in composites
- 1.4 Nanocomposites for thermal conductivity
  - 1.4.1 CNT-based nanocomposites preparation methods
  - 1.4.2 General issues on thermal conductivity of CNT-based nanocomposites

## 2 Thermal Conductivity of CNTs

- 2.1 Structure and Morphology
  - 2.1.1 Nanotube Morphology
  - 2.1.2 Atomic Structure
  - 2.1.3 Topological Defects
- 2.2 Size Parameters

2.2.1 Diameter

2.2.2 Length

2.3 Purification and Graphitization

2.3.1 Purification

2.3.2 Graphitization

2.4 Functionalization of CNTs

### **3 Thermal Conductivity of Polymer/CNTs Nanocomposites**

3.1 Effect of interfaces on thermal transfer

3.1.1 Interfacial Resistance

3.1.2 Contact Resistance

3.2 Dispersion

3.2.1 Effect of Functionalization

3.2.2 Effect of Mixing Conditions

3.2.3 Localization of Thermally Conductive Paths

3.3 Alignment

3.3.1 Alignment During Processing

3.3.2 Alignment from CNT Array

3.3.3 Alignment by External Field

3.4 Polymer Crystallization

### **4 Concluding Remarks**

### **Acknowledgements**

## Nomenclature

ABS	poly(acrylonitrile-butadiene-styrene) copolymer
AlN	aluminum nitride
BeO	beryllium oxide
BN	boron nitride
BNNT	boron nitride nanotubes
CNT	carbon nanotube
$C_p$	heat capacity
DSC	differential scanning calorimetry
DWCNT	double-walled carbon nanotube
EG	expanded graphite
EPDM	ethylene propylene diene rubber
EVA	poly(ethylene vinyl acetate)
GNP	graphite nanoplatelet
HDPE	high density polyethylene
$k$	thermal conductivity (in some figures taken from literature referred as $K_e$ =effective thermal conductivity)
$k_c$	thermal conductivity of composite
$k_m$	thermal conductivity of matrix
$k_p$	thermal conductivity of particle
$l$	phonon mean free path
$L$	length parameter
LDPE	low density polyethylene
MD	molecular dynamics
MWCNT	multi-walled carbon nanotube
ODA	oxydianiline
PA6	polyamide 6
PA66	polyamide 6-6
PBT	poly(butylene terephthalate)
PC	polycarbonate
PDMS	poly(dimethylsiloxane)
PE	polyethylene
PEEK	polyetheretherketone
PET	poly(ethylene terephthalate)
PEVA	poly(ethylene vinyl alcohol)
PI	polyimide
PMDA	pyromellitic dianhydride
PMMA	polymethylmethacrylate

PP	polypropylene
PPS	polyphenylene sulfide
PPSU	polyphenylsulfone
PS	polystyrene
PSU	polysulfone
PTFE	polytetrafluoroethylene
PU	polyurethane
PVB	poly(vinyl butyral)
PVC	polyvinyl chloride
PVDF	polyvinylidene difluoride
$R_k$	interfacial resistance
SDS	sodium dodecyl sulphate
SiC	silicon carbide
SWCNT	single-walled carbon nanotube
$T_g$	glass transition temperature
$v$	average phonon velocity
VGCF	vapor grown carbon fiber
$\alpha$	thermal diffusivity
$\rho$	density of the material
$\Phi_m$	volume fractions of matrix
$\Phi_p$	volume fractions of particles

# 1 Introduction

## 1.1 Limitation of Thermal Conductivity of Polymers

### 1.1.1 Low Thermal Conductivity

Heat transfer involves the transport of energy from one place to another by energy carriers. In a gas phase, gas molecules carry energy either by random molecular motion (diffusion) or by an overall drift of the molecules in a certain direction (advection). In liquids, energy can be transported by diffusion and advection of molecules. In solids, phonons, electrons, or photons transport energy. Phonons, quantized modes of vibration occurring in a rigid crystal lattice, are the primary mechanism of heat conduction in most polymers since free movement of electrons is not possible [1]. In view of theoretical prediction, the Debye equation is usually used to calculate the thermal conductivity of polymers.

$$\lambda = \frac{C_p \cdot v \cdot l}{3} \quad (1)$$

Where  $C_p$  is the specific heat capacity per unit volume;  $v$  is the average phonon velocity; and  $l$  is the phonon mean free path.

For amorphous polymers,  $l$  is an extremely small constant (i.e., a few angstroms) due to phonon



scattering from numerous defects, leading to a very low thermal conductivity of polymers [2]. Table 1 displays the thermal conductivities of some polymers [3,4,5].

### **1.1.2 Crystallinity and Temperature Dependence**

Polymer crystallinity strongly affects their thermal conductivity, which roughly varies from 0.2 W/m·K for amorphous polymers such as polymethylmethacrylate (PMMA) or polystyrene (PS), to 0.5 W/m·K for highly crystalline polymers as high-density polyethylene (HDPE) [4]. The thermal conductivity of semi-crystalline polymers is reported to increase with crystallinity. As an example, the thermal conductivity of polytetrafluoroethylene (PTFE) was found to increase linearly with crystallinity at 232°C [6].

However, there is a large scatter in the reported experimental data of thermal conductivity of crystalline polymers, even including some contradictory results. It should be noticed that the thermal conductivities of polymers depend on many factors, such as chemical constituents, bond strength, structure type, side group molecular weight, molecular density distribution, type and strength of defects or structural faults, size of intermediate range order, processing conditions and temperature, etc. Furthermore, due to the phonon scattering at the interface between the amorphous and crystalline phase and complex factors on crystallinity of polymer, the prediction of the thermal conductivity vs crystallinity presents a significant degree of complexity.

Semicrystalline and amorphous polymers also vary considerably in the temperature dependence of the thermal conductivity. At low temperature, semicrystalline polymers display a temperature

dependence similar to that obtained from highly imperfect crystals, having a maximum in the temperature range near 100 K, shifting to lower temperatures and higher thermal conductivities as the crystallinity increases [7,8], while amorphous polymers display temperature dependence similar to that obtained for inorganic glasses with no maximum, but a significant plateau region at low temperature range [9]. The thermal conductivity of an amorphous polymer increases with increasing temperature to the glass transition temperature ( $T_g$ ), while it decreases above  $T_g$  [10, 11]. The study of the thermal conductivity of some amorphous and partially crystalline polymers (PE, PS, PTFE and epoxy resin) as a function of temperature in a common-use range (273-373 K) indicates that the conductivity of amorphous polymers increases with temperature and that the conductivity is significantly higher in crystalline than amorphous regions [12].

From the general overview given in the preceding, it appears that very limited thermal conductivity is usually characteristic of polymers. On the other hand, there are many reasons to increase thermal conductivity of polymer-based materials in various industrial applications including circuit boards in power electronics, heat exchangers, electronics appliances and machinery. This justifies the recent significant research efforts on thermally conductive composite materials to overcome the limitations of traditional polymers.

## **1.2 Fillers for Thermally Conductive Composites**

Many applications would benefit from the use of polymers with enhanced thermal conductivity. For example, when used as heat sinks in electric or electronic systems, composites with a thermal

conductivity approximately from 1 to 30 W/m·K are required [13]. The thermal conductivity of polymers has been traditionally enhanced by the addition of thermally conductive fillers, including graphite, carbon black, carbon fibers, ceramic or metal particles (see Table 2) [14, 15, 16, 17, 18]. It is worth noticing that significant scatter of data are typical of data reported for thermal conductivity of fillers. This is caused by several factors, including filler purity, crystallinity, particle size and measurement method. It is also important to point out that some materials, typically fibers and layers, are highly anisotropic and can show much higher conductivity along a main axis or on a plane, compared to perpendicular direction.

High filler loadings (> 30 vol.%) are typically necessary to achieve the appropriate level of thermal conductivity in thermally conductive polymer composites, which represents a significant processing challenge. Indeed, the processing requirements, such as possibility to be extruded and injection molded, often limit the amount of fillers in the formulation and, consequently, the thermal conductivity performance [19]. Moreover, high inorganic filler loading dramatically alters the polymer mechanical behavior and density. For these reasons, obtaining composites having thermal conductivities higher than 4 W/m·K and usual polymer processability is very challenging at present.

### **1.2.1 Carbon-Based Fillers**

Carbon-based fillers appear to be the best promising fillers, coupling high thermal conductivity and lightweight. Graphite, carbon fiber and carbon black are well-known traditional carbon-based fillers. Graphite is usually recognized as the best conductive filler because of its good thermal conductivity,

low cost and fair dispersability in polymer matrix [20,21]. Single graphene sheets constituting graphite show intrinsically high thermal conductivity of about 800 W/m·K [22] or higher (theoretically estimated to be as high as 5300 W/m·K [23,24]), this determining the high thermal conductivity of graphite, usually reported in the range from 100 to 400 W/m·K. Expanded graphite (EG), an exfoliated form of graphite with layers of 20 nm to 100 nm thickness, has also been used in polymer composites [25], for which the thermal conductivity depends on the exfoliation degree [26], its dispersion in matrix [27] and the aspect ratio of the EG [28].

Carbon fiber, typically vapor grown carbon fiber (VGCF), is another important carbon-based filler. Polymer/VGCF composites have been reviewed by Tibbetts et al. [29]. Since VGCF is composed of an annular geometry parallel to the fiber axis, thermal conductive properties along the fiber axis are very different from the transverse direction (estimated up to 2000 W/m·K in the axial direction versus 10~110 W/m·K in the transverse direction [[30, 31]), directly affecting the thermal conductivity of aligned composites [32,33].

Carbon black particles are aggregates of graphite microcrystals and characteristic of their particle size (10-500 nm) and surface area (25-150 m<sup>2</sup>/g) [14]. Carbon black is reported to contribute to electrical conductivity rather than thermal conductivity [34, 35, 36].

### **1.2.2 Metallic Fillers**

The filling of a polymer with metallic particles may result in both increase of thermal conductivity and electrical conductivity in the composites. However, a density increase is also obtained when

adding significant metal loadings to the polymer matrix, thus limiting applications when lightweight is required. Metallic particles used for thermal conductivity improvement include powders of aluminum, silver, copper and nickel. Polymers modified with the inclusion of metallic particles include polyethylene [37] polypropylene [38], polyamide [39], polyvinylchloride and epoxy resins [40], showing thermal conductivity performance depending on the thermal conductivity of the metallic fillers, the particle shape and size, the volume fraction and spatial arrangement in the polymer matrix.

### **1.2.3 Ceramic Fillers**

Ceramic powder reinforced polymer materials have been used extensively as electronic materials. Being aware of the high electrical conductivity of metallic particles, several ceramic materials such as aluminum nitride (AlN), boron nitride (BN), silicon carbide (SiC) and beryllium oxide (BeO) gained more attention as thermally conductive fillers due to their high thermal conductivity and electrical resistivity [41, 42]. Thermal conductivities of composites with ceramic filler are influenced by filler packing density [43], particle size and size distribution [44, 45], surface treatment [46] and mixing methods [47].

## **1.3 Thermal conductivity - Measurement and Modelling**

### **1.3.1 Methods for thermal conductivity measurements**

Several methods, as reviewed elsewhere [48, 49], have been proposed and used for measurement of

the thermal conductivity of polymers and composites. Classical steady-state methods measure the temperature difference across the specimens in response to an applied heating power, either as an absolute value or by comparison with a reference material put in series or in parallel to the sample to be measured. However, these methods are often time consuming and require relatively bulky specimens.

Several non steady-state methods have also been developed, including hot wire and hot plate methods, temperature wave method and laser flash techniques [49]. Among these, laser-flash thermal diffusivity measurement is widely used, being a relatively fast method, using small specimens [<sup>50</sup>, <sup>51</sup>, <sup>52</sup>]. In this method, the sample surface is irradiated with a very short laser pulse and the temperature rise is measured on the opposite side of the specimen, permitting calculation of the thermal diffusivity of the material, after proper mathematical elaboration. The thermal conductivity  $k$  is then calculated according to equation 2.

$$k = \alpha \cdot C_p \cdot \rho \quad (2)$$

Where  $\alpha$ ,  $C_p$  and  $\rho$  are the thermal diffusivity, heat capacity and density, respectively.

Differential scanning calorimetry (DSC) methods may also be used, applying an oscillary [<sup>53</sup>] or step temperature profile [<sup>54</sup>] and analyzing the dynamic response.

Significant experimental error may be involved in thermal conductivity measurements, due to difficulties in controlling the test conditions, such as the thermal contact resistance with the sample,

leading to accuracy of thermal conductivity measurements typically in the range of 5~10%. In indirect methods, such as those calculating the thermal conductivity from the thermal diffusivity, experimental errors on density and heat capacity values will also contribute to the experimental error in the thermal conductivity.

### 1.3.2 Modelling of thermal conductivity in composites

Several different models developed to predict the thermal conductivity of traditional polymer composites are reviewed elsewhere [55, 56, 57, 58]. The fundamentals are recalled in this section.

The two basic models representing the upper bound and the lower bound for thermal conductivity of composites are the rule of mixture and the so-called series model, respectively. In the rule of mixture model, also referred to as the parallel model, each phase is assumed to contribute independently to the overall conductivity, proportionally to its volume fraction (Equation 3).

$$k_c = k_p \cdot \Phi_p + k_m \cdot \Phi_m \quad (3)$$

where  $k_c, k_p, k_m$  are the thermal conductivity of the composite, particle, matrix, respectively, and  $\Phi_p, \Phi_m$  volume fractions of particles and matrix, respectively. The parallel model maximizes the contribution of the conductive phase and implicitly assumes perfect contact between particles in a fully percolating network. This model has some relevance to the case of continuous fiber composites in the direction parallel to fibers, but generally results in very large overestimation for other types of composites.

On the other hand, the basic series model assumes no contact between particles and thus the contribution of particles is confined to the region of matrix embedding the particle. The conductivity of composites accordingly with the series model is predicted by equation 4.

$$k_c = \frac{1}{\left( \frac{\Phi_m}{k_m} + \frac{\Phi_p}{k_p} \right)} \quad (4)$$

Most of the experimental results were found to fall in between the two models. However, the lower bound model is usually closer to the experimental data compared to the rule of mixture [55], which brought to a number of different models derived from the basic series model, generally introducing some more complex weighted averages on thermal conductivities and volume fractions of particles and matrix. These so-called second-order models including equations by Hashin and Shtrikman, Hamilton and Crosser, Hatta and Taya, Agari, Cheng and Vachon as well as by Nielsen [55,56,<sup>59</sup>], appear to reasonably fit most of the experimental data for composites based on isotropic particles as well as short fibers and flakes with limited aspect ratio, up to loadings of about 30% in volume. For higher loadings, the Nielsen's model appear to best fit the rapid increase of thermal conductivity above 30 vol.%, thanks for the introduction of the maximum packing factor into the fitting equation, despite the evaluation of maximum packing factor in real composites may present difficulties due to particle size distribution and particle dispersion in the matrix. However, the basic assumption of separated particles in the effective medium approach is not valid in principle for highly filled composites, where contacts are likely to occur, possibly leading to thermally conductive paths [<sup>60</sup>].



In order to take into account fluctuations in thermal conductivity in the composites, Zhou et al. [56] proposed the concept of heat-transfer passages, to model the conduction in regions where interparticle distance is low, applying the series model to “packed-belt” of conductive particles.

Even though these macroscopic approaches may be of interest from the engineering point of view, they deliver little or no information about the physical background of the observed behavior. As an example, very limited interpretation is given to the rapidly increasing conductivity with filler content above a certain filler loading (typically above 30 vol.%), or why the experimental results are so far away from the upper bound conductivity, even for highly percolated systems.

Attempts to model thermal conductivity taking into account the interfacial thermal resistance between conductive particles and matrix have been reported by several research groups [<sup>61</sup>, <sup>62</sup>, <sup>63</sup>, <sup>64</sup>, <sup>65</sup>] and applied particles with different geometries and topologies, including aligned continuous fibers, laminated flat plates, spheres, as well as misoriented ellipsoidal particles. In general, these models provided an improved fit with experimental data for ceramic based composites than models not accounting for interface thermal resistance. These approaches generally assume conductive particles to be isolated in the matrix and take into account the thermal resistance in heat transfer between conductive particle and matrix, also known as Kapitza resistance, from the name of the discoverer of the temperature discontinuity at the metal-liquid interface. A very simple proof of thermal interfacial resistance is the fact that a thermal conductivity lower than the reference matrix was experimentally found with some composites containing particles with thermal conductivity

higher than the matrix [61,62]. This phenomenon is explained by the very low efficiency of heat transfer between particles and matrix, so that the higher thermal conductivity of the filler cannot be taken into advantage and the composite behaves like a hollow material, thus reducing its conductivity compared to the dense reference matrix.

#### **1.4 Nanocomposites for thermal conductivity**

Recently, nanotechnology has gained much attention in research to develop materials with unique properties. Nanotechnology can be broadly defined as the creation, processing, characterization and use of materials, devices, and systems with dimensions in the range 0.1-100 nm, exhibiting novel or significantly enhanced physical, chemical, and biological properties, functions, phenomena, and processes due to their nanoscale size [66]. Nanocomposites, i.e., composites containing dispersed particles is in the nanometer range, are a significant part of nanotechnology and one of the fastest growing areas in materials science and engineering.

Polymer based nanocomposites can be obtained by the addition of nanoscale particles which are classified into three categories depending on their dimensions: nanoparticles, nanotubes and nanolayers. The interest in using nanoscaled fillers in polymer matrices is the potential for unique properties deriving from the nanoscopic dimensions and inherent extreme aspect ratios of the nanofillers. Kumar et al. [67] summarized six interrelated characteristics of nanocomposites over conventional micro-composites: (1) low-percolation threshold (about 0.1-2 vol.%), (2) particle-particle correlation (orientation and position) arising at low-volume fractions (less than

0.001), (3) large number density of particles per particle volume ( $10^6$ - $10^8$  particles/ $\mu\text{m}^3$ ), (4) extensive interfacial area per volume of particles ( $10^3$ - $10^4$   $\text{m}^2/\text{ml}$ ), (5) short distances between particles (10-50 nm at 1-8 vol.%), (6) comparable size scales among the rigid nanoparticles inclusion, distance between particles, and the relaxation volume of polymer chains.

Different nanoparticles have been used to improve thermal conductivity of polymers. As a few examples, HDPE filled with 7 vol.% nanometer size expanded graphite has a thermal conductivity of 1.59 W/m·K, twice that of microcomposites (0.78 W/m·K) at the same volume content [68]. Poly(vinyl butyral) (PVB), PS, PMMA and poly(ethylene vinyl alcohol) (PEVA) based nanocomposites with 24 wt.% boron nitride nanotubes (BNNT) have thermal conductivities of 1.80, 3.61, 3.16 and 2.50 W/m·K, respectively [69]. Carbon nanofiber was also reported to improve the thermal conductivity of polymer composites [70,71]. However, the most widely used and studied nanoparticles for thermal conductivity are certainly carbon nanotubes (either single wall -SWCNT or multi wall -MWCNT), which have attracted growing research interest. Indeed, CNT couples very high thermal conductivity with outstanding aspect ratio, thus forming percolating network at very low loadings.

#### **1.4.1 CNT-based nanocomposites preparation methods**

As the bulk properties of composite materials strictly depend on the structure formed during the processing step [72], a brief review on CNT-based composites preparation methods is given here, including solution mixing, melt blending, and in situ polymerization. Detailed information may be

found in reviews on this topic [73, 74, 75, 76].

**Solution Mixing** is one of the most commonly used techniques for preparing CNT based polymer–matrix composites. Solution mixing generally involves three major steps: dispersing CNTs in a suitable solvent, mixing with a polymer solution, and recovering the composite by precipitating or casting a film [77]. The difficulties in dispersing the pristine CNTs in a solvent by simple stirring, often require the use of high-power ultrasonication to make metastable suspensions of CNT or CNT/polymer mixtures [78]. Heat-treated [79], acid-treated [80] or functionalized CNTs [81, 82, 83] are often used to improve the dispersion of CNTs. Many polymer/CNT composites have been successfully prepared by the solution mixing method, including polyacrylonitrile/SWCNT [84], poly(methyl methacrylate)/SWCNT [85], poly(ethylene oxide)/MWCNT [86], poly(L-lactic acid)/MWCNT [87], chitosan/MWCNT [88]. However, the solution mixing approach is limited to polymers that freely dissolve in solvents suitable that also lead to stable suspension of CNTs.

**In-situ Polymerization** involves dispersion of nanotubes in a monomer followed by polymerization [89]. As in solution blending, functionalized CNTs can improve the initial dispersion of the nanotubes in the liquid (monomer, solvent) and consequently in the composites. Furthermore, in-situ polymerization methods enable covalent bonding between functionalized nanotubes and the polymer matrix using various chemical reactions. A few examples are mentioned here: composites of polyimides/MWCNTs were obtained by the reaction of 4,4'-oxydianiline (ODA) and pyromellitic dianhydride (PMDA) [90]; composites of polyaniline/MWCNT (acid treated) were

synthesized by chemical oxidative polymerization [91]; and composites of polypyrrole/MWCNT were prepared by in-situ inverse microemulsion [92] and in-situ chemical polymerization [93].

**Melt Blending** is a convenient method to produce CNT based nanocomposites owing to its cost effectiveness, fast production and environmental benefits, being a solvent-free process. Melt blending uses high temperature and high shear forces to disperse nanotubes in a thermoplastic polymer matrix, using conventional equipment for industrial polymer processing. Compatibilizers such as end-grafted macromolecules and coupling agents are often used to enhance dispersion of CNTs [94, 95]. Melt-blending approach has been reported for all the main polymer types, including polyolefines (PE, PP), polyamides, polyesters (PET, PBT and others), polyurethane, polystyrene, etc. However, compared with solution mixing, melt blending is generally less effective at dispersing nanotubes in polymers, and limited to lower concentrations due to the high viscosity of the composites at higher nanotubes loadings [96].

Masterbatches, i.e., thermoplastic polymers containing high loading of CNTs (typically 15-20 wt.%), have recently become widely used in the melt preparation of CNT based polymer nanocomposites. For industrial applications of the melt mixing extrusion technique, the masterbatch dilution seems to be favorable compared to the direct nanotube incorporation since it reduces dispersion difficulties, offers a dust-free environment and reduced safety-risk concerns, and easy handling [97, 98]. The state of a CNT dispersion in the diluted composites is influenced by the state of the CNT dispersion in the masterbatches [99], processing conditions [100] and compatibility between

the CNTs and polymer matrix [101]. Instead of the thermal conductivity of CNT based nanocomposites prepared from CNT masterbatch, the rheological and electrical properties have been given considerable attention [102, 103].

#### **1.4.2 General issues on thermal conductivity of CNT-based nanocomposites**

CNTs exhibit longitudinal thermal conductivity of 2,800~6,000 W/m·K for a single nanotube at room temperature [104, 105, 16], comparable to diamond and higher than graphite and carbon fibers, as well as aspect ratio usually in the order  $10^3$  [106]. Based on these two properties, several authors claimed CNT suitable to obtain a breakthrough in thermal conductivity by the formation of a thermally conductive percolating network, similar to electrical conductivity [107, 108, 109, 110, 111]. However, the literature on the thermal conductivity of traditional composites summarized in section 1.3.1 is most often neglected, even though very similar scenario may apply to nanocomposites.

Indeed, the reported experimental results for thermal conductivities of CNT/polymer composites are much lower than the values estimated from the intrinsic thermal conductivity of CNTs and the simple rule of mixing model [112, 113]. Very large scatter in the experimental data was also found; ranging from a remarkable enhancement of thermal conductivity by a small amount of CNT [111] to a decrease in the conductivity by CNT loading [114], evidencing the complexity of the problems and the difficulties in providing general rules for the thermal conductivity in polymer/CNTs nanocomposites.

Recent research revealed two main critical issues associated with the use of CNTs as thermally

conductive fillers in polymer composites [<sup>115</sup>]: (1) CNTs tend to aggregate into ropes or bundles when dispersed in polymers due to the strong intrinsic Van der Waals forces and the inert graphite-like surface, causing poor dispersion and making it a challenging task to disperse CNTs properly to realize their full potential in improvement of thermal conductivities of composites; (2) the other is related to interfacial thermal resistance caused by the phonon mismatch at the interface of the CNTs and the polymer results in a high interface thermal resistance, leading to severe phonon scattering at the interface and a drastic reduction of thermal transport properties. In addition, the thermal transport through CNT network by phonons will be strongly hindered by the gaps between adjacent tubes. The attainment of polymer/CNT nanocomposites with high thermal conductivity is challenged to address these two critical issues and build effective conductive networks for heat transfer.

This review aims at the identification and discussion of the several parameters affecting the thermal conductivity of CNT-based polymer composites. The thermal conductivity of CNTs is first reviewed on the base of the dependence of thermal conductivity of nanotubes on the atomic structure, the tube size, the morphology, the defect, the purification and the functionalization. Then, the thermal conductivity of polymer/CNT nanocomposites is discussed, summarizing factors such as interfacial resistance, dispersion and alignment of CNTs and polymer crystallization.

## 2 Thermal Conductivity of CNTs

Since their first observation nearly two decades ago by Iijima [<sup>116</sup>], CNTs have been the focus of considerable research efforts. Numerous investigators have reported remarkable physical and mechanical properties for this new form of carbon, among which the thermal conductivity of CNTs has received considerable attention [16,<sup>117</sup>]. Recent measurements of the conductivity of a single CNTs confirmed conductivities of about 3,000 W/m·K for multi-walled carbon nanotubes (MWCNTs) [104] and above 2,000 W/m·K for single-walled carbon nanotubes (SWCNTs) [105]. However, the direct and quantitative measurement of thermal transport properties of individual nanotube remains challenging, due to technological difficulties associated with nano-scale experimental measurements [<sup>118</sup>]. For this reason, the thermal conductivity of CNTs is mostly based on the theoretical simulations and calculations from indirect experiments [<sup>119, 120, 121, 122</sup>], providing significantly scattered results, usually in the range between 2,000 to 6,000 W/m·K.

Similar to other non-metallic materials, the transport of thermal energy in CNTs is assumed to occur via a phonon conduction mechanism. The phonon conduction in nanotubes is influenced by several processes such as the number of phonon active modes, the boundary surface scattering, the length of the free path for the phonons and inelastic Umklapp-scattering (an anharmonic phonon-phonon or electron-phonon scattering process) [<sup>123, 124</sup>]. The thermal conductivity of CNTs depends on atomic arrangement (i.e., how the sheets of graphite are “rolled”), the diameter and length of the tubes, the number of structural defects and the morphology, as well as on the presence



of impurities [<sup>125</sup>, <sup>126</sup>, <sup>127</sup>]. The factors affecting CNTs thermal conductivity are discussed in detail in this section.

## **2.1 Structure and Morphology**

### **2.1.1 Nanotube Morphology**

There are two main kinds of nanotubes: single-walled carbon nanotubes (SWCNTs), individual cylinders 1-2 nm in diameter, consisting of a single rolled graphene sheet, and multi-walled carbon nanotubes (MWCNTs), a “Russian doll” structure constituting several concentric graphene cylinders, with weak Van der Waals forces binding the tubes together [<sup>128</sup>]. Thus, SWCNTs are significantly smaller in diameter compared to MWCNTs and the thermal properties may differ significantly.

The thermal conductivity of a single SWCNT was evaluated by Yu et al, using a suspended microdevice on which a single tube was grown by chemical vapor deposition method [105]. Despite some uncertainty on the actual CNT diameter, the conductivity was evaluated to be higher than 2,000 W/m·K, and to decrease with decreasing temperature. Due to aggregation of SWCNTs in bundles [<sup>129</sup>], the thermal conductivity of individual SWCNT is often measured on SWCNT mats. For example, Hone et al. [<sup>130</sup>] estimated the room temperature thermal conductivity of SWCNT to be in the range of 1,750 and 5,800 W/m·K, based on the measured thermal conductivity of

high-purity mats of tangled nanotube bundles,. However, due to the high thermal contact resistance between tubes (see section 3.1.2) , the experimental results obtained on the SWCNT mats are usually two order of magnitude lower than for single CNTs (e.g., about 35 W/m·K for dense-packed SWCNT mat accordingly to Hone et al. [<sup>131</sup>]).

Simulation studies usually report thermal conductivities in the range of 2,800~6,000 W/m·K for SWCNTs at room temperature [<sup>132</sup>]. Berber et al. [<sup>133</sup>] evaluated the temperature dependence of the thermal conductivity of an isolated SWCNT by combining equilibrium and non-equilibrium molecular dynamics simulations. Their results indicated room temperature conductivity value of 6,600 W/m·K, increasing for lower temperature, with a maximum of 37,000 W/m·K at 100 K, this trend being in disagreement the experimental result by Yu et al reported above. Osman et al. [<sup>134</sup>] also found a maximum in the thermal conductivity of SWCNTs over a temperature range of 100–500 K by molecular dynamics simulations, higher temperatures corresponding to larger diameters, before falling off at higher temperatures. Gu et al. [<sup>135</sup>] used the complete phonon dispersion relations to calculate the temperature dependence of thermal conductivity of SWCNT, finding a similar trend and a conductivity value of 474 W/m·K at 300 K.

MWCNTs consists of nested graphene cylinders coaxially arranged around a central hollow core with interlayer separations of about 0.34 nm, indicative of the interplane spacing of graphite. The temperature dependence of thermal conductivity of MWCNTs was discussed by Small et al. [<sup>136</sup>], reporting monotonically decreasing conductivity below room temperature. Kim et al. [104] reported

the room temperature thermal conductivity of over 3,000 W/m·K for an isolated MWCNT, determined using a suspended microdevice. Other experiments on isolated MWCNTs showed values of thermal conductivity between 200 and 3,000 W/m·K at room temperature [137]. The large difference between single-tube and bulk measurements (usually using films or macroscopic mat samples) was attributed to the numerous and high thermal contact resistance of MWCNTs [138]. The thermal conductivities of MWCNT films were reported to be about 15 W/m·K by a pulsed photothermal reflectance technique [139] and 25 W/m·K by a self-heating  $3\omega$  method [140].

In a comparison between theoretical properties of SWCNTs and MWCNTs Liu et al. [141] reported a non-contact Raman spectra shift method, by which the measured thermal conductivity of an individual SWCNT and a MWCNT were 2,400 W/m·K and 1,400 W/m·K, respectively. The lower thermal conductivity of MWCNT was attributed to two factors: (i) the assumption that thermal transport is mainly by the outermost wall, and (ii) the occurrence of intertube Umklapp scattering processes. The SWCNTs also show a high number of phonon vibrational modes from theoretical calculations, and a relatively low defect density compared to MWCNT, leading to a potentially higher thermal conductivity [142, 143, 144].

### 2.1.2 Atomic Structure

The atomic structure of nanotubes is described in terms of the tube chirality, or helicity, defined by the chiral vector ( $c_h = n\mathbf{a}_1 + m\mathbf{a}_2$ ) and the chiral angle, see Fig. 1a [145]. The two limiting cases for

which the chiral angle is at  $0^\circ$  and  $30^\circ$  are referred to as zig-zag ( $0^\circ$ ) and armchair ( $30^\circ$ ) based on the geometry of the carbon bonds around the circumference of the nanotube. The difference in armchair and zig-zag nanotube structures is shown in Fig. 1b and Fig. 1c. Thus, the structure of CNT can be specified by  $(n, m)$ , that is arm chair ( $n = m$ ), zigzag ( $n = 0$  or  $m = 0$ ), or chiral (all others).

Since the mechanism of heat conduction by phonons or electrons depends profoundly on the band gaps of materials [120,<sup>146</sup>], the heat transfer mechanism of CNTs is found to depend strongly on the chirality, which determines the size of their band gaps and electronic properties [<sup>147</sup>]. The largest band gap (on the order of 1.5 eV) is found in nanotubes with  $(n, m)$  chiral indices defining the chiral vector satisfying the condition:  $|n-m| \neq 3p$ , where  $p$  is an integer [<sup>148</sup>]. For other types of nanotubes, the band gap is considerably smaller in the case of armchair nanotubes ( $n = m$ ). Thus, the electronic contribution to the thermal conductivity will be significant in metallic CNTs with a small band gap [<sup>149</sup>]. On the other hand, thermal conductivity of chiral CNT is mainly governed by the phonon component [<sup>150</sup>].

The phonon thermal conductivity of a CNT was found to depend on its chirality by Zhang et al. [<sup>151</sup>]. Using the homogeneous non-equilibrium Green–Kubo method based on the Brenner potential, the temperature dependences of the thermal conductivities of (11, 11), (20, 0), (10, 13) nanotubes with nearly equal radii were calculated. As shown in Fig. 2, the thermal conductivities of these three types of nanotube seem to have similar temperature dependences. In the range from 100 to 400 K, the conductivity of the (11, 11) nanotube was lower than that of the (20, 0) nanotube, while the (10,

13) nanotube showed lower values of thermal conductivity compared with the two other types.

Unlike phonon thermal conductivity, electron thermal conductivity of CNTs for metallic CNTs is seldom reported. An additional contribution from electronic states to the thermal conductance of metallic CNTs may be profound even though heat transport in CNT is thought to be dominated by phonons. For instance, based on a solution to the Boltzmann kinetic equation Mensah et al. [152] predicted the electron thermal conductivity of a chiral SWCNT exceed 200,000 W/m·K at about 80 K and 41,000 W/m·K at about 104 K, much higher than phonon thermal conductivity. Despite the decrease of thermal conductivity above 100 K, the room temperature value of about 11,000 W/m·K was still very high. However, since only a small fraction of the crystalline ropes of CNTs in the experiment will be metallic, the thermal conductance is dominated by phonons rather than electrons [130,153].

### **2.1.3 Topological Defects**

Whereas theoretical calculations are typically performed on perfect structures, it is nearly impossible to obtain perfect, defect-free CNT samples. In the process of the growth of CNTs, a variety of structural defects inevitably occur, some of which may have a pronounced impact on the properties of the CNTs. Defining a perfect nanotube to be a cylindrical graphene sheet composed only of hexagons having a minimum of defects at the tips to form a closed seamless structure, Ebbesen and Takada [154] classified the defects into three groups: topological defects,

rehybridization defects, incomplete bonding and other defects. Topological defects like non-hexagonal carbon rings or vacancy-related defects can form during the nanotube growth process or be introduced after synthesis, for example by chemical purification or irradiation by charged particles [155]. The formation mechanism of topological defects has been theoretically investigated, especially for SWCNT [156,157].

The Stone-Wales (SW) defect is one of the most important topological defects in CNTs. A SW defect comes from the 90° rotation of a C–C bond, resulting in the transformation of four hexagons into two pentagons and two heptagons, i.e., a dipole consisting of two pentagon-heptagon pairs in a hexagonal network of CNT [158,159,160]. A pentagon-heptagon pair introduced on a SWCNT can change the chirality of the tube and thereby form a seamless junction [161].

Vacancies in SWCNTs can be engendered by the release of carbon atoms in CNTs under electron or ion irradiation [162,163]. The local structures around single vacancies can be reconstructed [164]. Molecular dynamics simulations showed that surface reconstruction and size reduction occurred through dangling bond saturation, forming non-hexagonal rings and 5-7 defects in the lattice [165].

Compared with SWCNT, theoretical prediction of MWCNT defects appears to be more difficult and is seldom reported. However, a highly complex structure and a variety of MWCNT morphologies have been observed by high-resolution transmission electron microscopy (HRTEM). Lavin et al. [166] delivered a detailed description of the complex structure of MWCNT with numerous defects, such as slip-planes, irregular layer spacings and internal caps.

About 5% of the carbon atoms were located at defective sites<sup>[167]</sup>. Such a significant number of defect sites on the graphene walls of the CNTs may exert significant influence on the thermal conductivity. Yamamoto and Watanabe <sup>[168]</sup> investigated the effects of vacancies and SW defects by the non-equilibrium Green's Function technique. By comparing the thermal conductance ratio  $\kappa_{\text{vac/SW}}/\kappa_{\text{p}}$  of CNTs with vacancy or SW defect and perfect CNTs, a defect-dependent thermal conductance of CNTs was revealed (Fig. 3). The incident phonons were scattered more strongly by the vacancies than by the SW defects and the influence of defect scattering in thin CNTs on the thermal conductance was more significant than that in thick CNTs. Che et al. <sup>[169]</sup> also found a decreasing thermal conductivity with increasing defect concentration, and a stronger scattering effect of vacancy than SW defects.

Branched or regularly coiled CNTs can form when non-hexagonal carbon rings are incorporated into the nanotube structure during the growth process <sup>[170]</sup>. The introduction of the junction on CNTs usually gives rise to an increase of the local thermal resistance, and reduces the thermal conductivity due to lattice defects in the form of non-hexagonal carbon rings at the junction <sup>[171]</sup>. For example, the thermal conductivity of X-shaped junctions decreased by ~20-80% compared with straight nanotubes <sup>[172]</sup>.

## **2.2 Size Parameters**

The phonon mean free paths are thought to be relatively long in nanotubes: 500nm for a MWCNT

and even longer for a SWCNT. [105,138,<sup>173</sup>,<sup>174</sup>]. Taking this into account, structure size of CNTs is of particular importance. It is well known that CNTs are characterized by a large aspect ratio and a huge surface area. Diameter and length are two key parameters to describe CNTs and directly affect the thermal conductivity of both CNTs and composites containing CNTs. The dependence of thermal conductivity on these two parameters is reviewed in this section.

### **2.2.1 Diameter**

Cao et al. [<sup>175</sup>] reported that theoretically, the thermal conductivity should be higher for SWCNTs with smaller diameters. According to their results (Fig. 4), the thermal conductivity at 300 K was approximately inversely proportional to the diameter of SWCNT. Fujii et al. [<sup>176</sup>] measured the thermal conductivity of a single MWCNT using a suspended sample-attached T-type nanosensor. The thermal conductivity of MWCNT at room temperature increased as its diameter decreased, i.e., the thermal conductivity increased as the number of walls decreased, varying from about 500 W/m·K for an outer diameter of 28 nm to 2069 W/m·K for a 10nm diameter.

### **2.2.2 Length**

Simulation results predict an effect of CNT length on its intrinsic thermal conductivity. By the molecular dynamics method, the thermal conductivity of SWCNTs with chiral indices (5,5) and (10,10) was found to increase with the length of the tube from 6 to 404 nm (Fig. 5) [<sup>177</sup>]. The length



dependence of the thermal conductivity at room temperature in Fig.6 was also revealed for SWCNTs with different chiral indices: (5, 5), (10, 0), (7, 7), (10, 10), (17, 0), (15, 15) by using reverse non-equilibrium molecular dynamics simulations [178]. For length parameters ( $L$ ) from 5 to 350 nm, the calculated thermal conductivity increased with increasing tube length and followed a  $L^\alpha$  law, with  $\alpha$  values between 0.54 ( $100 \text{ nm} < L < 350 \text{ nm}$ ) and 0.77 ( $L < 25 \text{ nm}$ ). These phenomena were explained by the variable ratio between the phonon mean free path and the CNT length [179]. Based on these results, the thermal conductivity is expected to become constant when the tube length is much longer than the mean free path of the energy-carrying phonons.

### **2.3 Purification and Graphitization**

Although some new methods are devised to synthesize high quality CNTs, presently CNTs are mainly produced by three techniques: arc discharge, laser ablation, and chemical vapor decomposition [180,181]. The raw CNT materials produced by these methods are far from perfect, and contain numerous defects and impurities which impair the thermal conductivities of the CNTs [182, 183]. Thus, the treatment of raw CNTs materials, including purification and graphitization are widely investigated [184]. In this section, the purification methods and graphitization procedures for CNTs will be briefly reviewed.

### 2.3.1 Purification

The impurities, residual metals from metal catalysts widely used in CNT production [185] and carbonaceous impurities such as amorphous carbon, graphitic particles, carbon shells, fullerenes and multi-shell carbon nanocapsules [186], cause a serious impediment in most CNT applications [187, 188]. To get advanced composite materials (e.g., strength, toughness, conductivity) [189, 190], the impurities have to be removed by further physical and chemical processing. Purification methods generally involving separation and elimination processes can be categorized into three major methods: physical separation, gas-phase oxidation and liquid phase oxidation [191].

Physical separations are often based on the use of SWCNT aqueous dispersions with a surfactant, such as sodium dodecyl sulphate (SDS), with separation achieved by sonication, filtration, centrifugation, or chromatographic methods [192, 193]. Physical methods are not very efficient because they leave some amorphous carbon particle and multi-shell nanocapsules in CNT samples and it is difficult to completely dissolve metal encapsulated within the carbonaceous tips of the nanotubes [194]. Moreover, sonicating CNTs for a long time and at high frequency can cause damage, breaking the nanotubes into shorter fragments [195].

Gas-phase oxidation is carried out by thermal annealing CNTs in the presence of an oxidizing gas (O<sub>2</sub>, Cl<sub>2</sub>, or their mixtures) at 300–600°C [196]. The oxidative treatment of raw CNTs is effective in removing non-nanotube carbon from bundles, and also promotes the removal of the carbon coating

from metal catalysts. Gas-phase oxidation method can be compromised by poor homogeneity of the gas/solid mixture and low efficiency in removing graphitic impurities and metallic catalytic impurities [197].

Liquid-phase oxidation is generally carried out with acid solutions such as  $\text{HNO}_3$  or mixtures of  $\text{H}_2\text{SO}_4/\text{HNO}_3$  or  $\text{H}_2\text{SO}_4/\text{KMnO}_4$  [198]. In removing metals and carbon impurities, in view of the resistance to oxidation, strong oxidants such as  $\text{H}_2\text{SO}_4/\text{KMnO}_4$  are used with MWCNTs, and nitric acid solutions are used with SWCNTs [199]. The treated nanotubes are thought to bear carboxylic acid groups at the tube ends, and in addition, partial destruction of the nanotube structure is also possible [200].

Combined purifications, generally made up of sonication, acid treatment, oxidation, heat treatment, etc., are generally found efficient for eliminating most impurities and have been widely investigated [201, 202]. By multi purification procedure, CNTs with high purity may be obtained and most importantly, the risk of structure destruction is reduced [203, 204, 205]. Unfortunately, most of present purification techniques result not only in the elimination of impurities, but also in structure alteration or even destruction [206, 207, 208], directly affecting the intrinsic CNT conductivity.

### **2.3.2 Graphitization**

As described in section 2.1.3, CNTs always contain structural defects, such as pentagons, pentagon–heptagon pairs, vacancies, interstitials, etc., which considerably affect their thermal

transport properties. Thermal treatments are needed to remove these imperfections, and possibly obtain a regular and defect-free graphitic structure. These treatments are often referred as to graphitization processes [14]. The graphitization behavior of CNTs depends on their microstructure and morphology. Complex morphological and structural transformations may occur at different temperatures.

For SWCNTs, graphitization may result in the transformation to SWCNTs with larger diameter or MWCNTs, depending on the temperature. For example, Metenier et al. [209] reported the first transformation due to SWCNT coalescence appearing at 1800°C, with an increase of the tube diameters from 2 to 4 nm, and the second one after 2200°C due to the formation of MWCNTs having at first two to three carbon layers, then reaching six layers. The temperature corresponding to the structural transformation differs to some extent for CNTs synthesized by different methods [210]. The transform process is also observed during heat treatment of double walled CNTs (DWCNTs). At temperatures higher than 2100°C, three different types of structures were reported: (a) large-diameter DWCNTs; (b) MWCNTs, and (c) flaky carbons [211]. For MWCNTs, the graphitization procedure annealed at temperatures between 1600 and 3000°C was found to reduce the wall defects [212]. The results of graphitization are: (a) an increase in the graphitic perfection of the annealed MWCNTs, (b) removal of metallic compounds, (c) removal of microstructural defects, (d) remain of gross defects, such as side grafts or kinks.

Typically, the ratio of intensities between the D and G bands ( $I_D/I_G$ ) of CNTs in Raman

spectroscopy is taken as a measure of defects in nanotubes [213]. An example of structure ordering is evidenced in Fig. 7, showing Raman spectra of disordered MWCNTs before and after treatment at 2800°C for 30 min in a high-purity argon atmosphere [214]. The structural transformation from a disordered CNT to a highly ordered MWCNT and also the healing of structural defects upon graphitization were confirmed by the upshift of the G band, an intensified 2D band (overtone of the D band), and a reduced  $I_D/I_G$  ratio from 0.98 to 0.23.

Although high temperature heat treatment can promote the graphitic perfection and ordering of CNTs, the faceted angles, junctions, kinks or other gross defects in graphitized CNTs are still detrimental to the thermal conductivities of CNTs. Being aware of the defects developed and surviving the graphitization process of CNTs [215], it seems essential to synthesize raw CNTs with fewer defects and higher crystallinity [166, 216].

## 2.4 Functionalization of CNTs

The functionalization of CNTs can be obtained by covalent and non-covalent methods with different substances, such as chemical groups [217, 218], surfactants [219, 220], polymers [221, 222] and metals [223, 224]. The main trends and recent achievements in CNT chemistry with special emphasis on the functionalization of CNTs were reviewed by Rakov [225] and Meng et al. [226].

Local strain in CNTs, which arises from pyramidalization and misalignment of the  $\pi$ -orbitals of the  $sp^2$ -hybridized carbon atoms, makes nanotubes more reactive than a flat graphene sheet, thereby

paving the way to covalently attach chemical species to nanotubes [149]. Defects of CNTs at the tube ends or on the sidewalls are important in the covalent chemistry of the tubes. Hirsch [<sup>227</sup>] described the typical defects of SWCNT and its functionalization methods detailedly. Defects-favored functionalization of MWCNT is also possible [73,<sup>228,229</sup>] and local oxidation of the graphene sheet is needed to obtain significant functionalization yields [200]. Depending on the oxidation degree of the CNTs, an oxidative treatment is usually needed prior to actual functionalization, usually done in liquid phase by acid treatment or gas phase oxidation, similar to the processes described for CNT purification (see section 2.3.1).

Covalent bonds can benefit phonon transferring between the nanotubes and the polymer matrix [<sup>230,231</sup>]. However, even when extensive damaging of CNT structure is avoided, a notable drawback of covalent functionalization is the disruption of the extended  $\pi$  conjugation in nanotubes, combined with the conversion of  $sp^2$  carbons to  $sp^3$  by hybridization [<sup>232,233,234,235</sup>]. Although the impact of disrupted  $\pi$  conjugation is limited for mechanical properties, the impact on thermal conductivity is expected to be profound because each covalent functionalization site scatters electrons and phonons [<sup>236</sup>]. Shenogin et al. [231] found a significant drop of thermal conductivity with increasing degree of functionalization when evaluating the effect of  $sp^3$  defect on thermal conductivity of CNT by equilibrium molecular dynamics (MD) simulations (see Fig. 8). However, once about 1% of carbon atoms are functionalized, further increase in defect density does not result in lowering thermal conductivity.

Non-covalent functionalization is an alternative method for tuning the interfacial properties of nanotubes [237]. Such functionalization is realized by adsorbing different moieties onto SWCNTs to “wrap” the nanotubes [238]. The non-covalent approach includes surfactant modification of CNT, polymer wrapping or absorption (with the polymers generated in-situ) by the non-covalent interaction between the  $\pi$ -system of CNT and the functional group comprising the polymer [239, 240]. The advantage of non-covalent attachment is that the CNT structure is not damaged so that their properties remain. The main disadvantage of non-covalent attachment is that the forces between the wrapping molecules and the CNT may be very weak, possibly leading to high interfacial thermal resistance [241, 242].

### **3 Thermal Conductivity of Polymer/CNTs Nanocomposites**

Most of the published results present a disappointing message, indicating that the enhancement in the thermal conductivity of CNT/polymer composites failed to match the theoretical prediction. Also, the concentration dependence of the thermal conductivity of polymer/CNT composites does not reveal percolation behavior in the vicinity of electrical percolation concentration [243].

An summary of thermal conductivity performances for CNT-based nanocomposites reported in literature is given in Fig. 9. It is clearly observable that the experimental results are much closer to the lower bound conductivity model rather than to the upper bound rule of mixing: this reflecting exactly the behavior of traditional microcomposites (see section 1.3.2). This appears to be

disappointing, considering that the outstanding aspect ratio easily leads to a percolation network in the polymer matrix.

Attempts to extend the classical composites modeling to nanocomposites were reported and recently reviewed elsewhere [244]. In particular, the Maxwell-Garnett effective medium approach was applied by Nan et al. [122], resulting in an overestimated prediction, based on an assumed CNT thermal conductivity. Later, this model was refined taking into account the effective aspect ratio, which is much lower than the assumed value for straight CNT, owing to bending of CNT in the matrix [245]. The effect of interfacial resistance has been addressed by several authors [246, 247, 113], as discussed in details in the following. However, serious limitations apply to these models, addressing only low amount of CNT, extremely high CNT length and no or negligible contact between CNTs, which is in clear contrast with the well-known percolation capability of CNT even at low concentration. An attempt to apply the Lewis-Nielsen model to thermal conductivity results for composites containing up to 49 vol.% SWCNT was reported by Xu et al. [248], obtaining a large conductivity overestimation, compared with the experimental results. However, the values for particle geometry and orientation ( $A$ ) and maximum packing fraction parameters are not obvious for nanocomposites, which may lead to significant deviations. Guthy et al. [106] also applied the Nielsen model to PMMA/SWCNT, confirming a very high sensitivity of the prediction to the geometrical parameter  $A$  defined above.

Based on this overview, it appears that the proper exploitation of the thermal conductivity and



aspect ratio of CNTs requires a very careful control of the micro- and nano-structure of the composite. Several parameters are recognized to play a role in the conductivity performance, including interfacial resistance, CNT distribution, dispersion and alignment. This remainder of this section reviews the influence of these parameters on thermal conductivity, based on the present state of the art. However, these factors are often interrelated and some difficulties apply to their independent discussion.

### **3.1 Effect of interfaces on thermal transfer**

In a polymer nanocomposite, the large surface area of the nanoparticles maximizes the extent of polymer/particle interfacial area. Furthermore, in the case of percolating network, the number of contact points between particles increases with decreasing particle size. It is therefore reasonable to expect a significant role of the interfaces in thermal conductivity of nanocomposites.

A significant amount of literature is reported on the thermal resistance at the solid-liquid or solid-solid interface, also referred to as Kapitza resistance from the name of the discoverer of the temperature discontinuity at the metal-liquid interface. This effect is assumed to apply at the interface between CNT and polymer matrix and possibly also in direct contact between CNT. In this paper, we refer to CNT-polymer and CNT-CNT interfaces by the terms interfacial resistance and contact resistance, respectively. An optimization of the polymer-CNT and CNT-CNT interfaces is certainly one of the key issues for the successful thermal transport of CNT/polymer composites.

### 3.1.1 Interfacial Resistance

The interfacial thermal resistance represents a barrier to the heat flow associated with the differences in the phonon spectra of the two phases (depending on atomic arrangement and density) and possible weak contact at the interface [246]. Interfacial thermal resistance between CNT and polymer was quantified both experimentally and theoretically [246,242] in the order of magnitude of  $10^{-8} \text{ m}^2 \cdot \text{K/W}$ , which correspond to the resistance of a layer of polymer with thickness in the ten nanometer range.

From a theoretical point of view, the scattering of phonons in composite materials is mainly due to the existence of an interfacial thermal barrier from acoustic mismatch. In a simplified model, the transmission of a phonon between two phases depends on the existence of common vibration frequencies for the two phases. Thus, it was supposed that only low frequency phonon modes of CNTs are effective when CNTs interact with a matrix only via weak dispersion forces [246].

Another source of interfacial resistance is the imperfect physical contact between CNT and matrix, which primarily depends on surface wettability. The packing of octane molecules around a CNT was studied by molecular dynamics simulation, showing a strong peak in octane density about 4 Å away of the tube wall [246]. A similar situation is expected with polymeric molecules, in which arrangements may be more complicated, depending on chain conformation and rigidity [241,243,244]. In addition, interface defects can arise from internal stresses due to mismatch in

particle and matrix thermal expansion coefficients. In the worst cases, gaseous products might also be present at the interface.

There are some experimental observations that indicate very good physical contact between polymers and CNTs. Strong interfacial interactions between CNT and polymer are suggested by TEM results of PE/MWCNT composites shown in Fig. 10, where MWCNTs were uniformly dispersed as single nanotubes and PE seemed to coat or wrap around the MWCNT [249]. MWCNTs well wetted in PP matrix have also been reported [250].

A significant number of modeling papers addressed the role of CNT interface thermal resistance. Nan et al. [113] first applied the effective medium approach previously developed for microcomposites to CNT nanocomposites, [61] including interfacial resistance. They reported a decrease of about one order of magnitude in the overall composite calculated conductivity as the thermal resistance increased from zero (perfect interface) to  $8 \cdot 10^{-8} \text{ m}^2 \cdot \text{K/W}$  (Fig. 11). This model, including interfacial resistance, was also found to approximate experimental data for a nanotube suspension in oil, whereas the equivalent model assuming perfect interfaces clearly overestimates the conductivity value (Fig. 12) [113]. Later, Haggenueller et al. [251] applied the same model to SWCNT/HDPE nanocomposites for CNT volume fraction  $<0,06$  and with an interfacial resistance of  $1 \cdot 10^{-8} \text{ m}^2 \cdot \text{K/W}$ . However, the model was found to strongly underestimate the conductivity at higher volume fractions.

Similar conclusions on the importance of interfacial resistance in CNT nanocomposites were also

reported by Xue [252], Ju and Li [241], Gao et al [253] and by Singh et al [254], based on purely theoretical work or compared with CNT suspensions in liquids. Duong et al. [255] also reported a computational model based on a Monte Carlo simulation, valid for composites in which particles are not in contact with each other, and found to be in good agreement with considered experimental results in polymer composites containing up to 5 wt.% CNT loading.

The modeling literature in the preceding provides some information on the phenomenology of interfacial thermal resistance, but does not discuss the relationship between chemical structure and overall thermal performance. The effect of linear hydrocarbon chains on functionalized CNTs on the thermal conductivity of poly(ethylene vinyl acetate) nanocomposites was studied by Clancy et al. using a multi-scale modeling approach (Fig. 13) [256]. The results predicted that grafting linear hydrocarbon chains to the surface of a SWCNT with covalent chemical bonds should result in an increase in the thermal conductivity of these nanocomposites due to the decrease in the interfacial thermal resistance between the SWCNT and the surrounding polymer matrix upon chemical functionalization. Shenogin et al. [231], using classical molecular dynamics simulations, also found the interfacial resistance reduced by more than three times when an octane molecule was attached to one out of 15 tube carbon atoms (Fig. 14).

The arguments reported above clearly evidence the role of interfacial resistance on the heat exchange between CNT and surrounding polymer, but the question remains as to how important this mechanism is in the objective of producing highly conductive composites based on CNTs. The

interfacial thermal resistance is usually addressed as a factor explaining the deviation from models derived from the basic parallel model (see also former section 1.3.1). Thus, in a best case of perfect contact, the composite exhibits a conductivity, which is still not satisfactory. Good thermal contact (i.e., low thermal resistance) between nanoparticle and polymer can in principle be obtained by close molecular contact and correspond to a relatively high efficiency in transferring thermal energy from CNT to the polymer. However, due to the very low mean free path for phonons in the polymer (a few angstroms) [2] compared to the mean free path on CNTs (hundreds of nanometers) [138,173,174], the theoretical scenario of perfectly dispersed CNT having no contact with each other and exchanging heat with the surrounding matrix does not appear to be convenient when aiming at efficient heat conduction. Indeed, preferential conduction of thermal energy along particles forming a percolating network is the basic idea behind the use of highly conductive and high aspect ratio nanoparticles such as CNTs.

Chen et al. [257] proposed that resistance along the lateral surfaces of CNTs could not be a major factor, whereas the effective composite conductivity may vary significantly depending on the thermal resistance at the ends of CNTs. In this convenient scenario, heat would be transported along the CNTs, taking advantage of their high aspect ratio, and exchanged at the nanotube tip, with efficiency depending on the local interfacial resistance with the matrix. In this case, the functionalization of CNT sidewalls to reduce the interfacial resistance would not be necessary. Moreover, surface functionalization may even be detrimental for CNT conductivity, as strong

coupling of CNT and polymer chains may lead to damping of phonon or scattering at the boundaries, reducing phonon speed and/or the mean free path, thus limiting the intrinsic thermal conductivity of the CNT. Unfortunately, experimental results reported do not provide a general trend for composite conductivity vs. chemical interaction at the interface. Indeed, either improved [258] or worsened [259] thermal conductivity performances are reported for composites based on organically functionalized CNT, compared to pristine ones.

The effect of CNT coupling with the matrix was argued for different types of CNTs, generally assuming that MWCNTs may be less sensitive to polymer coupling, thanks to the internal layer that is not in direct contact with polymer. However, some authors reported the heat conduction contribution of inner walls of MWCNT to be negligible [260].

Based on the facts discussed in this section, the effects of interfacial resistance appear to be complex, and the advisability of maximizing the heat exchange efficiency between CNT and matrix will also depend on the presence of other possible heat exchange mechanisms, such as the CNT-CNT interactions discussed in the following section.

### **3.1.2 Contact Resistance**

It is well known that CNT polymer nanocomposites easily form percolating network at very low concentration, as evidenced by electrical conductivity above the percolation threshold. This fact is usually taken as a proof that CNTs are in contact with each other. However, the features of these

CNT-CNT contacts are mostly unknown, especially in terms of thermal conduction.

Even though no rapid increase was observed in the thermal conductivity at the percolation threshold, the percolation model was also applied to thermal conductivity of CNT-based nanocomposites and suspensions. Foygel et al. [261] applied Monte Carlo simulations for classical percolation in a model to estimate parameters for thermal conductivity percolation, based on the equation 5.

$$k(\Phi; a) = k_0 [\Phi - \Phi_c(a)]^{t(a)} \quad (5)$$

Where  $k$  is the thermal conductivity,  $k_0$  is a pre-exponential factor that takes into account conductivity of nanotubes and of their contacts with each other,  $\Phi$  is the volume fraction,  $\Phi_c$  is the critical volume fraction for percolation,  $a$  is the aspect ratio and  $t$  is a factor accounting for the percolating network characteristics. Calculation from CNT suspension experimental data led to  $k_0$  in the range between 64 and 137 W/m·K, this value representing the effective conductivity of the CNT network. This value is obviously much lower than both the theoretical and measured CNT conductivities reported above in this paper and this fact is related to the contact resistance between CNTs in the network. Based on the  $k_0$  calculation, the authors also estimated the value of the network resistance (including the thermal resistance of the nanotube and the contact between the nanotubes) to be in the range of  $10^7 \sim 10^8$  K/W.

Bonnet et al. [262] also reported that the enhancement in thermal conductivity is quantified by percolation model and calculated a thermal conductivity of SWCNT network of  $\sim 55$  W/m·K, which is consistent with results discussed above.

Haggenmueller et al [251] applied the percolation model to SWCNT/HDPE nanocomposites, showing that the percolation model fits experimental data up to CNT loading of 20 vol.%, while the effective medium approach by Nan et al only fit data up to 6 vol.% (Fig. 15). Improved data fits with percolation model compared with an effective medium approach at high CNT loading was also reported by Kumar et al [263].

Further evidence of low efficiency in thermal contact between CNTs has been reported by other authors. Hone et al. [264] reported the thermal conductivity of SWCNT free-standing networks, showing much higher thermal conductivity from 10 to 400 K in the alignment direction compared to that for un-aligned SWCNT as illustrated in Fig. 16. At room temperature, the thermal conductivity of aligned SWCNT network was about 200 W/m·K for the aligned direction and only about 30 W/m·K in the unaligned one. This strong effect of orientation may be related to the lower number of contact points when CNT are oriented, thanks to their high aspect ratio, but there might also have an effect on the contact efficiency, in term of CNT-CNT overlap.

Similar results were reported by Gonnet et al. [265] for magnetically aligned buckypapers (a preformed nanotube network or nanotube mat), which showed much higher thermal conductivity along the alignment direction compared to the perpendicular direction or the unoriented buckypaper (see Fig. 17). The thermal conductivity of the random buckypaper epoxy composites was lower than both parallel and perpendicular nanocomposites, suggesting that reduced contact resistance for the oriented buckypaper is retained in the nanocomposites.



The contact between CNTs was modeled by Shenogina et al [247], who concluded that heat flow by CNT-CNT direct contact is very ineffective because of the weak Van der Waals forces binding CNTs, resulting in a significant thermal resistance, and because of the small contact area. The authors proposed an explanation for the difference in electrical vs thermal behavior based on the very different CNT/polymer conductivity ratio for thermal (about  $10^4$ ) and for electrical conductivity (in the range of  $10^{12}\sim 10^{16}$ ). With this relatively low thermal conductivity ratio, the dominant channel for heat flow was proposed to involve the matrix, rather than the percolating network.

The contact resistance between CNTs was modeled by Zhong and Lukes (Fig. 18), showing clear reduction in tube-tube resistance with longer CNT, larger overlap and smaller spacing [<sup>266</sup>].

Improvement in CNT-CNT contact is therefore a must to obtain a more efficient heat transfer between CNTs [<sup>267</sup>]. The resistance to heat transfer at the inter-CNT contact and the total contact area are crucial in polymer nanocomposites, given that the low thermal conductivity of the matrix makes CNT-CNT heat exchange through the polymer matrix a very low efficiency process. Both dispersion and preferential orientation of CNT strongly affect the total contact area in a polymer nanocomposite: as a first approximation, the more aggregated and oriented are the CNT, the higher the thermal contact they can exhibit. Randomly dispersed nanotubes in polymer composites are difficult to provide proper pathways for phonon transport, as the point interconnections in the random nanotubes network pose severe limitation to effective phonon transfer. In contrast,

interconnections formed by alignment are able to build a two-dimensional structure of the CNT network and extensive tube-tube overlap of individual tubes, which are desirable features for effective heat transport from one nanotube to the other.

Functionalization of carbon nanotubes may in principle be oriented to reduce the thermal contact resistance between adjacent CNTs, despite little work has been done so far on this way. In particular, interactions stronger than Van der Waals forces are assumed to be beneficial for phonon transfer from one tube to another. CNTs decorated with silver showed slightly improved performance in epoxy resin compared to reference CNTs [223], possibly due to reduced contact resistance.

The use of two or more fillers with different shapes may also be beneficial in term of particle contact surface. A synergistic effect between graphite nanoplatelets (GNPs) and SWCNTs in the enhancement of the thermal conductivity of epoxy composites was reported by Yu et al. [268], ascribed to the formation of a more efficient percolating hybrid CNT/GNP network with significantly reduced thermal contact resistance. Similar results were obtained for PP composites, in which thermal conductivity is also synergistically enhanced by combining CNTs with carbon black and synthetic graphite [269, 270].

### **3.2 Dispersion**

Dispersion, i.e., the separation of single nanoparticles, is one of the critical issues with regard to the processing of polymer/CNT composites due to the small size and high aspect ratio, leading to the

formation of CNT bundles and aggregates [66,<sup>271</sup>]. Many techniques, such as high power ultrasonication, surfactant-assisted processing and functionalization of nanotubes, have been proposed and used to get well dispersed CNTs in polymers [78,<sup>272</sup>,<sup>273</sup>]. Xie et al. [<sup>274</sup>] reviewed the recent progress made towards the improvement of dispersion of CNTs in polymer matrices. However, in contrast to the usual idea to disperse CNT, a key issue in producing superior CNT nanocomposites for thermally conductive applications appears to be the ability to control aggregation of the CNT in polymeric matrices to obtain an interconnecting network suitable for heat transfer. Indeed, dispersion of CNT into isolated particles with little or no contact with each others has been shown to lead to very low efficiency for thermal conductivity, as discussed in previous section 3.1.

However, it appears very difficult to provide general rules for the relationship between the dispersion of nanotubes and thermal conductivity of their nanocomposites for several reasons. First, the dispersion of CNT is a relative concept, dependent on the experimental techniques used, as well as the authors' interpretation, and little or no quantitative parameters are used in literature, making difficult or impossible the comparison between results reported in different papers. Moreover, dispersion is often dependent on other parameters affecting thermal conductivity. For example, dispersion is obviously related to CNT functionalization, but functionalization affects the thermal conductivity of the CNTs, so that the two effects cannot be studied independently. Similarly, dispersion depends on the mixing energy imposed, but mixing energy may also affect the thermal

conductivity of the CNTs, by introducing defects and/or shortening.

### 3.2.1 Effect of Functionalization

Van der Waals interactions between CNTs, result in rope-like aggregates or entangled bundles, depending on their flexibility [<sup>275</sup>]. Dissociation of agglomerated CNTs is usually pursued to maximize material properties including thermal conductivity [<sup>276, 277</sup>]. Aggregation is usually suppressed by ultrasonic treatment [<sup>278</sup>]. Comparison of thermal conductivities of epoxy resin based composites with raw MWCNTs and those treated under ultrasonication exhibit better dispersion and higher thermal conductivity for the composites with treated MWCNTs (Fig. 19) [<sup>279</sup>].

While untreated aggregates of CNTs are difficult to separate into dispersed and interconnected nanotubes, functionalization is usually helpful to disperse or individualize CNT in polymers [<sup>280, 281</sup>]. Compared with dispersions of MWCNT in epoxy with functionalized MWCNT (Fig.20), the dispersion of the unmodified MWCNT resulted in large clusters with dimension of few microns, while MWCNT-COOH mainly led to individual nanotubes or smaller clusters with reduced entanglement [<sup>282</sup>].

However, conventional acid treatment used to obtain COOH groups on CNT may lead to structural defects of CNT, which is detrimental to thermal conductivity. As an example, the thermal conductivity obtained in PMMA-based composites was higher for untreated CNTs [<sup>283</sup>]. Indeed, conductivities of 2.43 and 3.44 W/m·K were obtained with 1.0 wt.% pristine SWCNTs and 4.0

wt.% MWCNTs, respectively, while the corresponding materials obtained with purified CNTs showed thermal conductivity of 0.60 and 0.70 W/m·K (Fig.21) [283]. It is worth noticing that, to the best of the authors' knowledge, these results obtained by Hong et al presently exhibit the best performance achieved with CNT nanocomposites, in term of conductivity/CNT loading. Unfortunately, the authors did not report characterization of CNT dispersion in the polymer.

Functionalization of CNT may significantly affect the thermal conductivity properties of polymer/CNT composite by changing the thermal conductivity of CNT, the thermal contact between adjacent CNTs in a network and the interface thermal resistance between CNTs and polymers, as well as CNT dispersion into a polymer (as discussed in 2.4 and 3.1).

### **3.2.2 Effect of Mixing Conditions**

Mixing conditions obviously determines dispersion, together with functionalization discussed above. The shortening of CNTs under the action of high shear mixing is usually observed, especially during melt processing, possibly affecting the thermal conductivity of the nanocomposites. As an example, a shortening of MWCNTs occurred during melt mixing with polystyrene and the tube length decreased down to a third of the origin length (Fig.22) [284]. At the same time, a better MWCNT dispersion was obtained with increasing mixing energy input.

Hong et al. [285] compared the thermal conductivity of poly(dimethyl siloxane) (PDMS)/MWCNT composites prepared with raw MWCNT and oxidized/master batched MWCNT. Better dispersion

and thermal conductivities of composites were obtained with the master-batched MWCNT. For composites using master-batched MWCNT, the thermal conductivity was about 10% higher than those prepared with raw MWCNT and the aspect ratio 1.7 times greater (see Table 3).

As mentioned in section 2.2.2, the thermal conductivity of CNT has a length dependence that is more obvious for CNTs with smaller diameter. However, the composite thermal conductivity was theoretically predicted to have different dependence on the CNT length. As a few examples, Xue [252] predicted an increasing thermal conductivity with increasing nanotube length, Song and Youn [286] found a limiting value, whereas Bagchi and Nomura [260] found a thermal conductivity not very sensitive to the nanotube length. From a practical point of view, CNT shortening may be acceptable to some extent, as this facilitates better dispersion and enhances the thermal conduction. Xie and Chen [287] reported a noticeable enhancement of thermal conductivity by controlling the ball milling time, known for decreasing CNT length [288]. Wang et al. [289] reported a mechanical method to shorten SWCNT for improving dispersion without reducing their thermal conductivity (see Fig.23). Compared with acid oxidized SWCNT, mechanically shortened samples preserve the pristine structure of CNT without significant damaging of the graphitic sidewall structure and shortened SWCNT was found easier to disperse into polymer matrices.

### **3.2.3 Localization of Thermally Conductive Paths**

In order to increase the thermal contact area between conductive particles, localization of fillers into

well defined co-continuous region can be advantageous. Some techniques reported to build conductive pathways by localizing CNTs or controlling aggregation are discussed in this section.

Localized aggregation of CNTs can be realized by colloidal-physics methods using polymer emulsions or latexes. When combined with nano-sized filler, the polymer particles create excluded volume that leads to a segregated network of filler. It may be possible to form a segregated network of CNTs and enhance thermal conductivity at very low concentration. For example, semi-crystalline polyurethane (PU) dispersions were used as a latex host to accommodate MWCNTs following the colloidal physics method [290]. The continuous nanotube-rich phase was found in the interstitial space among the latex particles. The thermal conductivity increased from 0.15 W/m·K to 0.47 W/m·K (i.e., by ~210%) with a MWCNTs content of 3 wt%.

In nanostructured latexes, CNTs are usually first dispersed in aqueous solution driven by sonication and then mixed with latex [291]. Suitable functionalization of CNTs or usage of surfactants will favor uniform dispersion of CNT in latex [292,293], but it may also increase the contact thermal resistance between CNTs and hinder the formation of interconnecting network of CNTs [294,295]. Grunlan et al. [296] ascribed the limited improvements of thermal conductivity, approximately 10% for a CNT content  $\leq 2$  vol.%, to the effects of surfactant when preparing poly(vinyl acetate)/CNT nanocomposites with this approach. Similar results were also found in MWCNT/water-based PU composites [297]. Even so, the colloidal-physics method appears very interesting in controlling the segregation of CNTs and forming interconnecting network to obtain thermally conductive

polymer/CNT composites at low CNT content [<sup>298</sup>].

Other methods may be also used to obtain controlled segregation of conductive particles. In particular, co-continuous immiscible polymer blends have proved to be an effective method to build percolation network for electrical conductivity [<sup>299, 300, 301</sup>]. Co-continuous structures can indeed be used to build a conductive path in the material, selectively dispersing CNT in one of the phases [<sup>302, 303</sup>]. Recently, CNT master batches have provided a useful way to build co-continuous structures, engendering significant reduction in electrical resistivity due to the interconnecting network of the confined CNTs [<sup>304, 305, 306</sup>]. Similar approaches may be useful in principle for thermal conductive enhancement of polymer/CNT composites; however, to the best of our knowledge, the only attempts at present to obtain co-continuous blends with a thermally conductive phase were reported by Droval et al., using a syndiotactic polystyrene filled with boron nitride or aluminum oxide, in combination with an electrically conductive phase, for electrothermal applications [<sup>307, 308</sup>].

Alternatively, impregnation of preformed conductive networks can be used to prepare composites with precise control of conductive pathways through their volume. For example, Ji et al. [<sup>309</sup>] prepared MWCNT/carbon/polystyrene composites by in situ polymerization of monomer in preformed MWCNT/C foams, which were preformed using polyurethane foam as template and had a more continuous conductive structure than the CNT networks formed by free assembly in composites. The thermal conductivity of composites with 1 wt.% loading of MWCNT/C foam had



an enhancement of 37%, and the enhancement increased to 155% with a 20 wt.% loading of MWCNT/C.

### **3.3 Alignment**

Alignment is understood as a preferred orientation of a tube (in its longitudinal axes) within a three-dimensional sample which may result in great advantage, when thermal conductivity enhancement is desired in a preferential direction, similarly to the case of pure CNT network previously discussed in section 3.1.2. CNTs can be aligned in polymer composites by processing, CNT arrays or external force.

#### **3.3.1 Alignment During Processing**

During melt processing of polymer/CNT composites, CNTs usually tend to align parallel to the flow direction. Alignment of CNTs during processing has attracted much interest in reinforcing the mechanical properties of composites [<sup>310,311,312</sup>]. The good dispersion and alignment of the nanotubes, along with good adhesion with polymers are key factors for mechanical property enhancement. Although alignment of CNTs is usually found to improve mechanical properties in the alignment direction, its influence on thermal conductivity is not clear owing to the complex factors in forming effective heat transfer network.

Ghose et al. [<sup>313</sup>] processed EVA/MWCNT samples with significant alignment, and observed

thermal conductivity parallel to alignment in aligned sample higher than in the unaligned case (see Table 4), suggesting successfully heat conduction along aligned CNTs. Moreover, the addition of isotropic Al nanofiller reduced the difference in the conduction in the axial and transverse directions, likely acting as a bridging agent between aligned conductive pathways.

Kim et al. [314] associated the alignment of CNTs with the deformation applied during the optimized milling process. Alignment of 5 wt.% CNTs in ethylene propylene diene rubber (EPDM) matrix (0.28 W/m·K) resulted in obvious improvements in thermal conductivities (0.70 W/m·K).

### **3.3.2 Alignment from CNT Array**

An anisotropic thermal conductivity of composites can be expected if all the CNTs embedded in the matrix are strictly aligned, which can be obtained using preformed CNT arrays (Fig.24) [315].

Sih et al. [316] used aligned CNTs to enhance the through-thickness thermal conductivity in adhesively bonded joints and obtained a through-thickness thermal conductivity of over 250 W/m·K, superseding the thermal conductivity of neat adhesive joint by several order of magnitudes. Huang et al. [317] obtained highly thermal conductive silicone elastomer/CNT composites by using in situ injection of polymers into CNT arrays. As shown in Fig.25, the thermal conductivity of the aligned composites with only a 0.4 vol.% loading is 116% and 105% higher than that of pure elastomer S160 and dispersed composites, respectively. Enhancement of the thermal conductivity (10 to 20 times larger than the polymer matrix) was also reported by Borca-Tasciuc et al. [318] for composites

prepared by infiltrating poly-dimethyl siloxane (PDMS) in aligned MWCNT arrays.

Cola et al. [319] revealed that theoretically the overall performance of CNT array interfaces was strongly influenced by the thermal resistance at the contacts between free CNT ends and the opposing substrate surface (one-sided interface) or the opposing CNT array (two-sided interface). Lin et al. [320] reported an in-situ functionalization method by microwave curing to improve the ACNT–epoxy interfaces while maintaining their well-aligned structures. Figure 26 shows thermal conductive results for a thermally cured ACNT–epoxy composite (TCOM), a microwave-cured ACNT/epoxy composite (MCOM), a thermally cured epoxy (TEP), and a microwave-cured epoxy (MEP). The much higher thermal conductivity of MCOM suggests that the interfacial bonding between the ACNTs and the epoxy matrix is dramatically improved by microwave treatment. Strong bonding between polymer and CNT by microwave irradiation was also obtained by Wang et al. [321].

### **3.3.3 Alignment by External Field**

Alignment of CNT in nanocomposites can also be realized by an external field, such as magnetic [322], electric [323, 324] or force fields (stretching process) [325]. However, unlike the electrical conductivity, the thermal conductivity of composites obtained by alignment under an external field is seldom reported.

Useful data are reported in the work of Hong et al. [326], who found that the thermal conductivity of heat transfer nanofluids containing CNTs and Fe<sub>2</sub>O<sub>3</sub> was enhanced after alignment by an external

magnetic field. The reasonable explanation was that the  $\text{Fe}_2\text{O}_3$  particles formed aligned chains under the applied magnetic field, and helped to connect the nanotubes, which resulted in improved thermal conductivity. However, clumping of CNTs together with magnetic particles during an extended application of magnetic field would disconnect the network. The maximum thermal conductivity was  $0.92 \text{ W/m}\cdot\text{K}$ , i.e., 35% higher than the nanofluid without magnetic field.

Gonnet et al. [265] achieved in-plane SWCNT alignment under a high magnetic field. However, similar thermal conductivities were found in the aligned and perpendicular direction of the epoxy nanocomposites, even though the magnetically pre-aligned buckypapers (a preformed nanotube network or nanotube mat) had a much higher thermal conductivity along the alignment direction.

### **3.4 Polymer Crystallization**

Since effective phononic conduction requires geometrically regular and strong bonds, the crystallinity of macromolecules, i.e., the packing of polymer chains in crystal lattice structures, is certainly important for the thermal conductivity of nanocomposites. The presence and features of a crystalline structure are expected to strongly influence heat transfer in both the polymer phase at the interface between CNT and polymer. Furthermore, in semi-crystalline/CNTs composites, CNT can provide nucleation sites for polymers and accelerate the crystal growth rate, as well as modify the crystal shape. The influences of polymer crystallization on the thermal conductivity of polymer/CNT composites are discussed in this section.

CNTs have been shown to alter the crystallization kinetics of semi-crystalline polymers, including polyolefins [249,<sup>327</sup>,<sup>328</sup>], polyamide [312,<sup>329</sup>], poly(vinyl alcohol) [310] and poly(vinylidene fluoride) [<sup>330</sup>], acting as a heteronucleation agent and/or imposing a nanoconfinement effect. This strongly affects the rate of crystallization, the crystalline fraction and the shape of crystalline domains, including the formation of peculiar shish-kebab structures, reviewed elsewhere [<sup>331</sup>].

A few papers report the influence of polymer crystallinity and its orientation on the thermal conductivity of polymer/CNT composites. Haggemueller et al. [251] investigated the thermal conductivities in nanocomposites of SWCNTs and PE vs. the degree of PE crystallinity and the PE alignment. A significant increase in thermal conductivity with increasing SWCNT loading in isotropic SWCNT/PE nanocomposites was found, reaching 1.8 and 3.5 W/m·K at 20 vol.% SWCNT in low-density PE (LDPE) and high-density PE (HDPE), respectively. The increase of thermal conductivity in SWCNT/HDPE compared to SWCNT/LDPE evidenced a strong effect of polymer crystallinity, possibly explained by a reduction of the interfacial thermal resistance when PE is highly crystalline. As shown in Fig. 27, the authors also reported that the thermal conductivity along the fiber direction increased with increasing Hermans orientation factor  $f_c$  for both HDPE fibers and SWCNT/HDPE composites ( $f_c$  increases from 0 to 1 with increasing uniaxial alignment): as an example, the thermal conductivity increased by as much as 150% as  $f_c$  increased from 0 (isotropic) to ~0.65. The observed increase in thermal conductivity with increasing HDPE orientation for HDPE fibers and SWCNT/HDPE composite fibers with low loadings was

predominately attributed to the alignment of the HDPE. Indeed, it is well known that PE can exhibit a dramatic increase in thermal conductivity with increasing alignment of polymer chains. The thermal conductivity of PE can be as high as 340 W/m·K in ultradrawn fibers [<sup>332</sup>].

The influence of crystallinity on the dispersion of MWCNTs in PP matrix was investigated by Liao et al. [<sup>333</sup>]. High crystallinity PP (HC-PP), medium crystallinity PP (MC-PP), low crystallinity PP (LC-PP) were used and MWCNTs was found to be best dispersed better in LC-PP, but thermal conductivity was not disclosed. The better dispersability of CNT in low crystallinity PP is likely related to the amorphous fraction. Indeed, beside the possible nucleation activity induced by CNTs, most of the nanotubes are in the amorphous phase in highly filled CNT nanocomposites. In polymers with relatively large crystalline domains and high crystallinity, this may result in CNT confinement in the amorphous phase, where high CNT concentration may possibly be exploited to maximize CNT-CNT thermal contact.

## **4 Concluding Remarks**

As electronic devices tend to become slimmer and more integrated, heat management become a central task for device design and application. Similar issues are faced in several other applications, including electric motors and generators, heat exchangers in power generation, automotive etc. Metallic materials are widely used as heat dissipation materials, but there have been many attempts to replace the metallic materials with highly thermally conductive polymer based composites due to

their lightweight, corrosion resistance, easy processing and lower manufacturing cost.

Thermally conductive polymer based composites are tentatively prepared by the incorporation of thermally conductive fillers. The outstanding thermal conductivity of CNTs makes them a promising candidate to obtain highly thermally conductive polymer based composites. The thermal conductivity of CNTs themselves depends on their morphology, chirality, defect, size and impurities. To obtain well structured, fewer defect, uniform CNTs with good thermal conductivity, purification and graphitization processes are necessary. Even so, the exploitation of CNTs faces a number of complicating factors: (a) a range of chiralities; (b) a wide length distribution; (c) various diameters; (d) aggregation or bundles of different diameters; (e) ends and sidewall defects. These factors result in diverse thermal conductive properties of CNTs and their composites.

Functionalization of CNTs, which can have a profound significance in dispersing CNT in polymeric matrixes, can be realized by covalent and non-covalent bonding. Covalent functionalization suffers from two potential drawbacks: CNT rupture, causing a decrease of aspect ratio and the disturbance of graphitic structure. By comparison, non-covalent functionalization typically leads to weakly bonded functional groups. These features directly affect thermal conductivity of CNTs, due to changes in CNT intrinsic conductivity, in terms of phonon mean free path and boundary scattering effects. These changes, combined with different distribution and dispersion level obtainable with different functionalizations, exert complicated influences on the thermal conductivity of polymer/CNT nanocomposites. Thus, the reported thermal conductivities of polymer/CNT

nanocomposites tend to be widely scattered.

The thermal conductivity of CNT-based nanocomposites has often been addressed in a strict analogy with electrical conductivity. However, significant differences apply between thermal and electrical conductivities, primarily in (i) the CNT/polymer conductivity ratio, being several orders of magnitude lower for the thermal conductivity, and (ii) in the phononic vs. electronic conduction mechanisms. Neglect of these two basic differences has led to a certain disappointment in literature reports, when obtaining thermal conductivity results that do not follow the same trend as electrical conductivity, and being much lower than expected with the simple rule of mixtures. However, previous literature on microcomposites for thermal conductivity show similar behavior, not often mentioned in discussions of CNT nanocomposites.

Strict control of the nanostructure and a detailed knowledge of the physical phenomena for thermal conduction are needed to take proper advantage of the outstanding aspect ratio and intrinsic thermal conductivity of CNTs. Indeed, two fundamental and critical issues associated with obtaining highly efficient thermal conductive polymer/CNT nanocomposites, irrespective of the fabrication method: the nanotubes should be properly distributed in the polymer matrix to form an effective conductive path, and the thermal resistances at CNT-polymer and/or at CNT-CNT interfaces must be minimized. The thermal interface resistance phenomena are believed to be the bottleneck for highly thermally conductive polymer/CNT composites. The CNT/polymer interface resistance can be tentatively reduced by improving the strength of interactions between filler and matrix; however,



due to the low thermal conductivity of polymers, heat transfer from CNT to the polymer does not appear to be an efficient scenario for improved overall heat transfer. On the other hand, in principle it could be more effective to exploit direct contacts between CNTs. Unfortunately, both the lower efficiency of thermal contact and low contact area typically apply to CNT-CNT contacts. Thus, the quality and quantity of CNTs interconnections appear to be crucial. These may be maximized at high CNT loadings, with obvious drawbacks related to cost and processability. Alternatively, alignment and strictly controlled segregation of CNT have been experimentally shown to be beneficial.

Based on the present state of the art reviewed here, CNTs remain one of the most promising thermally conductive filler type for polymers. However, significant advances are still needed to obtain thermally conductive composites sufficiently efficient to meet the requirements of most market applications.

## **Acknowledgements**

The authors are grateful to Prof. Giovanni Camino and Prof. Guido Saracco at Politecnico di Torino for discussion and support during the preparation of this work. A. Fina also thanks Dr. Donald R. Paul at the University of Texas at Austin for the useful discussiosn on themal conductivity modeling in polymer composites.

The research leading to this results has received funding from the European Community's Seventh Framework Programme (FP7 2007-2013) under grant agreement n° 227407 - Thermonano

Z. Han is grateful to the Post-Doc Fellowship for Senior Researcher programme of Politecnico di Torino for financial support.

#### References

- 
- <sup>1</sup>Majumdar A. Microscale transport phenomena. In: Rohsenow WM, Hartnett JR, Cho Y I, editors. Handbook of Heat Transfer (3rd Edition). New York: McGraw-Hill, 1998. pp. 8.1-8.8.
  - <sup>2</sup>Agari Y, Ueda A, Omura Y, Nagai S. Thermal diffusivity and conductivity of PMMA-PC blends. *Polymer* 1997; 38: 801-807.
  - <sup>3</sup>T'Joen C, Park Y, Wang Q, Sommers A, Han X, Jacobi A. A review on polymer heat exchangers for HVAC&R applications. *Int J Refrig* 2009; 32: 763-779.
  - <sup>4</sup>Hu M, Yu D, Wei J. Thermal conductivity determination of small polymer samples by differential scanning calorimetry. *Polymer Testing* 2007; 26: 333-337.
  - <sup>5</sup>Speight JG. Lange's Handbook of Chemistry (Sixteenth Edition), Section 2: Organic Chemistry, 2.20 POLYMERS. New York: McGraw-Hill, 2005. pp. 2.794-2.797.
  - <sup>6</sup>Price DM, Jarratt M. Thermal conductivity of PTFE and PTFE composites. *Thermochimica Acta* 2002; 392-393: 231-236.
  - <sup>7</sup>Greig D, Hardy ND. The thermal conductivity of semicrystalline polymers at very low temperatures. *Journal de Physique Colloques* 1981; 42(C6): 69-71.
  - <sup>8</sup>Yano O, Yamaoka H. Cryogenic properties of polymers. *Prog Polym Sci* 1995; 20: 585-613.
  - <sup>9</sup>Reese W. Thermal Properties of Polymers at Low Temperatures. *J Macromol Sci A* 1969; 3: 1257-1295.
  - <sup>10</sup>Zhong C, Yang Q, Wang W. Correlation and prediction of the thermal conductivity of amorphous polymers. *Fluid Phase Equilibria* 2001; 181: 195-202.
  - <sup>11</sup>Dashora P, Gupta G. On the temperature dependence of the thermal conductivity of linear amorphous polymers. *Polymer* 1996; 37: 231-234.
  - <sup>12</sup>Kline DE. Thermal conductivity studies of polymers. *J Polym Sci* 1961; 50: 441-450.
  - <sup>13</sup>King JA, Tucker KW, Vogt BD, Weber EH, Quan C. Electrically and thermally conductive nylon 6,6. *Polym Compos* 1999; 20: 643-654.
  - <sup>14</sup>Pierson HO. Handbook of Carbon, Graphite, Diamond and Fullerenes: Properties, Processing and Applications. New Jersey: Noyes Publications, 1993.
  - <sup>15</sup>Wypych G. Handbook of Fillers: Physical Properties of Fillers and Filled Materials. Toronto: ChemTec Publishing, 2000.
  - <sup>16</sup>Fischer JE. Carbon nanotubes: structure and properties. In: Yury Gogotsi, editor. Carbon Nanomaterials. New York: Taylor and Francis Group, 2006. pp. 51-58.
  - <sup>17</sup>Wolff S, Wang MJ. Carbon Black Science & Technology (2nd Ed). New York: Marcel Dekker, 1993.
  - <sup>18</sup> Kelly BT. Physics of Graphite. Barking (UK):Applied Science Publishers, 1981.
  - <sup>19</sup>King JA, Barton RL, Hauser RA, Keith JM. Synergistic effects of carbon fillers in electrically and

- 
- thermally conductive liquid crystal polymer based resins. *Polym Compos* 2008; 29: 421-428.
- <sup>20</sup>Causin V, Marega C, Marigo A, Ferrara G, Ferraro A. Morphological and structural characterization of polypropylene/conductive graphite nanocomposites. *Eur Polym J* 2006; 42: 3153-3161.
- <sup>21</sup>Tu H, Ye L. Thermal conductive PS/graphite composites. *Polym Adv Technol* 2009; 20: 21-27
- <sup>22</sup>Liu Z, Guo Q, Shi J, Zhai G, Liu L. Graphite blocks with high thermal conductivity derived from natural graphite flake. *Carbon* 2008; 46: 414-421.
- <sup>23</sup>Veca ML, Meziani MJ, Wang W, Wang X, Lu F, Zhang P, Lin Y, Fee R, Connell JW, Sun Y. Carbon nanosheets for polymeric nanocomposites with high thermal conductivity. *Adv Mater* 2009; 21: 2088-2092.
- <sup>24</sup>Stankovich S, Dikin DA, Dommett GHB, Kohlhaas KM, Zimney EJ, Stach EA, Piner RD, Nguyen ST, Ruoff RS. Graphene-based composite materials. *Nature* 2006; 442: 282-286
- <sup>25</sup>Ganguli S, Roy AK, Anderson DP. Improved thermal conductivity for chemically functionalized exfoliated graphite/epoxy composites. *Carbon* 2008; 46: 806-817.
- <sup>26</sup>Park SH, Hong CM, Kim S, Lee YJ. Effect of fillers shape factor on the performance of thermally conductive polymer composites. *ANTEC 2008 Plastics - Annual Technical Conference Proceedings 2008*: 39-43.
- <sup>27</sup>Mu Q, Feng S. Thermal conductivity of graphite/silicone rubber prepared by solution intercalation. *Thermochimica Acta* 2007; 462: 70-75.
- <sup>28</sup>Kalaitzidou K, Fukushima H, Drzal LT. Multifunctional polypropylene composites produced by incorporation of exfoliated graphite nanoplatelets. *Carbon* 2007; 45: 1446-1452.
- <sup>29</sup>Tibbetts GG, Lake ML, Strong KL, Rice BP. A review of the fabrication and properties of vapor-grown carbon nanofiber/polymer composites. *Compos Sci Technol* 2007; 67: 1709-1718.
- <sup>30</sup>Chen Y, Ting J. Ultra high thermal conductivity polymer composites. *Carbon* 2002; 40: 359-362.
- <sup>31</sup>Zhang X, Fujiwara S, Fujii M. Measurements of Thermal Conductivity and Electrical Conductivity of a Single Carbon Fiber. *Int J Thermophys* 2000; 21: 965-980.
- <sup>32</sup>Mohammed H A, Uttandaraman S. A review of vapor grown carbon nanofiber/polymer conductive composites. *Carbon* 2009; 47: 2-22.
- <sup>33</sup>Kuriger RJ, Alam MK, Anderson DP, Jacobsen RL. Processing and characterization of aligned vapor grown carbon fiber reinforced polypropylene. *Compos A* 2002; 33: 53-62.
- <sup>34</sup>Wong YW, Lo KL, Shin FG. Electrical and thermal properties of composite of liquid crystalline polymer filled with carbon black. *J Appl Polym Sci* 2001; 82: 1549-1555.
- <sup>35</sup>Abdel-Aal N, El-Tantawy F, Al-Hajry A, Bououdina M. Epoxy resin/plasticized carbon black composites. Part I. Electrical and thermal properties and their applications. *Polym Compos* 2008; 29: 511-517.
- <sup>36</sup>King JA, Morrison FA, Keith JM, Miller MG, Smith RC, Cruz M, Neuhalfen AM, Barton RL. Electrical conductivity and rheology of carbon-filled liquid crystal polymer composites. *J Appl Polym Sci* 2006; 101: 2680-2688.
- <sup>37</sup>Kumlutaş D, Tavmana IS, Çoban MT. Thermal conductivity of particle filled polyethylene composite materials. *Compos Sci Technol* 2003; 63: 113-117.
- <sup>38</sup>Boudenne A, Ibos L, Fois M, Majeste JC, Géhin E. Electrical and thermal behavior of polypropylene filled with copper particles. *Compos A* 2005; 36: 1545-1554.
- <sup>39</sup>Tekce HS, Kumlutas D, Tavman IH. Effect of particle shape on thermal conductivity of copper reinforced polymer composites. *J Reinf Plast Compos* 2007; 26: 113-121.
- <sup>40</sup>Mamunya YP, Davydenko VV, Pissis P, Lebedev EV. Electrical and thermal conductivity of polymers filled

---

with metal powders. *Eur Polym J* 2002; 38: 1887-1897.

- <sup>41</sup>Momentive Performance Materials. Boron nitride finds new applications in thermoplastic compounds. *Plastics Additives & Compounding* 2008; May/June: 26-31.
- <sup>42</sup>Ishida H, Rimdusit S. Very high thermal conductivity obtained by boron nitride-filled polybenzoxazine. *Thermochimica Acta* 1998; 320: 177-186.
- <sup>43</sup>Ohashi M, Kawakami S, Yokogawa Y. Spherical aluminum nitride fillers for heat-conducting plastic packages. *J Am Ceram Soc* 2005; 88: 2615-2618.
- <sup>44</sup>Yu S, Hing P, Hu X. Thermal conductivity of polystyrene–aluminum nitride composite. *Compos A* 2002; 33: 289-292.
- <sup>45</sup>Mu Q, Feng S, Diao G. Thermal conductivity of silicone rubber filled with ZnO. *Polym Compos* 2007; 28:125-130.
- <sup>46</sup>Gu J, Zhang Q, Dang J, Zhang J, Yang Z. Thermal conductivity and mechanical properties of aluminum nitride filled linear low-density polyethylene composites. *Polym Eng Sci* 2009; 49: 1030-1034.
- <sup>47</sup>Zhou W, Qi S, An Q, Zhao H, Liu N. Thermal conductivity of boron nitride reinforced polyethylene composites. *Mater Res Bull* 2007; 42: 1863–1873.
- <sup>48</sup>Tritt T M, Weston D. Measurement techniques and considerations for determining thermal conductivity of bulk materials. In : Tritt T M, editor. *Thermal Conductivity Theory, Properties, and Applications*. New York: Kluwer Academic/Plenum Publishers, 2004. pp. 187-203.
- <sup>49</sup>Rides M, Morikawa J, Halldahl L, Hay B, Lobo H, Dawson A, Allen C. Intercomparison of thermal conductivity and thermal diffusivity methods for plastics. *Polym Test* 2009; 28: 480-489.
- <sup>50</sup>Nunes dos Santos W. Thermal properties of polymers by non-steady-state techniques. *Polym Test* 2007; 26: 556-566.
- <sup>51</sup>Nunes dos Santos W, Mummery P, Wallwork A. Thermal diffusivity of polymers by the laser flash technique. *Polym Test* 2005; 24: 628-634.
- <sup>52</sup>Gaal PS, Thermitus MA, Stroe DE. Thermal conductivity measurements using the flash method. *J Therm Anal Calorim* 2004; 78: 185-189.
- <sup>53</sup>Marcus SM, Blaine RL. Thermal conductivity of polymers, glasses and ceramics by modulated DSC. *Thermochim Acta* 1994; 243: 231-239
- <sup>54</sup>Merzlyakov M, Schick C. Thermal conductivity from dynamical response of DSC. *Thermochim Acta* 2001; 377: 183-191.
- <sup>55</sup>Bigg DM. Thermal conductivity of heterophase polymer compositions. *Adv Polym Sci* 1995; 119: 1-30.
- <sup>56</sup>Zhou H, Zhang S, Yang M. The effect of heat-transfer passages on the effective thermal conductivity of high filler loading composite materials. *Compos Sci Technol* 2007; 67: 1035-1040
- <sup>57</sup>Zeng J, Fu R, Agathopoulos S, Zhang S, Song X, He H. Numerical Simulation of Thermal Conductivity of Particle Filled Epoxy Composites. *J Electron Packaging* 2009; 131: 041006.
- <sup>58</sup>Wang J, Carson JK, North MF, Cleland DJ. A new structural model of effective thermal conductivity for heterogeneous materials with cocontinuous phases. *Int J Heat Mass Trans* 2008; 51: 2389-2397
- <sup>59</sup>Okamoto S, Ishida H. A new theoretical equation for thermal conductivity of two-phase systems. *J Appl Polym Sci* 1999; 72: 1689-1697
- <sup>60</sup>Tavman IH. Thermal and mechanical properties of aluminum powder-filled high-density polyethylene composites. *J Appl Polym Sci* 1996; 62: 2161-2167.
- <sup>61</sup>Nan CW, Birringer R, Clarke DR, Gleiter H. Effective thermal conductivity of particulate composites with interfacial thermal resistance. *J Appl Phys* 1997; 10: 6692-6699.

- 
- <sup>62</sup>Every AG, Tzou Y, Hasselman DPH, Ray R. The effect of particle size on the thermal conductivity of ZnS /diamond composites. *Acta Metall Mater* 1992; 40: 123-129.
- <sup>63</sup>Dunn ML, Taya M. The effective thermal conductivity of composites with coated reinforcement and the application to imperfect interfaces. *J Appl Phys* 1993; 73: 1711-1722.
- <sup>64</sup>Lipton R, Vernescu B. Composites with imperfect interface. *Proc R Soc Lond A* 1996; 452: 329-358.
- <sup>65</sup>Torquato S, Rintoul MD. Effect of interface on the properties of composite media. *Phys Rev Lett* 1995; 75: 4067-4070.
- <sup>66</sup>Thostenson EK, Li C, Chou TW. Nanocomposites in context. *Compos Sci Technol* 2005; 65: 491-516.
- <sup>67</sup>Kumar AP, Depan D, Tomer NS, Singh RP. Nanoscale particles for polymer degradation and stabilization—Trends and future perspectives. *Prog Polym Sci* 2009; 34: 479-515.
- <sup>68</sup>Ye CM, Shentu BQ, Weng ZX. Thermal conductivity of high density polyethylene filled with graphite. *J Appl Polym Sci* 2006; 101: 3806-3810.
- <sup>69</sup>Zhi C, Bando Y, Terao T, Tang C, Kuwahara H, Golberg D. Towards thermoconductive, electrically insulating polymeric composites with boron nitride nanotubes as fillers. *Adv Funct Mater* 2009; 19: 1857-1862
- <sup>70</sup>Sui G, Jana S, Zhong WH, Fuqua MA, Ulven CA. Dielectric properties and conductivity of carbon nanofiber/semi-crystalline polymer composites. *Acta Materialia* 2008; 56: 2381-2388.
- <sup>71</sup>Elgafy A, Lafdi K. Effect of carbon nanofiber additives on thermal behavior of phase change materials. *Carbon* 2005; 43: 3067-3074.
- <sup>72</sup>Bokobza L. Multiwall carbon nanotube elastomeric composites: A review. *Polymer* 2007; 48: 4907-4920.
- <sup>73</sup>Harris PJF. Carbon nanotube composites. *Int Mater Rev* 2004; 49: 31-43.
- <sup>74</sup>Moniruzzaman M, Winey KI. Polymer nanocomposites containing carbon nanotubes. *Macromolecules* 2006; 39: 5194-5205.
- <sup>75</sup>McClory C, Chin SJ, McNally T. Polymer/carbon nanotube composites. *Aust J Chem* 2009 ; 62: 762-785.
- <sup>76</sup>Martínez-Hernández AL, Velasco-Santos C, Castaño VM. Carbon Nanotubes Composites: Processing, Grafting and Mechanical and Thermal Properties. *Curr Nanosci* 2010; 6: 12-39.
- <sup>77</sup>Safadi B, Andrews R, Grulke EA. Multiwalled carbon nanotube polymer composites: synthesis and characterization of thin films. *J Appl Polym Sci* 2002; 84: 2660-2669.
- <sup>78</sup>Paredes JI, Burghard M. Dispersions of individual single-walled carbon nanotubes of high length. *Langmuir* 2004; 20: 5149-5152.
- <sup>79</sup>Chang TE, Kisliuk A, Rhodes SM, Brittain WJ, Sokolov AP. Conductivity and mechanical properties of well-dispersed single-wall carbon nanotube/polystyrene composite. *Polymer* 2006; 47: 7740-7746.
- <sup>80</sup>Kwon JY, Kim HD. Preparation and properties of acid-treated multiwalled carbon nanotube/waterborne polyurethane nanocomposites. *J Appl Polym Sci* 2005; 96: 595-604
- <sup>81</sup>Zhu BK, Xie SH, Xu ZK, Xu YY. Preparation and properties of the polyimide/multi-walled carbon nanotubes (MWNTs) nanocomposites. *Compos Sci Technol* 2006; 66: 548-554.
- <sup>82</sup>Feng X, Liao G, He W, Sun Q, Jian X, Du J. Preparation and characterization of functionalized carbon nanotubes/poly(phthalazinone ether sulfone ketone)s composites. *Polym Compos* 2009; 30: 365-373.
- <sup>83</sup>Liu YL, Chang YH, Liang M. Poly(2,6-dimethyl-1,4-phenylene oxide) (PPO) multi-bonded carbon nanotube (CNT): Preparation and formation of PPO/CNT nanocomposites. *Polymer* 2008; 49: 5405-5409.
- <sup>84</sup>Guo H, Sreekumar TV, Liu T, Minus M, Kumar S. Structure and properties of polyacrylonitrile/single wall carbon nanotube composite films. *Polymer* 2005; 46: 3001-3005.

- 
- <sup>85</sup>Liu J, Rasheed A, Minus ML, Kumar S. Processing and Properties of Carbon Nanotube/Poly(methyl methacrylate) Composite Films. *J Appl Polym Sci* 2009; 112: 142-156.
- <sup>86</sup>Abraham TN, Ratna D, Siengchin S, Karger-Kocsis J. Rheological and thermal properties of poly(ethylene oxide)/multiwall carbon nanotube composites. *J Appl Polym Sci* 2008; 110: 2094-2101.
- <sup>87</sup>Moon SI, Jin F, Lee C, Tsutsumi S, Hyon SH. Novel carbon nanotube/poly(L-lactic acid) nanocomposites; their modulus, thermal stability and electrical conductivity. *Macromol Symp* 2005; 224: 287-295.
- <sup>88</sup>Liu YL, Chen WH, Chang YH. Preparation and properties of chitosan/carbon nanotube nanocomposites using poly(styrene sulfonic acid)-modified CNTs. *Carbohydr Polym* 2009; 76: 232-238.
- <sup>89</sup>Yang Z, Chen X, Pu Y, Zhou L, Chen C, Li W, Xu L, Yi B, Wang Y. Facile approach to obtain individual-nanotube dispersion at high loading in carbon nanotubes/polyimide composites. *Polym Adv Technol* 2007; 18: 458-462.
- <sup>90</sup>Srivastava R, Banerjee S, Jehnichen D, Voit B, Böhme F. In situ preparation of polyimide composites based on functionalized carbon nanotubes. *Macromol Mater Eng* 2009; 294: 96-102.
- <sup>91</sup>Kim DK, OH KW, Kim SH. Synthesis of polyaniline/multiwall carbon nanotube composite via inverse emulsion polymerization. *J Polym Sci B: Polym Phys* 2008; 46: 2255-2266.
- <sup>92</sup>Yu Y, Ouyang C, Gao Y, Si Z, Chen W, Wang Z, Xue GI. Synthesis and characterization of carbon nanotube/polypyrrole core-shell nanocomposites via in situ inverse microemulsion. *J Polym Sci A: Polym Chem* 2005; 43: 6105-6115
- <sup>93</sup>Sahoo NG, Jung YC, So HH, Cho JW. Polypyrrole coated carbon nanotubes: Synthesis, characterization, and enhanced electrical properties. *Synthetic Met* 2007; 157: 374-379.
- <sup>94</sup>Lee SS, Park CY, Lee DS. Properties of nanocomposites based on sulfonated poly(styrene-*b*-ethylenebutylene-*b*-styrene) and multiwalled carbon nanotubes. *Colloid Surface A: Physicochem Eng Aspects* 2008; 313-314: 239-241.
- <sup>95</sup>Xie XL, Aloys K, Zhou XP, Zeng FD. Ultrahigh molecular mass polyethylene/carbon nanotube composites Crystallization and melting properties. *J Therm Anal Calorim* 2003; 74: 317-323.
- <sup>96</sup>Jin Z, Pramoda KP, Goh SH, Xu G. Poly(vinylidene fluoride)-assisted melt-blending of multi-walled carbon nanotube/poly(methyl methacrylate) composites. *Mater Res Bull* 2002; 37: 271-278.
- <sup>97</sup>Prashantha K, Soulestin J, Lacrampe MF, Krawczak P, Dupin G, Claes M. Masterbatch-based multi-walled carbon nanotube filled polypropylene nanocomposites: Assessment of rheological and mechanical properties. *Compos Sci Technol* 2009; 69: 1756-1763.
- <sup>98</sup>Pötschke P, Bhattacharyya AR, Janke A. Melt mixing of polycarbonate with multiwalled carbon nanotubes: microscopic studies on the state of dispersion. *Eur Polym J* 2004; 40: 137-148.
- <sup>99</sup>Villmow T, Pötschke P, Pegel S, Häussler L, Kretzschmar B. Influence of twin-screw extrusion conditions on the dispersion of multi-walled carbon nanotubes in a poly(lactic acid) matrix. *Polymer* 2008; 49: 3500-3509.
- <sup>100</sup>Pegel S, Pötschke P, Petzold G, Alig I, Dudkin SM, Lellinger D. Dispersion, agglomeration, and network formation of multiwalled carbon nanotubes in polycarbonate melts. *Polymer* 2008; 49: 974-984.
- <sup>101</sup>Lee SH, Kim MW, Kim SH, Youn JR. Rheological and electrical properties of polypropylene/MWCNT composites prepared with MWCNT masterbatch chips. *Eur Polym J* 2008; 44: 1620-1630.
- <sup>102</sup>Abdel-Goad M, Pötschke P. Rheological characterization of melt processed polycarbonate-multiwalled carbon nanotube composites. *J Non-Newton Fluid* 2005; 128: 2-6.
- <sup>103</sup>Pötschke P, Fornes TD, Paul DR. Rheological behavior of multiwalled carbon nanotube/polycarbonate composites. *Polymer* 2002; 43: 3247-3255.

- 
- <sup>104</sup>Kim P, Shi L, Majumdar A, McEuen PL. Thermal transport measurements of individual multiwalled nanotubes. *Phys Rev Lett* 2001; 87: 215502.
- <sup>105</sup>Yu C, Shi L, Yao Z, Li D, Majumdar A. Thermal conductance and thermopower of an individual single-wall carbon nanotube. *Nano Lett* 2005; 5: 1842-1846.
- <sup>106</sup>Guthy C, Du F, Brand S, Winey KI, Fischer JE. Thermal conductivity of single-walled carbon nanotube/PMMA nanocomposites. *J Heat Transfer* 2007; 129: 1096-1099.
- <sup>107</sup>Choi ES, Brooks JS, Eaton DL, Al-Haik MS, Hussaini MY, Garmestani H, Li D, Dahmen K. Enhancement of thermal and electrical properties of carbon nanotube polymer composites by magnetic field processing. *J Appl Phys* 2003; 94: 6034-6039.
- <sup>108</sup>Kim HS, Chae YS, Park BH, Yoon JS, Kang M, Jin HJ. Thermal and electrical conductivity of poly(L-lactide)/multiwalled carbon nanotube nanocomposites. *Curr Appl Phys* 2008; 8: 803-806.
- <sup>109</sup>Choi SUS, Zhang ZG, Yu W, Lockwood FE, Grulke EA. Anomalous thermal conductivity enhancement in nanotube suspensions. *Appl Phys Lett* 2001; 79: 2252-2254.
- <sup>110</sup>Wen DS, Ding YL. Effective thermal conductivity of aqueous suspensions of carbon nanotubes (nanofluids). *J Thermophys Heat Transf* 2004; 18: 481-485.
- <sup>111</sup>Biercuk MJ, Llaguno MC, Radosavljevic M, Hyun JK, Johnson AT, Fischer JE. Carbon nanotube composites for thermal management. *Appl Phys Lett* 2002; 80: 2767-2769.
- <sup>112</sup>Shen Z, Bateman S, Wu DY, McMahon P, Dell'Olio M, Gotama J. The effects of carbon nanotubes on mechanical and thermal properties of woven glass fibre reinforced polyamide-6 nanocomposites. *Compos Sci Technol* 2009; 69: 239-244.
- <sup>113</sup>Nan CW, Liu G, Lin Y, Li M. Interface effect on thermal conductivity of carbon nanotube composites. *Appl Phys Lett* 2004; 85: 3549-3551.
- <sup>114</sup>Li MQ, Kinloch IA, Windle AH. Thermal and electrical conductivity of single- and multi-walled carbon nanotube-epoxy composites. *Compos Sci Technol* 2006; 66: 1285-1288.
- <sup>115</sup>Das A, Stöckelhuber KW, Jurk R, Saphiannikova M, Fritzsche J, Lorenz H, Klüppel M, Heinrich G. Modified and unmodified multiwalled carbon nanotubes in high performance solution-styrene-butadiene and butadiene rubber blends. *Polymer* 2008; 49: 5276-5283.
- <sup>116</sup>Iijima S. Helical microtubules of graphitic carbon. *Nature* 1991; 354: 56-58.
- <sup>117</sup>Ruoff RS, Lorents DC. Mechanical and thermal properties of carbon nanotubes. *Carbon* 1995; 33: 925-930.
- <sup>118</sup>Xie H, Cai A, Wang X. Thermal diffusivity and conductivity of multiwalled carbon nanotube arrays. *Phys Lett A* 2007; 369: 120-123.
- <sup>119</sup>Stroschio MA, Dutta M, Kahn D, Kim KW. Continuum model of optical phonons in a nanotube. *Superlattices and Microstructures* 2001; 29: 405-409.
- <sup>120</sup>Grujicic M, Cao G, Gersten B. Atomic-scale computations of the lattice contribution to thermal conductivity of single-walled carbon nanotubes. *Mater Sci Eng B* 2004; 107: 204-216.
- <sup>121</sup>Hepplestone SP, Ciavarella AM, Janke C, Srivastava GP. Size and temperature dependence of the specific heat capacity of carbon nanotubes. *Surface Science* 2006; 600: 3633-3636.
- <sup>122</sup>Nan CW, Shi Z, Lin Y. A simple model for thermal conductivity of carbon nanotube-based composites. *Chem Phys Lett* 2003; 375: 666-669.
- <sup>123</sup>Maultzsch J, Reich S, Thomsen C, Dobardžić E, Milošević I, Damnjanović M. Phonon dispersion of carbon nanotubes. *Solid state commun* 2002; 121: 471-474.
- <sup>124</sup>Ishii H, Kobayashi N, Hirose K. Electron-phonon coupling effect on quantum transport in carbon

- 
- nanotubes using time-dependent wave-packet approach. *Physica E* 2007; 40: 249-252.
- <sup>125</sup>Maeda T, Horie C. Phonon modes in single-wall nanotubes with a small diameter. *Physica B* 1999; 263-264: 479-481.
- <sup>126</sup>Kasuya A, Saito Y, Sasaki Y, Fukushima M, Maeda T, Horie C, Nishina Y. Size dependent characteristics of single wall carbon nanotubes. *Mater Sci Eng A* 1996; 217/218: 46-47.
- <sup>127</sup>Popov VN. Theoretical evidence for T<sup>1/2</sup> specific heat behavior in carbon nanotube systems. *Carbon* 2004; 42: 991-995.
- <sup>128</sup>Breuer O, Sundararaj U. Big returns from small fibers: a review of polymer/carbon nanotube composites. *Polym Compos* 2004; 25: 630-641.
- <sup>129</sup>Sauvajol JL, Anglaret E, Rols S, Alvarez L. Phonons in single wall carbon nanotube bundles. *Carbon* 2002; 40: 1697-1714.
- <sup>130</sup>Hone J, Whitney M, Piskoti C, Zettl A. Thermal conductivity of single-walled carbon nanotubes. *Phys Rev B* 1999; 59: R2514-R2516.
- <sup>131</sup>Hone J, Whitney M, Zettl A. Thermal conductivity of single-walled nanotubes. *Synthetic Met* 1999; 103: 2498-2499.
- <sup>132</sup>Lindsay L, Broido DA, Mingo N. Lattice thermal conductivity of single-walled carbon nanotubes: Beyond the relaxation time approximation and phonon-phonon scattering selection rules. *Phys Rev B* 2009; 80: 125407.
- <sup>133</sup>Berber S, Kwon YK, Tománek D. Unusually High Thermal Conductivity of Carbon Nanotubes. *Phys Rev Lett* 2000; 84: 4613-4616.
- <sup>134</sup>Osman MA, Srivastava D. Temperature dependence of the thermal conductivity of single-wall carbon nanotubes. *Nanotechnology* 2001; 12: 21-24.
- <sup>135</sup>Gu Y, Chen Y. Thermal conductivities of single-walled carbon nanotubes calculated from the complete phonon dispersion relations. *Phys Rev B* 2007; 76: 134110.
- <sup>136</sup>Small JP, Shi L, Kim P. Mesoscopic thermal and thermoelectric measurements of individual carbon nanotubes. *Solid State Commun* 2003; 127: 181-186.
- <sup>137</sup>Yang DJ, Wang SG, Zhang Q, Sellin PJ, Chen G. Thermal and electrical transport in multi-walled carbon nanotubes. *Phys Lett A* 2004; 329: 207-213.
- <sup>138</sup>Prasher R. Thermal boundary resistance and thermal conductivity of multiwalled carbon nanotubes. *Phys Rev B* 2008; 77: 075424.
- <sup>139</sup>Yang DJ, Zhang Q, Chen G, Yoon SF, Ahn J, Wang SG, Zhou Q, Wang Q, Li JQ. Thermal conductivity of multiwalled carbon nanotubes. *Phys Rev B* 2002; 66: 165440.
- <sup>140</sup>Yi W, Lu L, Zhang DL, Pan ZW, Xie SS. Linear specific heat of carbon nanotubes. *Phys Rev B* 1999; 59: R9015- R9018.
- <sup>141</sup>Li Q, Liu C, Wang X, Fan S. Measuring the thermal conductivity of individual carbon nanotubes by the Raman shift method. *Nanotechnology* 2009; 20: 145702.
- <sup>142</sup>Mingo N, Broido DA. Carbon nanotube ballistic thermal conductance and its limits. *Phys Rev Lett* 2005; 95: 096105.
- <sup>143</sup>Dresselhaus MS, Dresselhaus G, Jorio A, Filho AGS, Saito R. Raman spectroscopy on isolated single wall carbon nanotubes. *Carbon* 2002; 40: 2043-2061.
- <sup>144</sup>Dimitrakopoulos GP, Dravid VP, Karakostas TH, Pond RC. The defect character of carbon nanotubes and nanoparticles. *Acta Cryst* 1997; A53: 341-351.
- <sup>145</sup>Thostenson ET, Ren Z, Chou TW. Advances in the science and technology of carbon nanotubes and their



- 
- composites: a review. *Compos Sci Technol* 2001; 61: 1899-1912.
- <sup>146</sup>Tománek D, Enbody RJ. *Science and Application of Nanotubes*. New York: Kluwer Academic Publishers, 2002.
- <sup>147</sup>Odom TW, Huang JL, Kim P, Lieber CM. Atomic structure and electronic properties of single-walled carbon nanotubes. *Nature* 1998; 391: 62-64.
- <sup>148</sup>Ando T. Quantum anomalies in carbon nanotubes. *Solid State Commun* 2003; 127: 69-78.
- <sup>149</sup>Odom TW, Huang JL, Kim P, Lieber CM. Structure and electronic properties of carbon nanotubes. *J Phys Chem B* 2000; 104: 2794-2809.
- <sup>150</sup>Ando T. Carbon nanotubes and exotic transport properties. *Physica E* 2004; 22: 656-661.
- <sup>151</sup>Zhang W, Zhu Z, Wang F, Wang T, Sun L, Wang Z. Chirality dependence of the thermal conductivity of carbon nanotubes. *Nanotechnology* 2004; 15: 936-939.
- <sup>152</sup>Mensah SY, Allotey FKA, Nkrumah G, Mensah NG. High electron thermal conductivity of chiral carbon nanotubes. *Physica E* 2004; 23: 152-158.
- <sup>153</sup>Yamamoto T, Watanabe S, Watanabe D. Universal features of quantized thermal conductance of carbon nanotubes. *Phys Rev Lett* 2004; 92: 075502.
- <sup>154</sup>Ebbesen TW, Takada T. Topological and  $sp^3$  defect structures in nanotubes. *Carbon* 1995; 33: 973-978.
- <sup>155</sup>Mera Y, Harada Y, Arima S, Hata K, Shin S, Maeda K. Defects generation in single-walled carbon nanotubes induced by soft X-ray illumination. *Chem Phys Lett* 2009; 473: 138-141.
- <sup>156</sup>Xia Y, Ma Y, Xing Y, Mu Y, Tan C, Mei L. Growth and defect formation of single-wall carbon nanotubes. *Phys Rev B* 2000; 61: 11088-11092.
- <sup>157</sup>Sternberg M, Curtiss LA, Gruen DM, Kedziora G, Horner DA, Redfern PC, Zapol P. Carbon ad-dimer defects in carbon nanotubes. *Phys Rev Lett* 2006; 96: 075506.
- <sup>158</sup>Stone AJ, Wales DJ. Theoretical studies of icosahedral C<sub>60</sub> and some related species. *Chem Phys Lett* 1986; 128: 501-503.
- <sup>159</sup>Meng FY, Zhou LG, Shi SQ, Yang R. Atomic adsorption of catalyst metals on Stone-Wales defects in carbon nanotubes. *Carbon* 2002; 41: 2009-2025.
- <sup>160</sup>Liu H, Chen J, Yang H. Structural and electronic properties of defect and intramolecular junctions for single-walled carbon nanotube. *phys stat sol (b)* 2004; 241: 127-133.
- <sup>161</sup>Meunier V, Lambin Ph. Scanning tunneling microscopy and spectroscopy of topological defects in carbon nanotubes. *Carbon* 2000 ; 38 : 1729-1733.
- <sup>162</sup>Bellucci S. Carbon nanotubes: physics and applications. *phys stat sol (c)* 2005; 2: 34-47.
- <sup>163</sup>Yuan J, Liew KM. Effects of vacancy defect reconstruction on the elastic properties of carbon nanotubes. *Carbon* 2009; 47: 1526-1533.
- <sup>164</sup>Lu AJ, Pan BC. Nature of single vacancy in achiral carbon nanotubes. *Phys Rev Lett* 2004; 92: 105504.
- <sup>165</sup>Ajayan PM, Ravikumar V, Charlier JC. Surface reconstructions and dimensional changes in single-walled carbon nanotubes. *Phys Rev Lett* 1998; 81:1437.
- <sup>166</sup>Lavin JG, Subramoney S, Ruoff RS, Berber S, Tomanek D. Scrolls and nested tubes in multiwall carbon nanotubes. *Carbon* 2002; 40: 1123-1130.
- <sup>167</sup>Mawhinney DB, Naumenko V, Kuznetsova A, Yates Jr JT, Liu J, Smalley RE. Surface defect site density on single walled carbon nanotubes by titration. *Chem Phys Lett* 2000; 324: 213-216.
- <sup>168</sup>Yamamoto T, Watanabe K. Nonequilibrium Green's function approach to phonon transport in defective carbon nanotubes. *Phys Rev Lett* 2006; 96: 255503.

- 
- <sup>169</sup>Che J, Cagin T, Goddard WA. Thermal conductivity of carbon nanotubes. *Nanotechnology* 2000; 11: 65-69.
- <sup>170</sup>Osváth Z, Tapasztó L, Vértesy G, Koós AA, Horváth ZE, Gyulai J, Biró LP. STM imaging of carbon nanotube point defects. *phys stat sol (a)* 2007; 204: 1825–1829.
- <sup>171</sup>Cummings A, Osman M, Srivastava D, Menon M. Thermal conductivity of Y-junction carbon nanotubes. *Phys Rev B* 2004; 70: 115405.
- <sup>172</sup>Meng FY, Ogata S, Xu DS, Shibutani Y, Shi SQ. Thermal conductivity of an ultrathin carbon nanotube with an X-shaped junction. *Phys Rev B* 2007; 75: 205403.
- <sup>173</sup>Chang CW, Okawa D, Garcia H, Majumdar A, Zettl A. Breakdown of Fourier's law in nanotube thermal conductors. *Phys Rev Lett* 2008; 101: 075903.
- <sup>174</sup>Donadio D, Galli G. Thermal conductivity of isolated and interacting carbon nanotubes: comparing results from molecular dynamics and the Boltzmann transport equation. *Phys Rev Lett* 2007; 99: 255502.
- <sup>175</sup>Cao JX, Yan XH, Xiao Y, Ding JW. Thermal conductivity of zigzag single-walled carbon nanotubes: Role of the umklapp process. *Phys Rev B* 2004; 69: 073407.
- <sup>176</sup>Fujii M, Zhang X, Xie H, Ago H, Takahashi K, Ikuta T, Abe H, Shimizu T. Measuring the thermal conductivity of a single carbon nanotube. *Phys Rev Lett* 2005; 95: 065502.
- <sup>177</sup>Maruyama S. A molecular dynamics simulation of heat conduction in finite length SWNTs. *Physica B* 2002; 323: 193-195.
- <sup>178</sup>Alaghemandi M, Algaer R, Böhm MC, Müller-Plathe F. The thermal conductivity and thermal rectification of carbon nanotubes studied using reverse non-equilibrium molecular dynamics simulations. *Nanotechnology* 2009; 20: 115704.
- <sup>179</sup>Chiu HY, Deshpande VV, Ch Postma HW, Lau CN, Mikó C, Forró L, Bockrath M. Ballistic phonon thermal transport in multiwalled carbon nanotubes. *Phys Rev Lett* 2005; 95: 226101.
- <sup>180</sup>Khare R, Bose S. Carbon nanotube based composites-A Review. *J Miner Mater Charact Eng* 2005; 4: 31-46.
- <sup>181</sup>Hahn J, Heo SB, Suh JS. Catalyst free synthesis of high-purity carbon nanotubes by thermal plasma jet. *Carbon* 2005; 43: 2638-2641.
- <sup>182</sup>Qian W, Liu T, Wei F, Wang Z, Luo G, Yu H, Li Z. The evaluation of the gross defects of carbon nanotubes in a continuous CVD process. *Carbon* 2003; 41: 2613-2617.
- <sup>183</sup>Zhang G, Li B. Thermal conductivity of nanotubes revisited: Effects of chirality, isotope impurity, tube length, and temperature. *J Chem Phys* 2005; 123: 114714.
- <sup>184</sup>Gong Q, Li Z, Bai X, Li D, Zhao Y, Liang J. Thermal properties of aligned carbon nanotube/carbon nanocomposites. *Mater Sci Eng A* 2004; 384: 209-214.
- <sup>185</sup>Lee CJ, Park J, Yu JA. Catalyst effect on carbon nanotubes synthesized by thermal chemical vapor deposition. *Chem Phys Lett* 2002; 360: 250-255.
- <sup>186</sup>Penza M, Tagliente MA, Aversa P, Re M, Cassano G. The effect of purification of single-walled carbon nanotube bundles on the alcohol sensitivity of nanocomposite Langmuir–Blodgett films for SAW sensing applications. *Nanotechnology* 2007; 18: 185502
- <sup>187</sup>Geng J, Kong BS, Yang SB, Youn SC, Park S, Joo T, Jung HT. Effect of SWNT defects on the electron transfer properties in P3HT/SWNT hybrid materials. *Adv Funct Mater* 2008; 18: 2659-2665.
- <sup>188</sup>Bruk R, Sae-Khow O, Mitra S. Stabilizing single-walled carbon nanotubes by removal of residual metal catalysts. *Chem Phys Lett* 2008; 459: 149-152.
- <sup>189</sup>Nardelli MV, Fattebert JL, Orlikowski D, Roland C, Zhao Q, Bernholc J. Mechanical properties, defects

- 
- and electronic behavior of carbon nanotubes. *Carbon* 2000; 38: 1703-1711.
- <sup>190</sup>Tien LG, Tsai CH, Li FY, Lee MH. Influence of vacancy defect density on electrical properties of armchair single wall carbon nanotube. *Diam Relat Mater* 2008; 17: 563-566.
- <sup>191</sup>Fan YY, Kaufmann A, Mukasyan A, Varma A. Single- and multi-wall carbon nanotubes produced using the floating catalyst method: Synthesis, purification and hydrogen up-take. *Carbon* 2006; 44: 2160-2170.
- <sup>192</sup>Duesberg GS, Muster J, Byrne HJ, Roth S, Burghard M. Towards processing of carbon nanotubes for technical applications. *Appl Phys A* 1999; 69: 269-274.
- <sup>193</sup>Holzinger M, Hirsch A, Bernier P, Duesberg GS, Burghard M. A new purification method for single-wall carbon nanotubes (SWCNTs). *Appl Phys A* 2000; 70: 599-602.
- <sup>194</sup>Jeong T, Kim WY, Hahn YB. A new purification method of single-wall carbon nanotubes using H<sub>2</sub>S and O<sub>2</sub> mixture gas. *Chem phys lett* 2001; 344: 18-22.
- <sup>195</sup>Bandow S, Rao AM, Williams KA, Thess A, Smalley RE, Eklund PC. Purification of single-wall carbon nanotubes by microfiltration. *J Phys Chem B* 1997; 101: 8839-8842.
- <sup>196</sup>Zimmerman JL, Bradley RK, Huffman CB, Hauge RH, Margrave JL. Gas-phase purification of single-wall carbon nanotubes. *Chem Mater* 2000; 12: 1361-1366.
- <sup>197</sup>Thess A, Lee R, Nikolaev P, Dai H, Petit P, Robert J, Xu C, Lee YH, Kim SG, Rinzler A, Colbert DT, Scuseria G, Tomanek D, Fischer JE, Smalley R. Nanocapillarity and Chemistry in Carbon Nanotubes. *Science* 1996; 273: 483-487.
- <sup>198</sup>Monthieux M, Smith BW, Claye A, Luzzi DE. Sensitivity of singlewall carbon nanotubes to chemical processing: an electron microscopy investigation. *Carbon* 2001; 39: 1251-72.
- <sup>199</sup>Chiang IW, Brinson BE, Smalley RE, Margrave JL, Hauge RH. Purification and characterization of single-wall carbon nanotubes. *J Phys Chem B* 2001; 105: 1157-1161.
- <sup>200</sup>Zhang J, Zou H, Qing Q, Yang Y, Li Q, Liu Z, Guo X, Du Z. Effect of chemical oxidation on the structure of single-walled carbon nanotubes. *J Phys Chem B* 2003; 107: 3712-3718.
- <sup>201</sup>Hou PX, Bai S, Yang QH, Liu C, Chen HM. Multi-step purification of carbon nanotubes. *Carbon* 2002; 40: 81-85.
- <sup>202</sup>Yuan JX, Chen XH, Chen XH, Fan ZF, Yang XG, Chen ZH. An easy method for purifying multi-walled carbon nanotubes by chlorine oxidation. *Carbon* 2008; 46: 1253-1269.
- <sup>203</sup>Huang W, Wang Y, Luo G, Wei F. 99.9% purity multi-walled carbon nanotubes by vacuum high-temperature annealing. *Carbon* 2003; 41: 2585-2590.
- <sup>204</sup>Montoro LA, Rosolen JM. A multi-step treatment to effective purification of single-walled carbon nanotubes. *Carbon* 2006; 44: 3293-3301.
- <sup>205</sup>Li F, Cheng HM, Xing YT, Tan PH, Su G. Purification of single-walled carbon nanotubes synthesized by the catalytic decomposition of hydrocarbons. *Carbon* 2000; 38: 2041-2045.
- <sup>206</sup>Chattopadhyay D, Galeska I, Papadimitrakopoulos F. Complete elimination of metal catalysts from single wall carbon nanotubes. *Carbon* 2002; 40: 985-988.
- <sup>207</sup>Wiltshire JG, Li LJ, Khlobystov AN, Padbury CJ, Briggs GAD, Nicholas RJ. Magnetic separation of Fe catalyst from single-walled carbon nanotubes in an aqueous surfactant solution. *Carbon* 2005; 43: 1151-1155.
- <sup>208</sup>Strong KL, Anderson DP, Lafdi K, Kuhn JN. Purification process for single-wall carbon nanotubes. *Carbon* 2003; 41: 1477-1488.
- <sup>209</sup>Metenier K, Bonnamy S, Beguin F, Journet C, Bernier P, M Lamy de La Chapelle, Chauvet O, Lefrant S. Coalescence of single-walled carbon nanotubes and formation of multi-walled carbon nanotubes under

- 
- high-temperature treatments. *Carbon* 2002; 40: 1765-1773.
- <sup>210</sup>Yudasaka M, Ichihashi T, Kasuya D, Kataura H, Iijima S. Structure changes of single-wall carbon nanotubes and single-wall carbon nanohorns caused by heat treatment. *Carbon* 2003; 41: 1273-1280.
- <sup>211</sup>Kim YA, Muramatsu H, Hayashi T, Endo M, Terrones M, Dresselhaus MS. Thermal stability and structural changes of double-walled carbon nanotubes by heat treatment. *Chem Phys Lett* 2004; 398: 87-92.
- <sup>212</sup>Andrews A, Jacques D, Qian D, Dickey EC. Purification and structural annealing of multiwalled carbon nanotubes at graphitization temperatures. *Carbon* 2001; 39: 1681-1687.
- <sup>213</sup>Dresselhaus MS, Dresselhaus G, Saito R, Jorio A. Raman spectroscopy of carbon nanotubes. *Phys Rep* 2005; 409: 47-99.
- <sup>214</sup>Kim YA, Hayashi T, Osawa K, Dresselhaus MS, Endo M. Annealing effect on disordered multi-wall carbon nanotubes. *Chem Phys Lett* 2003; 380: 319-324.
- <sup>215</sup>Endo M, Kim YA, Fukai Y, Hayashi T, Terrones M, Terrones H, Dresselhaus MS. Comparison study of semi-crystalline and highly crystalline multiwalled carbon nanotubes. *Appl Phys Lett* 2001; 79: 1531-1533.
- <sup>216</sup>Huh Y, Yong Lee JY, Cheon J, Hong YK, Koo JY, Lee TJ, Lee CJ. Controlled growth of carbon nanotubes over cobalt nanoparticles by thermal chemical vapor deposition. *J Mater Chem* 2003; 13: 2297-2300.
- <sup>217</sup>Kuzmany H, Kukovec A, Simon F, Holzweber M, Kramberger Ch, Pichler T. Functionalization of carbon nanotubes. *Synthetic Met* 2004; 141: 113-122.
- <sup>218</sup>Wang Y, Iqbal Z, Malhotra SV. Functionalization of carbon nanotubes with amines and enzymes. *Chem Phys Lett* 2005; 402: 96-101.
- <sup>219</sup>Liu X, Chan-Park MB. Facile Way To Disperse Single-Walled Carbon Nanotubes Using a Noncovalent Method and Their Reinforcing Effect in Poly(methyl methacrylate) Composites. *J Appl Polym Sci* 2009; 114: 3414-3419.
- <sup>220</sup>Geng Y, Liu MY, Li J, Shi XM, Kim JY. Effects of surfactant treatment on mechanical and electrical properties of CNT/epoxy nanocomposites. *Compos A* 2008; 39: 1876-1883.
- <sup>221</sup>Wang C, Guo ZX, Fu S, Wu W, Zhu D. Polymers containing fullerene or carbon nanotube structures. *Prog Polym Sci* 2004; 29: 1079-1141.
- <sup>222</sup>Liu P. Modifications of carbon nanotubes with polymers. *Eur Polym J* 2005; 41: 2693-2703.
- <sup>223</sup>Ma PC, Tang BZ, Kim JK. Effect of CNT decoration with silver nanoparticles on electrical conductivity of CNT-polymer composites. *Carbon* 2008; 46: 1497-1505.
- <sup>224</sup>Bittencourt C, Felten A, Ghijsen J, Pireaux JJ, Drube W, Erni R, Tendeloo GV. Decorating carbon nanotubes with nickel nanoparticles. *Chem Phys Lett* 2007; 436: 368-372.
- <sup>225</sup>Rakov EG. Chemistry of carbon nanotubes. In: Gogotsi Y, editor. *Carbon Nanomaterials*. New York: Taylor and Francis Group, 2006. pp. 78-117.
- <sup>226</sup>Meng L, Fu C, Lu Q. Advanced technology for functionalization of carbon nanotubes. *Prog Nat Sci* 2009; 19: 801-810.
- <sup>227</sup>Hirsch A. Functionalization of Single-Walled Carbon Nanotubes. *Angew Chem Int Ed* 2002; 41: 1853-1859.
- <sup>228</sup>Chen CC, Chen CF, Chen CM, Chuang FT. Modification of multi-walled carbon nanotubes by microwave digestion method as electrocatalyst supports for direct methanol fuel cell applications. *Electr Commun* 2007; 9: 159-163.

- 
- <sup>229</sup>Čech J, Curran SA, Zhang D, Dewald JL, Avadhanula A, Kandadai M, Roth S. Functionalization of multi-walled carbon nanotubes: Direct proof of sidewall thiolation. *phys stat sol (b)* 2006; 243: 3221–3225.
- <sup>230</sup>Sun YP, Fu K, Lin Y, Huang W. Functionalized carbon nanotubes: properties and applications. *Acc Chem Res* 2002; 35: 1096-1104.
- <sup>231</sup>Shenogin S, Bodapati A, Xue L, Ozisik R, Keblinski P. Effect of chemical functionalization on thermal transport of carbon nanotube composites. *Appl Phys Lett* 2004; 85: 2229-2231.
- <sup>232</sup>Kuan HC, Ma CM, Chang WP, Yuen SM, Wu HH, Lee TM. Synthesis, thermal, mechanical and rheological properties of multiwall carbon nanotube/waterborne polyurethane nanocomposite. *Compos Sci Technol* 2005; 65: 1703-1710.
- <sup>233</sup>Lefrant S, Baibarac M, Baltog I, Mevellec JY, Godon C, Chauvet O. Functionalization of single-walled carbon nanotubes with conducting polymers evidenced by Raman and FTIR spectroscopy. *Diam Relat Mater* 2005; 14: 867-872.
- <sup>234</sup>Hayden H, Gun'ko YK, Perova TS. Chemical modification of multi-walled carbon nanotubes using a tetrazine derivative. *Chem Phys Lett* 2007; 435: 84-89.
- <sup>235</sup>Garg A, Sinnott SB. Effect of chemical functionalization on the mechanical properties of carbon nanotubes. *Chem Phys Lett* 1998; 295: 273–278
- <sup>236</sup>Liu CH, Fan SS. Effects of chemical modifications on the thermal conductivity of carbon nanotube composites. *Appl Phys Lett* 2005; 86: 123106.
- <sup>237</sup>Zhou W, Lv S, Shi W. Preparation of micelle-encapsulated single-wall and multi-wall carbon nanotubes with amphiphilic hyperbranched polymer. *Eur Polym J* 2008; 44: 587-601.
- <sup>238</sup>Zheng D, Ye J, Zhang W. Some properties of sodium dodecyl sulfate functionalized multiwalled carbon nanotubes electrode and its application on detection of dopamine in the presence of ascorbic acid. *Electroanalysis* 2008; 20: 1811-1818.
- <sup>239</sup>Yang LP, Pan CY. A non-covalent method to functionalize multi-walled carbon nanotubes using six-armed star poly(L-lactic acid) with a triphenylene core. *Macromol Chem Phys* 2008; 209: 783-793.
- <sup>240</sup>Baskarana D, Mays JW, Bratcher MS. Polymer adsorption in the grafting reactions of hydroxyl terminal polymers with multi-walled carbon nanotubes. *Polymer* 2005; 46: 5050-5057.
- <sup>241</sup>Ju S, Li ZY. Theory of thermal conductance in carbon nanotube composites. *Phys Lett A* 2006; 353: 194-197.
- <sup>242</sup>Huxtable ST, Cahill DG, Shenogin S, Xue L, Ozisik R, Barone P, Ursey M, Strano MS, Siddons G, Shim M, Keblinski P. Interfacial heat flow in carbon nanotube suspensions. *Nature Mater* 2003; 2:731-734.
- <sup>243</sup>Mamunya Ye, Boudenne A, Lebovka N, Ibos L, Candau Y, Lisunova M. Electrical and thermophysical behaviour of PVC-MWCNT nanocomposites. *Compos Sci Technol* 2008; 68: 1981-1988.
- <sup>244</sup>Deng F, Zheng Q. Interaction models for effective thermal and electric conductivity of carbon nanotube composites. *Acta Mech Solida Sinica* 2009; 22: 1-16.
- <sup>245</sup>Deng F, Zheng QS, Wang LF. Effects of anisotropy, aspect ratio, and nonstraightness of carbon nanotubes on thermal conductivity of carbon nanotube composites. *Appl Phys Lett* 2007; 90: 021914.
- <sup>246</sup>Shenogin S, Xue L, Ozisik R, Keblinski P, Cahill DG. Role of thermal boundary resistance on the heat flow in carbon-nanotube composites. *J Appl Phys* 2004; 95: 8136-8144
- <sup>247</sup>Shenogina N, Shenogin S, Xue L, Keblinski P. On the lack of thermal percolation in carbon nanotube composites. *Appl Phys Lett* 2005; 87: 133106.
- <sup>248</sup>Xu Y, Ray G, Abdel-Magid B. Thermal behavior of single-walled carbon nanotube polymer–matrix

---

composites. *Compos A* 2006; 37: 114-121.

- <sup>249</sup>McNally T, Pötschke P, Halley P, Murphy M, Martin D, Bell SEJ, Brennan GP, Bein D, Lemoine P, Quinn JP. Polyethylene multiwalled carbon nanotube composites. *Polymer* 2005; 46: 8222-8232.
- <sup>250</sup>Assouline E, Lustiger A, Barber AH, Cooper CA, Klein E, Wachtel E, Wagner HD. Nucleation ability of multiwall carbon nanotubes in polypropylene composites. *J Polym Sci B: Polym Phys* 2003; 41: 520-527.
- <sup>251</sup>Haggenmueller R, Guthy C, Lukes JR, Fischer JE, Winey KI. Single Wall Carbon Nanotube/Polyethylene Nanocomposites: Thermal and Electrical Conductivity. *Macromolecules* 2007; 40: 2417-2421.
- <sup>252</sup>Xue QZ. Model for the effective Thermal conductivity of carbon nanotube composites. *Nanotechnology* 2006; 17: 1655-1660.
- <sup>253</sup>Gao L, Zhou X, Ding Y. Effective thermal and electrical conductivity of carbon nanotube composites. *Chem Phys Lett* 2007; 434: 297-300.
- <sup>254</sup>Singh IV, Tanaka M, Endo M. Effect of interface on the thermal conductivity of carbon nanotube composites. *Int J Therm Sci* 2007; 46: 842-847.
- <sup>255</sup>Duong HM, Papavassiliou DV, Mullen KJ, Maruyama S. Computational modeling of the thermal conductivity of single-walled carbon nanotube-polymer composites. *Nanotechnology* 2008; 19: 065702.
- <sup>256</sup>Clancy TC, Gates TS. Modeling of interfacial modification effects on thermal conductivity of carbon nanotube composites. *Polymer* 2006; 47: 5990-5996.
- <sup>257</sup>Chen T, Weng GJ, Liu WC. Effect of Kapitza contact and consideration of tube-end transport on the effective conductivity in nanotube-based composites. *J Appl Phys* 2005; 97: 104312.
- <sup>258</sup>Yang K, Gu M, Guo Y, Pan X, Mu G. Effects of carbon nanotube functionalization on the mechanical and thermal properties of epoxy composites. *Carbon* 2009; 47: 1723-1737.
- <sup>259</sup>Gojny FH, Wichmann MHG, Fiedler B, Kinloch IA, Bauhofer W, Windle AH, Schulte K. Evaluation and identification of electrical and thermal conduction mechanisms in carbon nanotube/epoxy composites. *Polymer* 2006; 47: 2036-2045.
- <sup>260</sup>Bagchi B, Nomura S. On the effective thermal conductivity of carbon nano tube reinforced polymer composites. *Compos Sci Technol* 2006; 66: 1703-1712.
- <sup>261</sup>Foygel M, Morris RD, Anez D, French S, Sobolev VL. Theoretical and computational studies of carbon nanotube composites and suspensions: Electrical and thermal conductivity. *Phys Rev B* 2005; 71: 104201.
- <sup>262</sup>Bonnet P, Sireude D, Garnier B, Chauvet O. Thermal properties and percolation in carbon nanotube-polymer composites. *Appl Phys Lett* 2007; 91: 201910.
- <sup>263</sup>Kumar S, Alam MA, Murthy JY. Effect of percolation on thermal transport in nanotube composites. *Appl Phys Lett* 2007; 90: 104105.
- <sup>264</sup>Hone J, Llaguno MC, Nemes NM, Johnson AT, Fischer JE, Walters DA, Casavant MJ, Schmidt J, Smalley RE. Electrical and thermal transport properties of magnetically aligned single wall carbon nanotube films. *Appl Phys Lett* 2000; 77: 666-668.
- <sup>265</sup>Gonnet P, Liang Z, Choi ES, Kadambala RS, Zhang C, Brooks JS, Wang B, Kramer L. Thermal conductivity of magnetically aligned carbon nanotube buckypapers and nanocomposites. *Curr Appl Phys* 2006; 6: 119-122.
- <sup>266</sup>Zhong H, Lukes JR. Interfacial thermal resistance between carbon nanotubes: Molecular dynamic simulations and analytical thermal modeling. *Phys Rev B* 2006; 74: 125403.
- <sup>267</sup>Pradhan NR, Duan H, Liang J, Iannacchione GS. The specific heat and effective thermal conductivity of composites containing single-wall and multi-wall carbon nanotubes. *Nanotechnology* 2009; 20: 245705.
- <sup>268</sup>Yu A, Ramesh P, Sun X, Bekyarova E, Itkis ME, Haddon RC. Enhanced thermal conductivity in a hybrid

- 
- graphite nanoplatelet-carbon nanotube filler for epoxy composites. *Adv Mater* 2008; 20: 4740-4744.
- <sup>269</sup> King JA, Johnson BA, Via MD, Ciarkowski CJ. Effects of carbon fillers in thermally conductive polypropylene based resins. *Polym Compos* 2010; 31: 497-506.
- <sup>270</sup> King JA, Gaxiola DL, Johnson BA, Keith JM. Thermal conductivity of carbon-filled polypropylene-based resins. *J Compos Mater* 2009; 44: 839-855.
- <sup>271</sup> Endo M, Hayashi T, Kim YA. Large-scale production of carbon nanotubes and their applications. *Pure Appl Chem* 2006; 78: 1703-1713.
- <sup>272</sup> Riggs JE, Guo Z, Carroll DL, Sun YP. Strong Luminescence of Solubilized Carbon Nanotubes. *J Am Chem Soc* 2000; 122: 5879-5880.
- <sup>273</sup> Ke G, Guan WC, Tang CY, Hu Z, Guan WJ, Zeng DL, Deng F. Covalent modification of multiwalled carbon nanotubes with a low molecular weight chitosan. *Chinese Chem Lett* 2007; 18: 361-364.
- <sup>274</sup> Xie XL, Mai YW, Zhou XP. Dispersion and alignment of carbon nanotubes in polymer matrix: A review. *Mat Sci Eng R* 2005; 49: 89-112.
- <sup>275</sup> Narh KW, Jallo L, Rhee KY. The effect of carbon nanotube agglomeration on the thermal and mechanical properties of polyethylene oxide. *Polym Compos* 2008; 29: 809-817.
- <sup>276</sup> Fujigaya T, Fukumaru T, Nakashima N. Evaluation of dispersion state and thermal conductivity measurement of carbon nanotubes/UV-curable resin nanocomposites. *Synthetic Met* 2009; 159: 827-830.
- <sup>277</sup> Thostenson ET, Chou TW. Processing-structure-multi-functional property relationship in carbon nanotube/epoxy composites. *Carbon* 2006; 44: 3022-3029.
- <sup>278</sup> Park C, Ounaies Z, Watson KA, Crooks RE, Jr JM, Lowther SE, Connell JW, Siochi EJ, Harrison JS, St Clair TL. Dispersion of single wall carbon nanotubes by in situ polymerization under sonication. *Chem Phys Lett* 2002; 364: 303-308.
- <sup>279</sup> Song YS, Youn JR. Influence of dispersion states of carbon nanotubes on physical properties of epoxy nanocomposites. *Carbon* 2005; 43: 1378-1385.
- <sup>280</sup> Zhou Z, Wang S, Lu L, Zhang Y, Zhang Y. Isothermal crystallization kinetics of polypropylene with silane functionalized multi-walled carbon nanotubes. *J Polym Sci B: Polym Phys* 2007; 45: 1616-1624.
- <sup>281</sup> Shen J, Hu Y, Qin C, Li C, Ye M. Dispersion behavior of single-walled carbon nanotubes by grafting of amphiphilic block copolymer. *Compos A* 2008; 39: 1679-1683.
- <sup>282</sup> Špitalský Z, Matějka L, Šlouf M, Konyushenko EN, Kovářová J, Zemek J, Kotek J. Modification of carbon nanotubes and its effect on properties of carbon nanotube/epoxy nanocomposites. *Polym Compos* 2009; 30: 1378-1387.
- <sup>283</sup> Hong WT, Tai NH. Investigations on the thermal conductivity of composites reinforced with carbon nanotubes. *Diam Relat Mater* 2008; 17: 1577-1581.
- <sup>284</sup> Andrews R, Jacques D, Minot M, Rantell T. Fabrication of carbon multiwall nanotube/polymer composites by shear mixing. *Macromol Mater Eng* 2002; 287: 395-403.
- <sup>285</sup> Hong J, Lee J, Hong CK, Shim SE. Effect of dispersion state of carbon nanotube on the thermal conductivity of poly(dimethyl siloxane) composites. *Curr Appl Phys* 2010; 10: 359-363.
- <sup>286</sup> Song YS, Youn JR. Evaluation of effective thermal conductivity for carbon nanotube/polymer composites using control volume finite element method. *Carbon* 2006; 44: 710-717.
- <sup>287</sup> Xie H, Chen L. Adjustable thermal conductivity in carbon nanotube nanofluids. *Phys Lett A* 2009; 373: 1861-1864
- <sup>288</sup> Pierard N, Fonseca A, Colomer JF, Bossuot C, Benoit JM, Van Tendeloo G, Pirard JP, Nagy JB. Ball milling effect on the structure of single-wall carbon nanotubes. *Carbon* 2004; 42: 1691-1697.

- 
- <sup>289</sup>Wang S, Liang R, Wang B, Zhang C. Dispersion and thermal conductivity of carbon nanotube composites. *Carbon* 2009; 47: 53-57.
- <sup>290</sup>Cai D, Song M. Latex technology as a simple route to improve the thermal conductivity of a carbon nanotube/polymer composite. *Carbon* 2008; 46: 2107-2112.
- <sup>291</sup>Yu J, Lu K, Sourty E, Grossiord N, Koning CE, Loos J. Characterization of conductive multiwall carbon nanotube/polystyrene composites prepared by latex technology. *Carbon* 2007; 45: 2897-2903.
- <sup>292</sup>Vandervorst P, Lei CH, Lin Y, Dupont O, Dalton AB, Sun YP, Keddie JL. The fine dispersion of functionalized carbon nanotubes in acrylic latex coatings. *Prog Org Coat* 2006; 57: 91-97.
- <sup>293</sup>Lisunova MO, Lebovka NI, Melezhyk OV, Boiko YP. Stability of the aqueous suspensions of nanotubes in the presence of nonionic surfactant. *J Colloid Interf Sci* 2006; 299: 740-746.
- <sup>294</sup>Sastry NNV, Bhunia A, Sundararajan T, Das SK. Predicting the effective thermal conductivity of carbon nanotube based nanofluids. *Nanotechnology* 2008; 19: 055704.
- <sup>295</sup>Chen L, Xie H, Li Y, Yu W. Applications of cationic gemini surfactant in preparing multi-walled carbon nanotube contained nanofluids. *Colloid Surface A: Physicochem Eng Aspects* 2008; 330: 176-179.
- <sup>296</sup>Grunlan JC, Kim YS, Ziaee S, Wei X, Abdel-Magid B, Tao K. Thermal and mechanical behavior of carbon-nanotube-filled latex. *Macromol Mater Eng* 2006; 291: 1035-1043.
- <sup>297</sup>Cai D, Song M. Water-based polyurethane filled with multi-walled carbon nanotubes prepared by a colloidal-physics method. *Macromol Chem Phys* 2007; 208: 1183-1189.
- <sup>298</sup>Koo J, Kang Y, Kleinstreuer C. A nonlinear effective thermal conductivity model for carbon nanotube and nanofiber suspensions. *Nanotechnology* 2008; 19: 375705.
- <sup>299</sup>Chen G, Lu J, Wu D. The electrical properties of graphite nanosheet filled immiscible polymer blends. *Mater Chem Phys* 2007; 104: 240-243.
- <sup>300</sup>Al-Saleh MH, Sundararaj U. Nanostructured carbon black filled polypropylene/polystyrene blends containing styrene-butadiene-styrene copolymer: Influence of morphology on electrical resistivity. *Eur Polym J* 2008; 44: 1931-1939.
- <sup>301</sup>Bose S, Bhattacharyya AR, Kulkarni AR, Pöschke P. Electrical, rheological and morphological studies in co-continuous blends of polyamide 6 and acrylonitrile-butadiene-styrene with multiwall carbon nanotubes prepared by melt blending. *Compos Sci Technol* 2009; 69: 365-372.
- <sup>302</sup>Pötschke P, Paul DR. Formation of Co-continuous Structures in Melt-Mixed Immiscible Polymer Blends. *J Macromol Sci C Polym Reviews* 2003; 43: 87-141.
- <sup>303</sup>Nazarenko S, Dennison M, Schuman T, Stepanov EV, Hiltner A, Baer E. Creating layers of concentrated inorganic particles by interdiffusion of polyethylenes in microlayers. *J Appl Polym Sci* 1999; 73: 2877-2885.
- <sup>304</sup>Pötschke P, Bhattacharyya AR, Janke A. Morphology and electrical resistivity of melt mixed blends of polyethylene and carbon nanotube filled polycarbonate. *Polymer* 2003; 44: 8061-8069.
- <sup>305</sup>Pötschke P, Bhattacharyya AR, Janke A. Carbon nanotube-filled polycarbonate composites produced by melt mixing and their use in blends with polyethylene. *Carbon* 2004; 42: 965-969.
- <sup>306</sup>Meincke O, Kaempfer D, Weickmann H, Friedrich C, Vathauer M, Warth H. Mechanical properties and electrical conductivity of carbon-nanotube filled polyamide-6 and its blends with acrylonitrile/butadiene/styrene. *Polymer* 2004; 45: 739-748.
- <sup>307</sup>Droval G, Feller JF, Salagnac P, Glouannec P. Conductive polymer composites with double percolated architecture of carbon nanoparticles and ceramic microparticles for high heat dissipation and sharp PTC switching. *Smart Mater Struct* 2008; 17: 025011.



- 
- <sup>308</sup>Droval G, Feller JF, Salagnac P, Glouannec P. Rheological properties of conductive polymer composite (CPC) filled with double percolated network of carbon nanoparticles and boron nitride powder. *e-Polymers* 2009, no. 023.
- <sup>309</sup>Ji L, Stevens MM, Zhu Y, Gong Q, Wu J, Liang J. Preparation and properties of multi-walled carbon nanotube/carbon/polystyrene composites. *Carbon* 2009; 47: 2733-2741.
- <sup>310</sup>Minus ML, Chae HG, Kumar S. Interfacial crystallization in gel-spun poly(vinyl alcohol)/single-wall carbon nanotube composite fibers. *Macromol Chem Phys* 2009; 210: 1799-1808.
- <sup>311</sup>Jose MV, Dean D, Tyner J, Price G, Nyairo E. Polypropylene/carbon nanotube nanocomposite fibers: process-morphology-property relationships. *J Appl Polym Sci* 2007; 103: 3844-3850.
- <sup>312</sup>Perrot C, Piccione PM, Zakri C, Gaillard P, Poulin P. Influence of the spinning conditions on the structure and properties of polyamide 12/carbon nanotube composite fibers. *J Appl Polym Sci* 2009; 114: 3515-3523.
- <sup>313</sup>Ghose S, Watson KA, Working DC, Connell JW, Smith Jr JG, Sun YP. Thermal conductivity of ethylene vinyl acetate copolymer/nanofiller blends. *Compos Sci Technol* 2008; 68: 1843-1853.
- <sup>314</sup>Kim YA, Hayashi T, Endo M, Gotoh Y, Wada N, Seiyama J. Fabrication of aligned carbon nanotube-filled rubber composite. *Scripta Materialia* 2006; 54: 31-35.
- <sup>315</sup>Shaikh S, Li L, Lafdi K, Huie J. Thermal conductivity of an aligned carbon nanotube array. *Carbon* 2007; 45: 2608-2613.
- <sup>316</sup>Sihn S, Ganguli S, Roy AK, Qu L, Dai L. Enhancement of through-thickness thermal conductivity in adhesively bonded joints using aligned carbon nanotubes. *Compos Sci Technol* 2008; 68: 658-665.
- <sup>317</sup>Huang H, Liu C, Wu Y, Fan S. Aligned carbon nanotube composite films for thermal management. *Adv Mater* 2005; 17: 1652-1656.
- <sup>318</sup>Borca-Tasciuc T, Mazumder M, Son Y, Pal SK, Schadler LS, Ajayan PM. Anisotropic thermal diffusivity characterization of aligned carbon nanotube-polymer composites. *J Nanosci Nanotechnol* 2007; 7: 1581-1588.
- <sup>319</sup>Cola BA, Xu J, Fisher TS. Contact mechanics and thermal conductance of carbon nanotube array interfaces. *Int J Heat Mass Tran* 2009; 52: 3490-3503.
- <sup>320</sup>Lin W, Moon KS, Wong CP. A combined process of in situ functionalisation and microwave treatment to achieve ultrasmall thermal expansion of aligned carbon nanotube-polymer nanocomposites: toward applications as thermal interface materials. *Adv Mater* 2009; 21: 2421-2424.
- <sup>321</sup>Wang C, Chen T, Chang S, Cheng S, Chin T. Strong carbon-nanotube-polymer bonding by microwave irradiation. *Adv Funct Mater* 2007; 17: 1979-1983.
- <sup>322</sup>Garmestani H, Al-Haik MS, Dahmen K, Tannenbaum R, Li D, Sablin SS, Hussaini MY. Polymer-mediated alignment of carbon nanotubes under high magnetic fields. *Adv Mater* 2003; 15: 1918-1921.
- <sup>323</sup>Park C, Wilkinson J, Banda S, Ounaies Z, Wise KE, Sauti G, Lillehei PT, Harrison JS. Aligned single-wall carbon nanotube polymer composites using an electric field. *J Polym Sci B: Polym Phys* 2006; 44: 1751-1762.
- <sup>324</sup>Duan J, Kim C, Jiang P. Effect of external electric field on the microstructures and properties of carbon nanotubes/thermosets nanocomposites. *Polym Compos* 2010; 31: 347-358.
- <sup>325</sup>Dai J, Wang Q, Li W, Wei Z, Xu G. Properties of well aligned SWNT modified poly (methyl methacrylate) nanocomposites. *Mater Lett* 2007; 61: 27-29.
- <sup>326</sup>Hong H, Wright B, Wensel J, Jin S, Ye XR, Roy W. Enhanced thermal conductivity by the magnetic field

---

in heat transfer nanofluids containing carbon nanotube. *Synthetic Metals* 2007; 157: 437-440.

- <sup>327</sup>Bhattacharyya AR, Sreekumar TV, Liu T, Kumar S, Ericson LM, Hauge RH, Smalley RE. Crystallization and orientation studies in polypropylene/single wall carbon nanotube composite. *Polymer* 2003; 44: 2373-2377
- <sup>328</sup>Sandler JKW, Pegel S, Cadek M, Gojny F, Es MV, Lohmar J, Blau WJ, Schulte K, Windle AH, Shaffer MSP. A comparative study of melt spun polyamide-12 fibres reinforced with carbon nanotubes and nanofibres. *Polymer* 2004; 45: 2001-2015.
- <sup>329</sup>Sahoo NG, Cheng HKF, Cai J, Li L, Chana SH, Zhao J, Yu S. Improvement of mechanical and thermal properties of carbon nanotube composites through nanotube functionalization and processing methods. *Mater Chem Phys* 2009; 117: 313-320.
- <sup>330</sup>Nam YW, Kim WN, Cho YH, Chae DW, Kim GH, Hong SP, Hwang SS, Hong SM. Morphology and physical properties of binary blend based on PVDF and multi-walled carbon nanotube. *Macromol Symp* 2007; 249-250: 478-484.
- <sup>331</sup>Li L, Li B, Hood M A, Li C Y. Carbon nanotube induced polymer crystallization: The formation of nanohybrid shish - kebabs. *Polymer* 2009; 50: 953-965.
- <sup>332</sup>Choy CL, Wong YW, Yang GW, Kanamoto T. Elastic modulus and thermal conductivity of ultradrawn polyethylene. *J Polym Sci B: Polym Phys* 1999; 37: 3359-3367.
- <sup>333</sup>Liao SH, Yen CY, Weng CC, Lin YF, Ma CM, Yang CH, Tsai MC, Yen MY, Hsiao MC, Lee SJ, Xie XF, Hsiao YH. Preparation and properties of carbon nanotube/polypropylene nanocomposite bipolar plates for polymer electrolyte membrane fuel cells. *J Power Sources* 2008; 185: 1225-1232.

---

## Figure Captions

- Fig.1 (a) Schematic diagram showing how a hexagonal sheet of graphite is “rolled” to form a CNT, (b) an armchair and (c) a ziz-zag nanotube. Reprinted with permission from Ref. [145] (Thostenson ET et al. *Compos Sci Technol* 2001; 61: 1899-1912, Copyright (2001) Elsevier).
- Fig.2 Thermal conductivities of (20, 0)-open squares, (11, 11)-solid circles, and (10, 13)-open triangles, nanotubes. Reprinted with permission from Ref. [151] (Zhang W et al. *Nanotechnology* 2004; 15: 936-939, Copyright (2004) IOP Publishing Ltd).
- Fig.3 The temperature dependence of the ratio  $\kappa_{vac}/SW/\kappa_p$  for (6,6), (8,8) and (10,10) CNTs with the vacancy (solid) or SW defect (dash). Reprinted with permission from Ref. [168] (Yamamoto T, Watanabe K. *Phys Rev Lett* 2006; 96: 255503, Copyright (2006) the American Physical Society).
- Fig.4 Thermal conductivity of (n, 0) SWCNTs (n=6~14) at 300K. Reprinted with permission from Ref. [175] (Cao JX et al. *Phys Rev B* 2004; 69: 073407, Copyright (2004) the American Physical Society).
- Fig.5 Dependence of thermal conductivity on length of CNTs for 300K. Reprinted with

---

permission from Ref. [177] (Maruyama S. *Physica B* 2002; 323: 193-195, Copyright (2002) Elsevier).

Fig.6 Thermal conductivity versus tube length of (5, 5), (10, 0), (7, 7), (10, 10), (17, 0), (15, 15), and (20, 20) SWCNTs at 300 K in a double-logarithmic scale. Reprinted with permission from Ref. [178] (Alaghemandi M et al. *Nanotechnology* 2009; 20: 115704, Copyright (2009) IOP Publishing Ltd).

Fig.7 Raman spectra of pristine (upper) and annealed (lower) MWCNTs. Reprinted with permission from Ref. [214] (Kim YA et al. *Chem Phys Lett* 2003; 380: 319-324, Copyright (2003) Elsevier).

Fig.8 CNT thermal conductivity vs. fraction of functionalized carbon atoms. Reprinted with permission from Ref. [231] (Shenogin S et al. *Appl Phys Lett* 2004; 85(12): 2229-2231, Copyright (2004) American Institute of Physics).

Fig.9 Overview of literature data on thermal conductivity enhancement compared with reference matrix, vs. CNT loading. Attention is driven on logarithmic scale on Y axis, enlarging differences between low thermal conductivity values.

Fig.10 HRTEM of a PE/MWCNT nanocomposite. The MWCNT is protruding from the side of

---

the extrudate and coated with PE. Reprinted with permission from Ref. [249] (McNally T et al. Polymer 2005; 46: 8222-8232, Copyright (2005) Elsevier).

Fig.11 Effect of the interface thermal resistance on the thermal conductivity enhancement in CNT composites.  $K_e$ =effective thermal conductivity,  $K_m$ = thermal conductivity of the matrix,  $R_k$ = interfacial thermal resistance. Reprinted with permission from Ref. [113] (Nan CW et al. Appl Phys Lett 2004; 85: 3549-3551, Copyright (2004) American Institute of Physics).

Fig.12 Normalised thermal conductivity vs CNT volume fraction, with perfect interface ( $R_k=0$ ) or with interfacial thermal resistance ( $R_k\neq 0$ ).  $K_e$ =effective thermal conductivity,  $K_m$ = thermal conductivity of the matrix. Reprinted with permission from Ref. [113] (Nan CW et al. Appl Phys Lett 2004; 85: 3549-3551, Copyright (2004) American Institute of Physics).

Fig.13 The interfacial thermal resistance,  $R_k$ , vs. the grafting density, for several end-grafted chain lengths. Reprinted with permission from Ref. [256] (Clancy TC, Gates TS. Polymer 2006; 47: 5990-5996, Copyright (2006) Elsevier).

Fig.14 Interfacial resistance in units of equivalent matrix thickness vs fraction of tube carbon atoms with covalently attached octane molecules. Reprinted with permission from Ref. [231] (Shenogin S et al. Appl Phys Lett 2004; 85(12): 2229-2231, Copyright (2004) American Institute of Physics).

- 
- Fig.15 Comparison between percolation model (solid line) and effective medium model (dotted line). Reprinted with permission from Ref. [251] (Haggenmueller R et al. *Macromolecules* 2007; 40: 2417-2421, Copyright (2007) American Chemical Society).
- Fig.16 Thermal conductivity of the “thick” annealed sample of aligned SWCNT, measured in the parallel direction. Effective thickness of 5  $\mu\text{m}$ . Reprinted with permission from Ref. [264] (Hone J et al. *Appl Phys Lett* 2000; 77(5): 666-668, Copyright (2000) American Institute of Physics).
- Fig.17 Thermal conductivities of pristine buckypapers and the corresponding composites for samples with different heat flow and alignment direction. Reprinted with permission from Ref. [265] (Gonnet P et al. *Curr Appl Phys* 2006; 6: 119-1224, Copyright (2005) Elsevier).
- Fig.18 2D-scenario for CNT-CNT contact and temperature profile along the contact. The temperature drop at the interface is the effect of thermal contact resistance. Reprinted with permission from Ref. [266] (Zhong H, Lukes JR. *Phys Rev B* 2006; 74: 125403, Copyright (2006) the American Physical Society).
- Fig.19 Thermal conductivity of nanocomposites with respect to CNT loading. Reprinted with permission from Ref. [279] (Song YS, Youn JR. *Carbon* 2005; 43: 1378-1385, Copyright

---

(2005) Elsevier).

Fig.20 TEM micrographs of 1 wt% CNTs in epoxy nanocomposites (a) as-received MWCNT, (b) MWCNT-COOH. Reprinted with permission from Ref. [282] (Špitalský Z et al. Polym Compos 2009; 30: 1378-1387, Copyright (2008) Society of Plastics Engineers).

Fig.21 Thermal conductivity of PMMA-based composites reinforced with (a) unpurified CNTs, (b) purified CNTs. Reprinted with permission from Ref. [283] (Hong WT, Tai NH. Diam Relat Mater 2008; 17: 1577-1581, Copyright (2008) Elsevier).

Fig.22 MWCNT dispersion and tube length vs mixing energy in polystyrene. Reprinted with permission from Ref. [284] (Andrews R et al. Macromol Mater Eng 2002; 287: 395-403, Copyright (2002) WILEY-VCH).

Fig.23 Thermal conductivity of 0.5wt% nanotubes integrated composites. Reprinted with permission from Ref. [289] (Wang S et al. Carbon 2009; 47: 53-57, Copyright (2008) Elsevier).

Fig.24 (a) SEM image of aligned CNTs on quartz substrate. (b) Higher magnification image showing the size and the orientation of CNTs. Reprinted with permission from Ref. [315] (Shaikh S et al. Carbon 2007; 45: 2608-2613, Copyright (2007) Elsevier).

---

Fig.25 The enhanced values of thermal conductivity vs. weight fractions of the CNTs. The inset is a comparison of measured thermal conductivity values of different samples. Reprinted with permission from Ref. [317] (Huang H et al. *Adv Mater* 2005; 17(13): 1652–1656, Copyright (2005) WILEY-VCH).

Fig.26 Thermal conductivities of TCOM, MCOM and epoxy resin. Reprinted with permission from Ref. [320] (Lin W et al. *Adv Mater* 2009; 21: 2421-2424, Copyright (2009) WILEY-VCH).

Fig.27 Thermal conductivity of various SWCNT/HDPE nanocomposites as a function of the PE chains orientation (fc): (tilted  $\Delta$ ) isotropic HDPE, ( $\blacktriangledown$ ) nominally isotropic 0.6 vol.% SWCNT/HDPE, ( $\Delta$ ) aligned HDPE fibres, ( $\bullet$ ) aligned 0.6 vol.% SWCNT/HDPE, and ( $\blacksquare$ ) aligned 1.2 vol.% SWCNT/HDPE. Thermal conductivities were measured along the alignment direction. Reprinted with permission from Ref. [251] (Haggenmueller R et al. *Macromolecules* 2007; 40: 2417-2421, Copyright (2007) American Chemical Society).



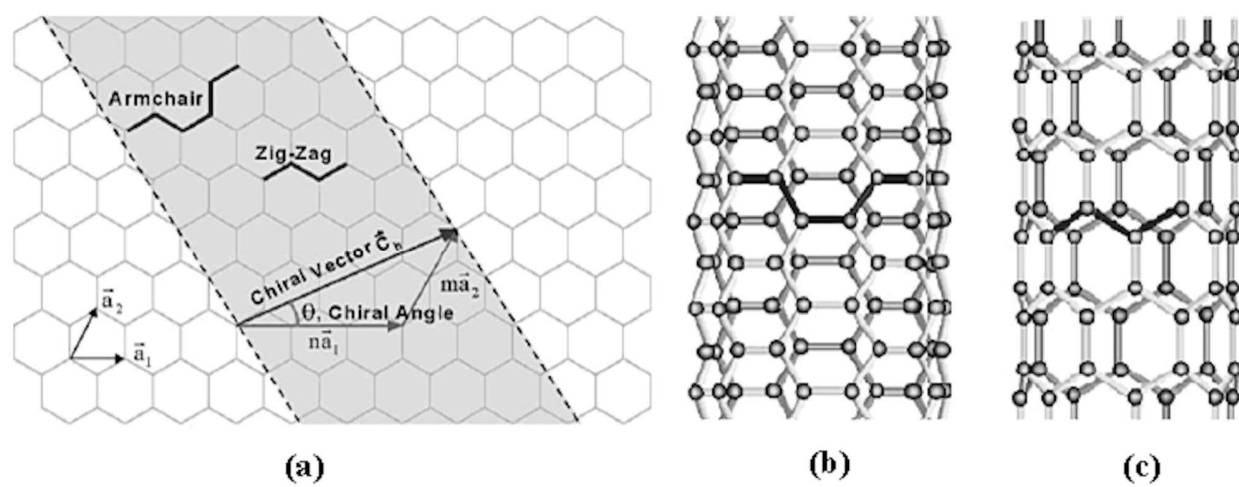


Fig.1

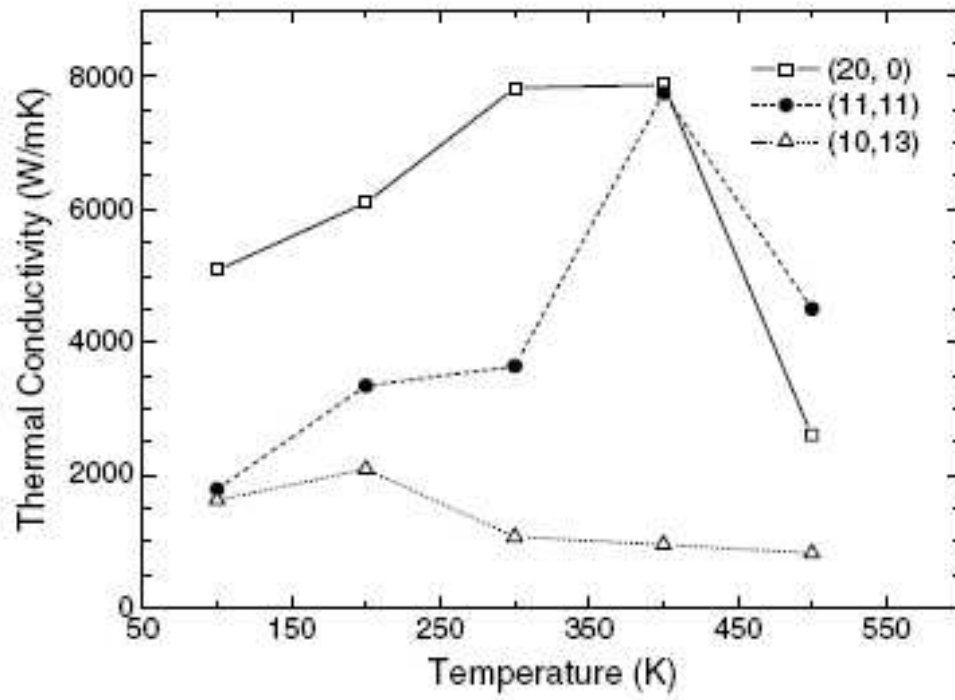


Fig.2

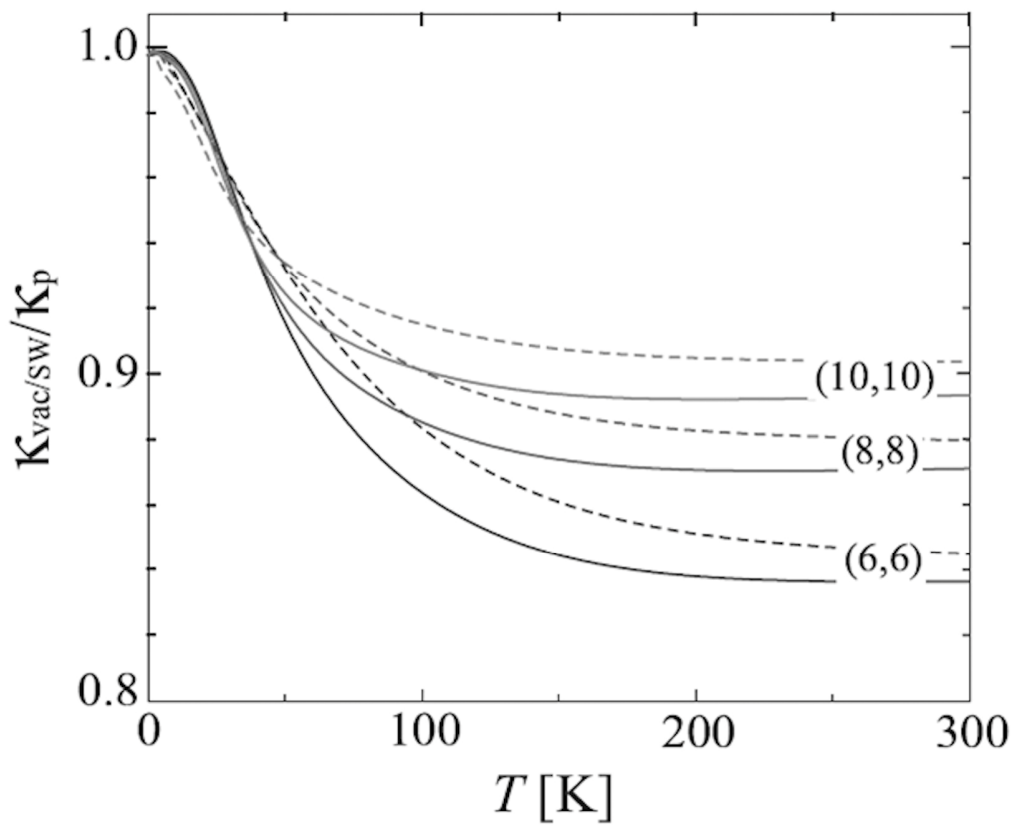


Fig.3

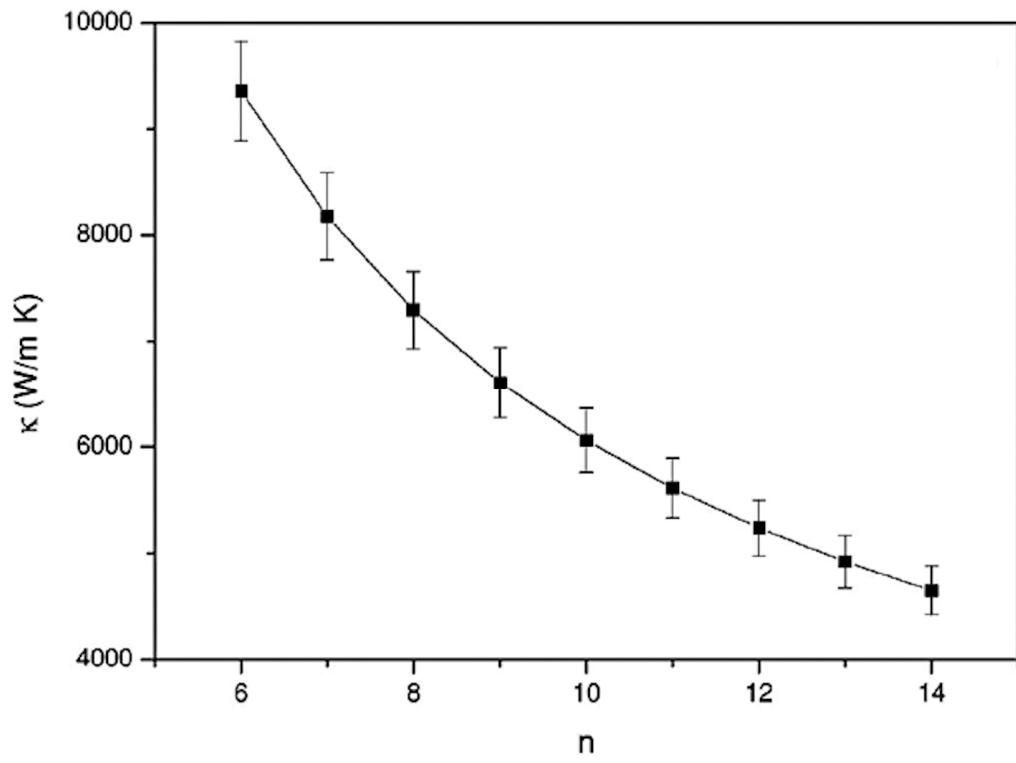


Fig.4

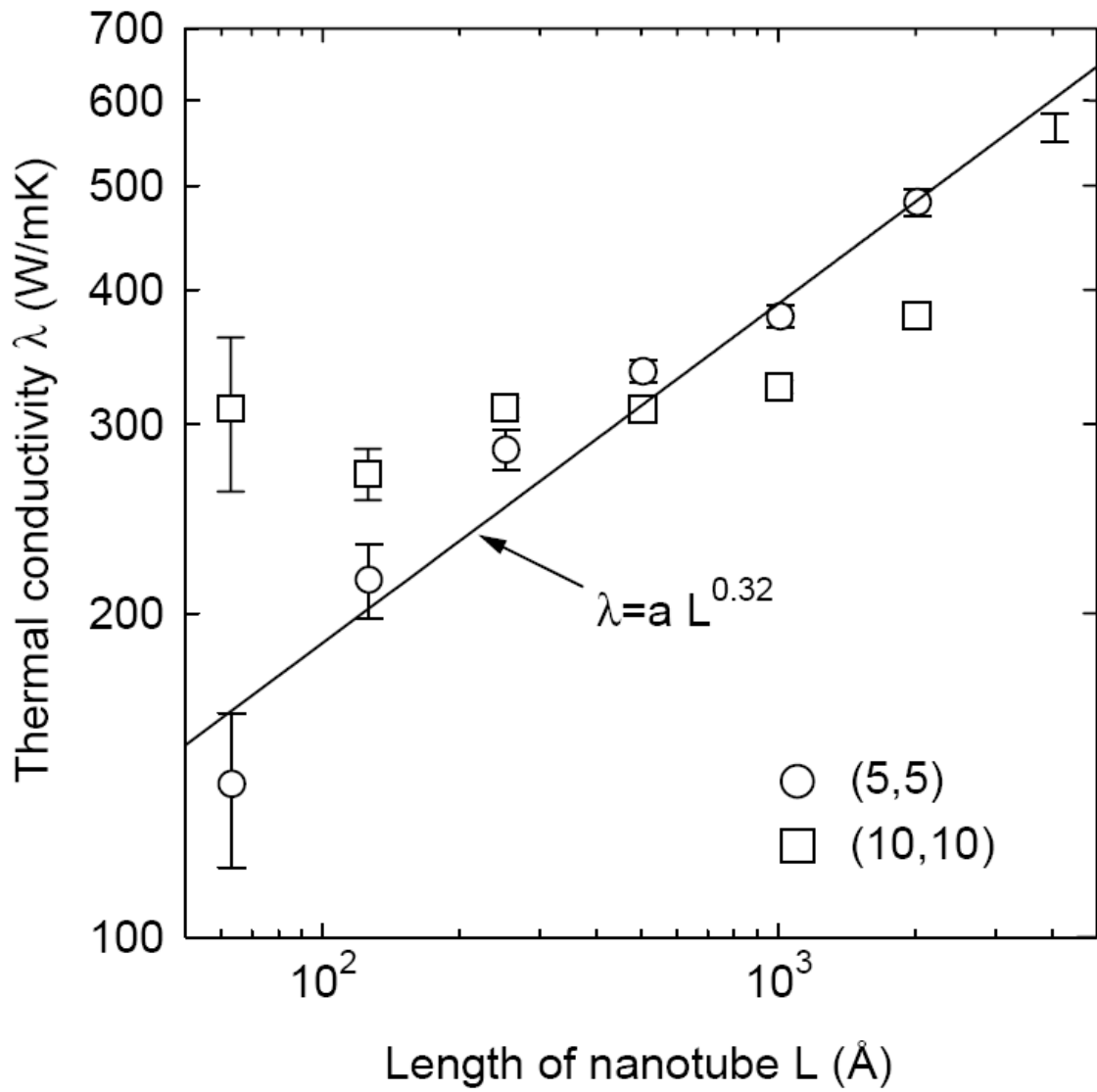


Fig.5

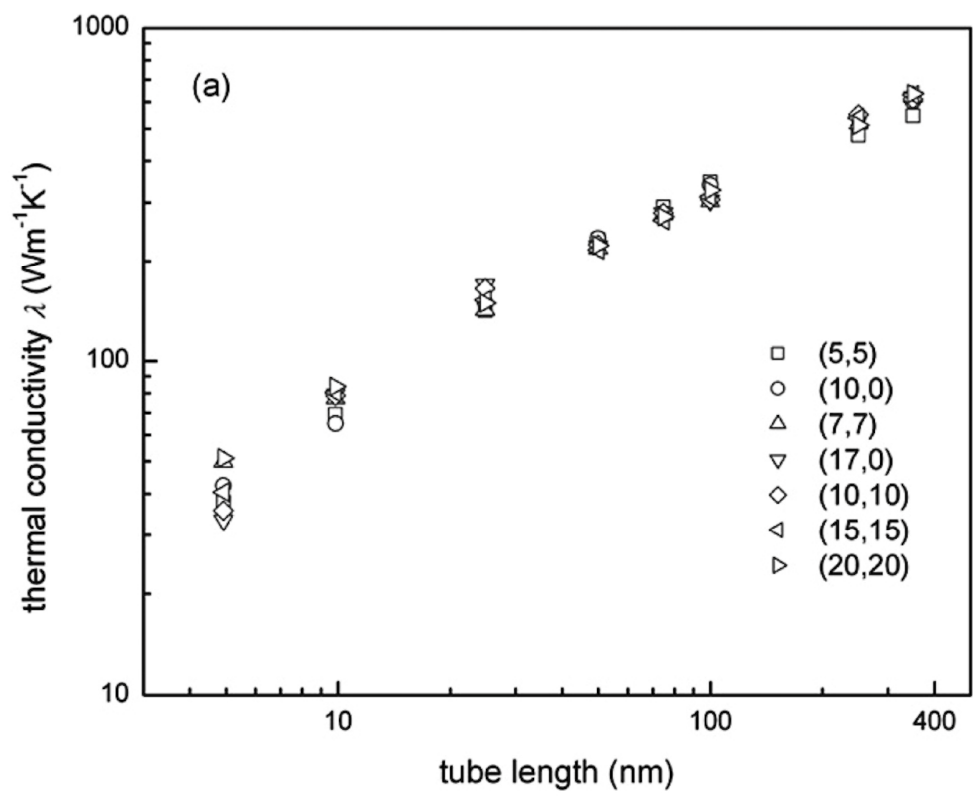


Fig.6

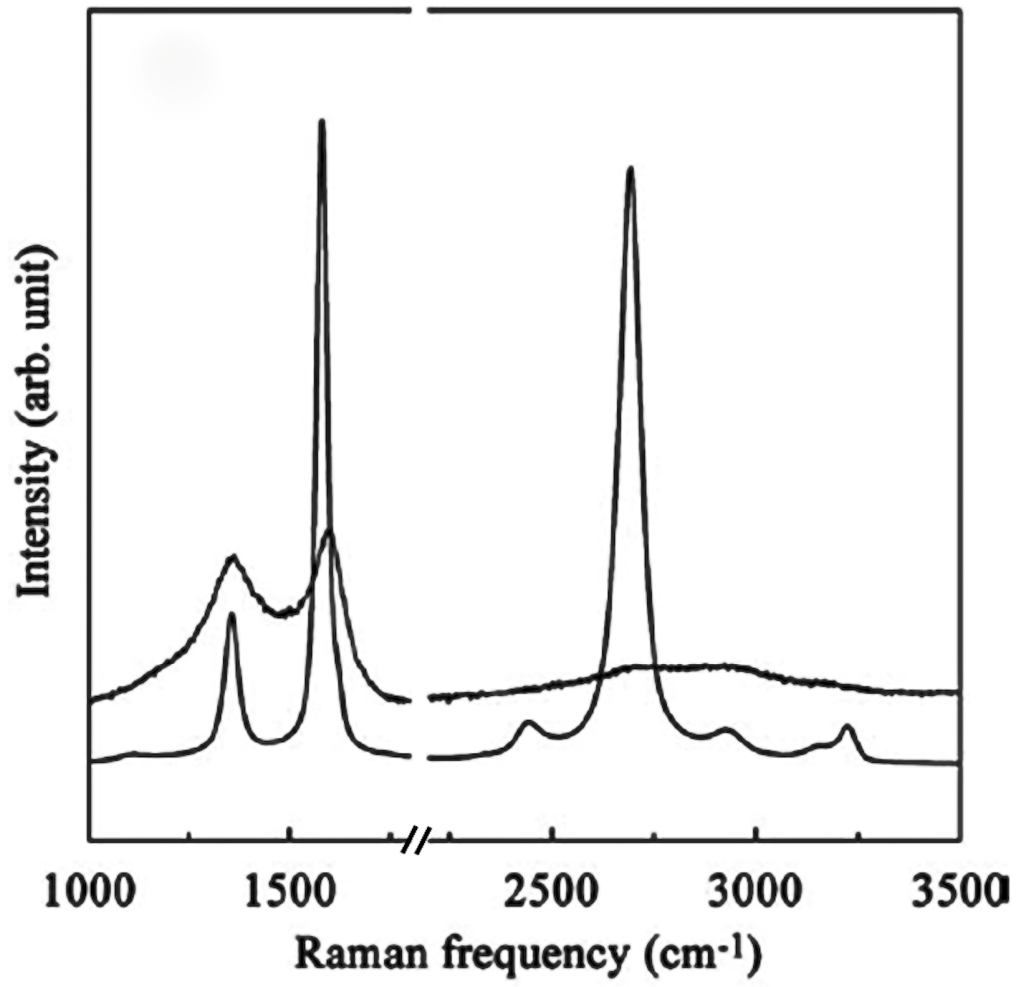


Fig.7

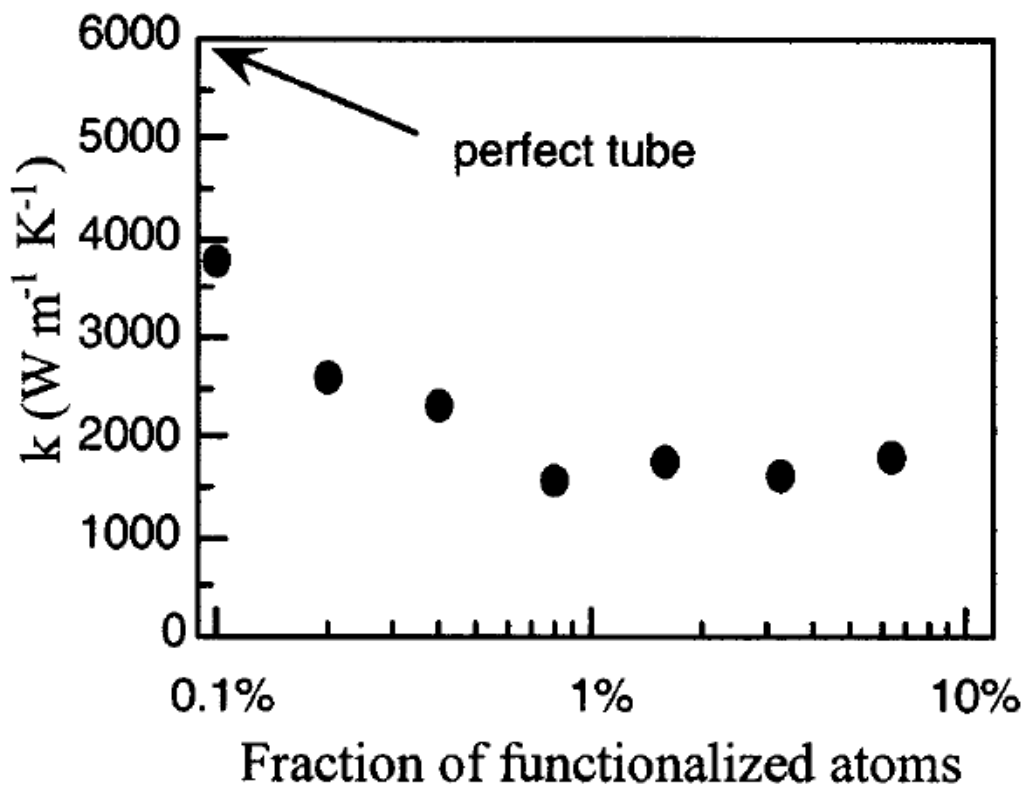


Fig.8



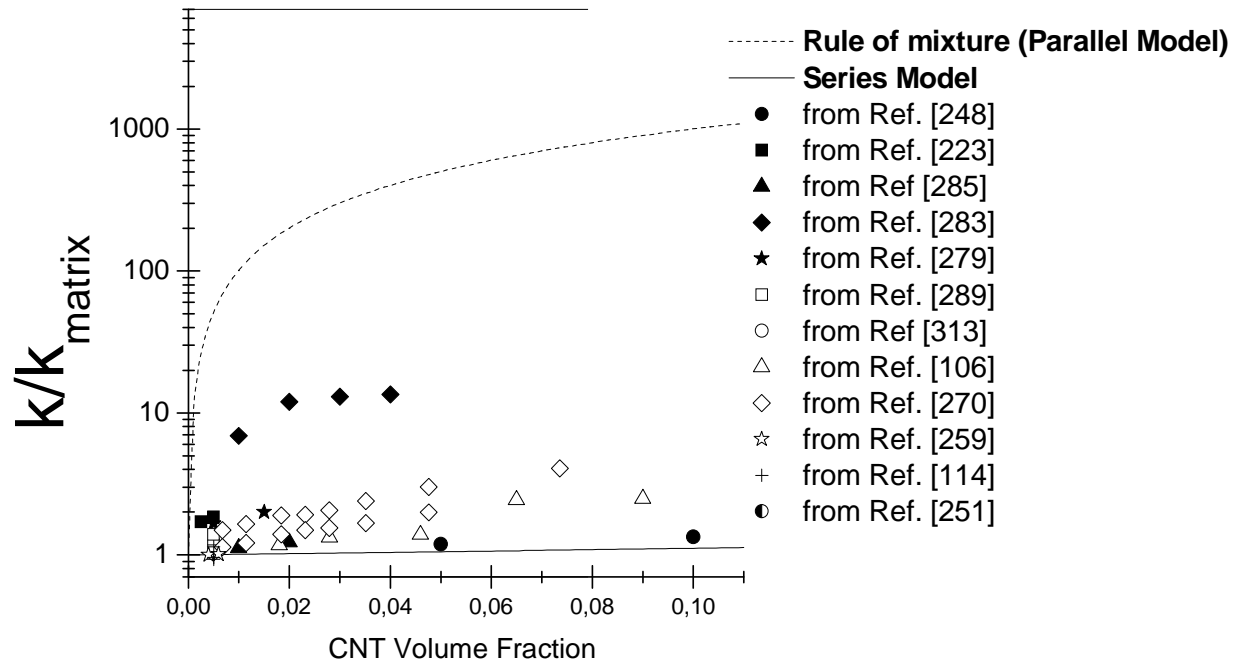


Fig.9

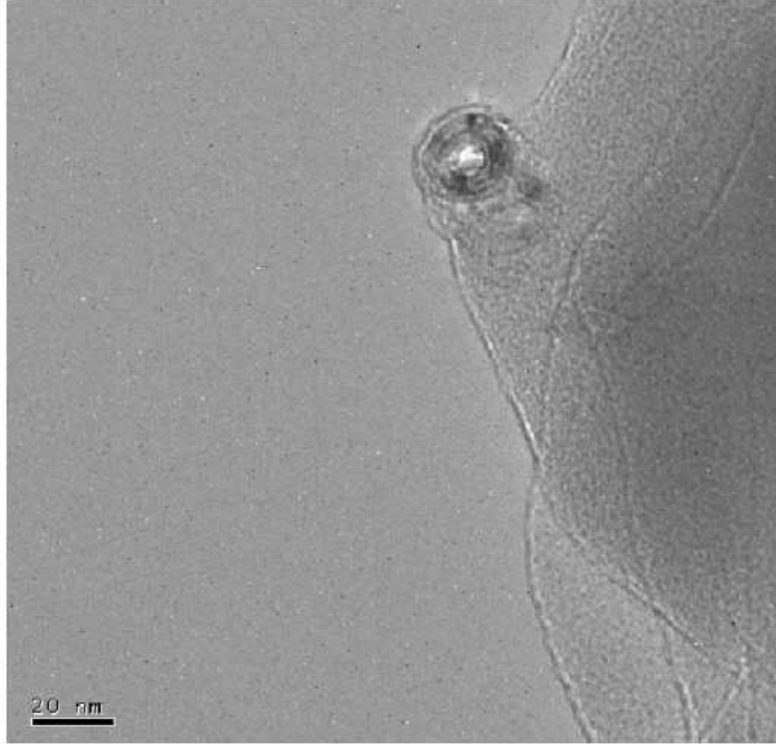


Fig.10

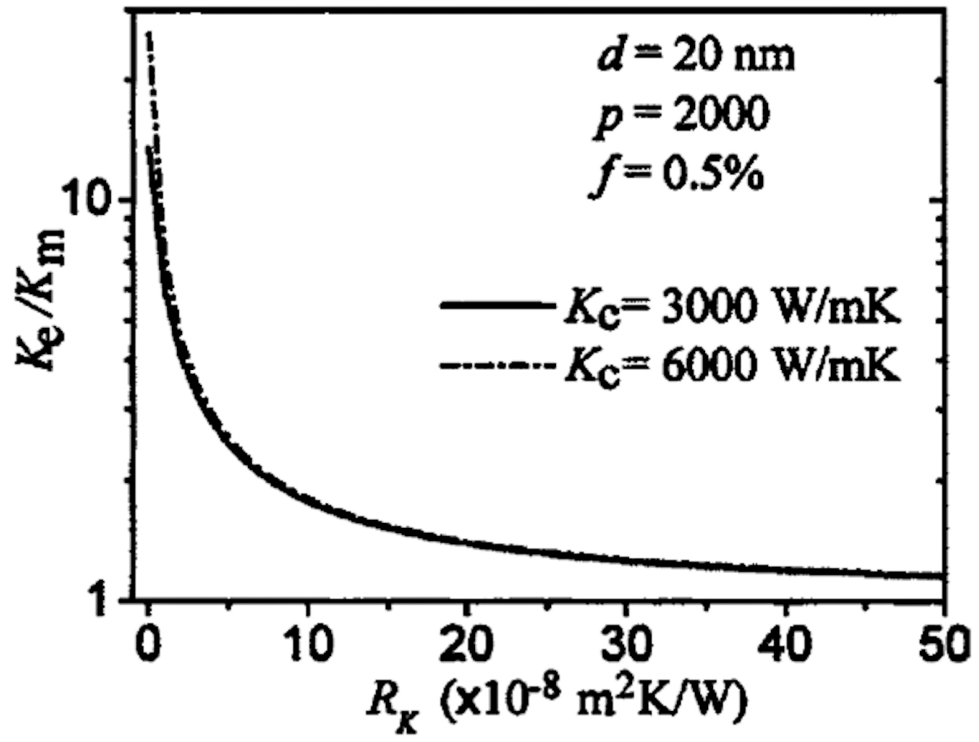


Fig.11

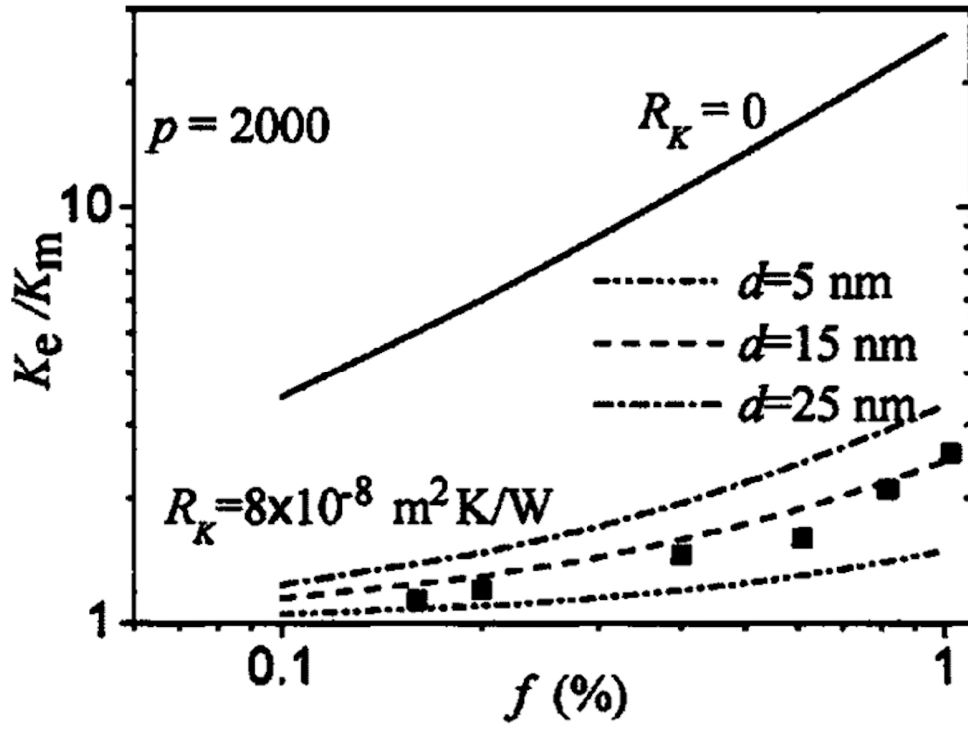


Fig.12

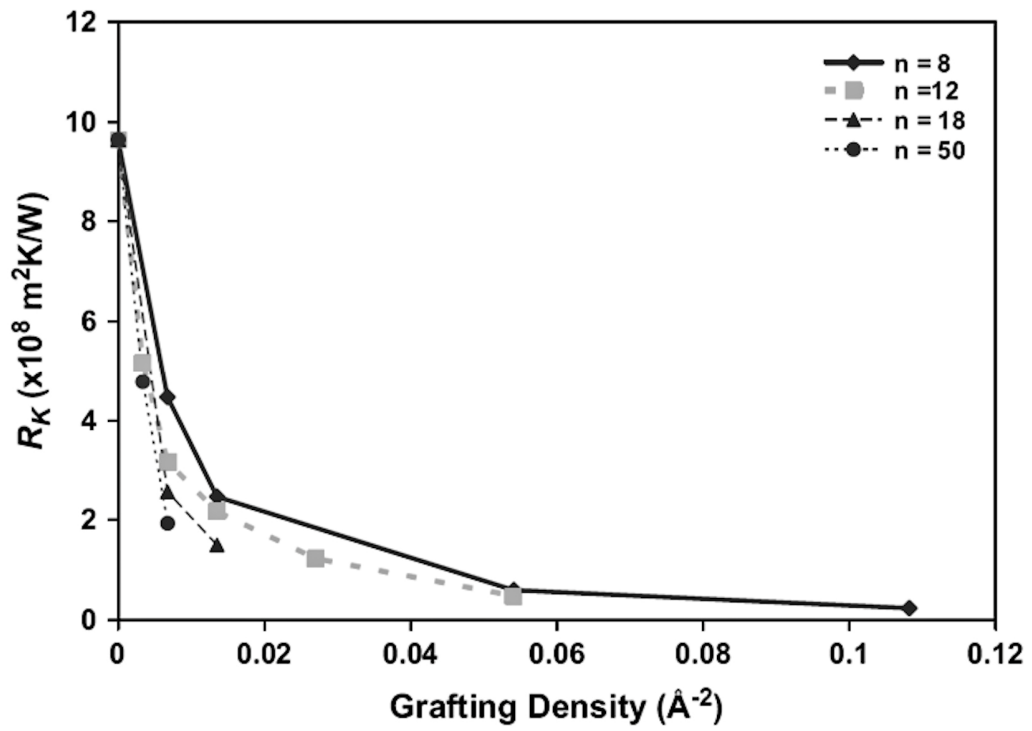


Fig.13

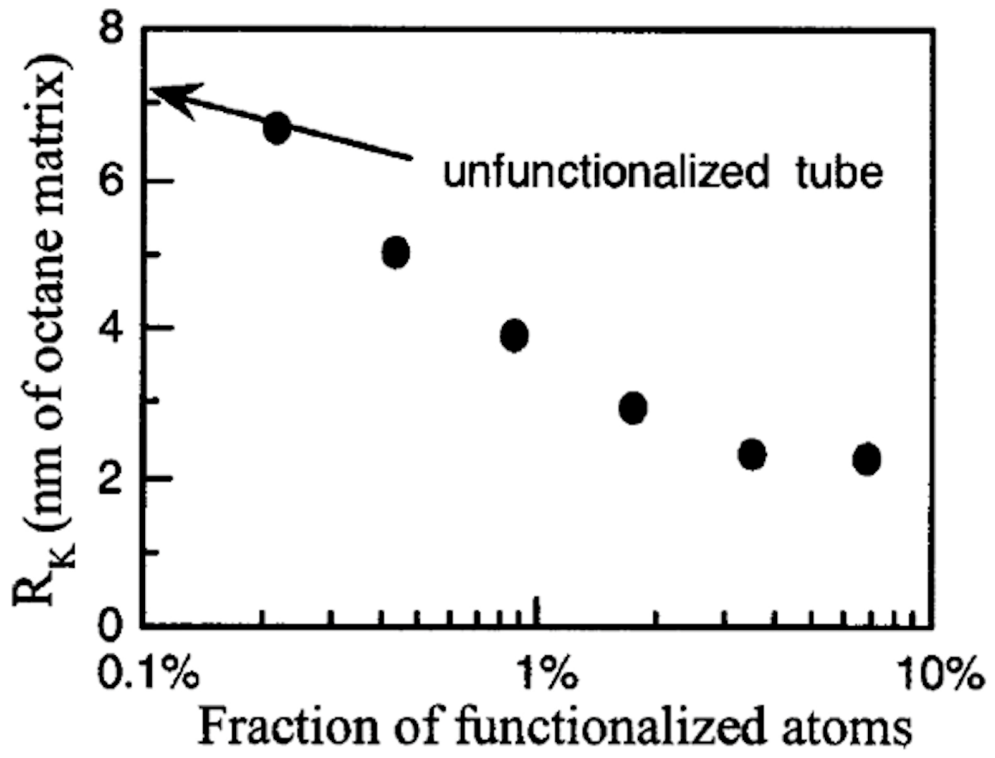


Fig.14

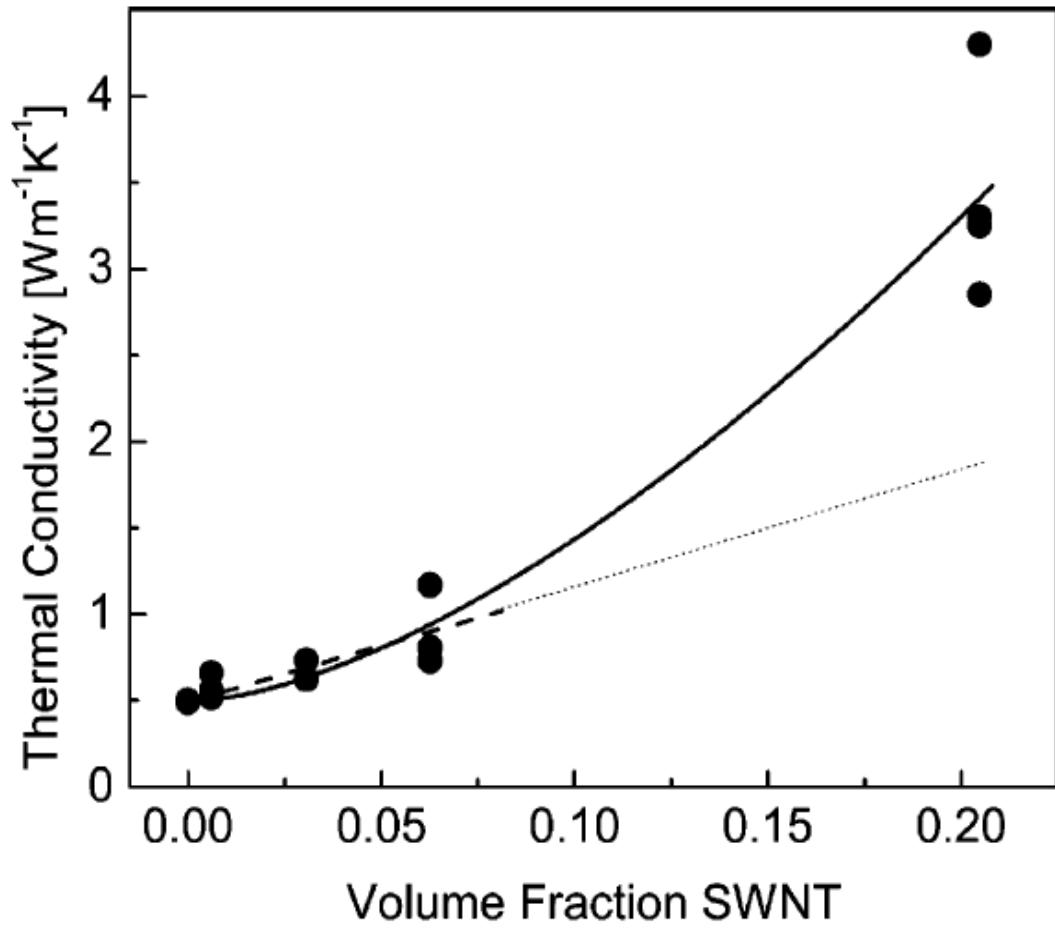


Fig.15

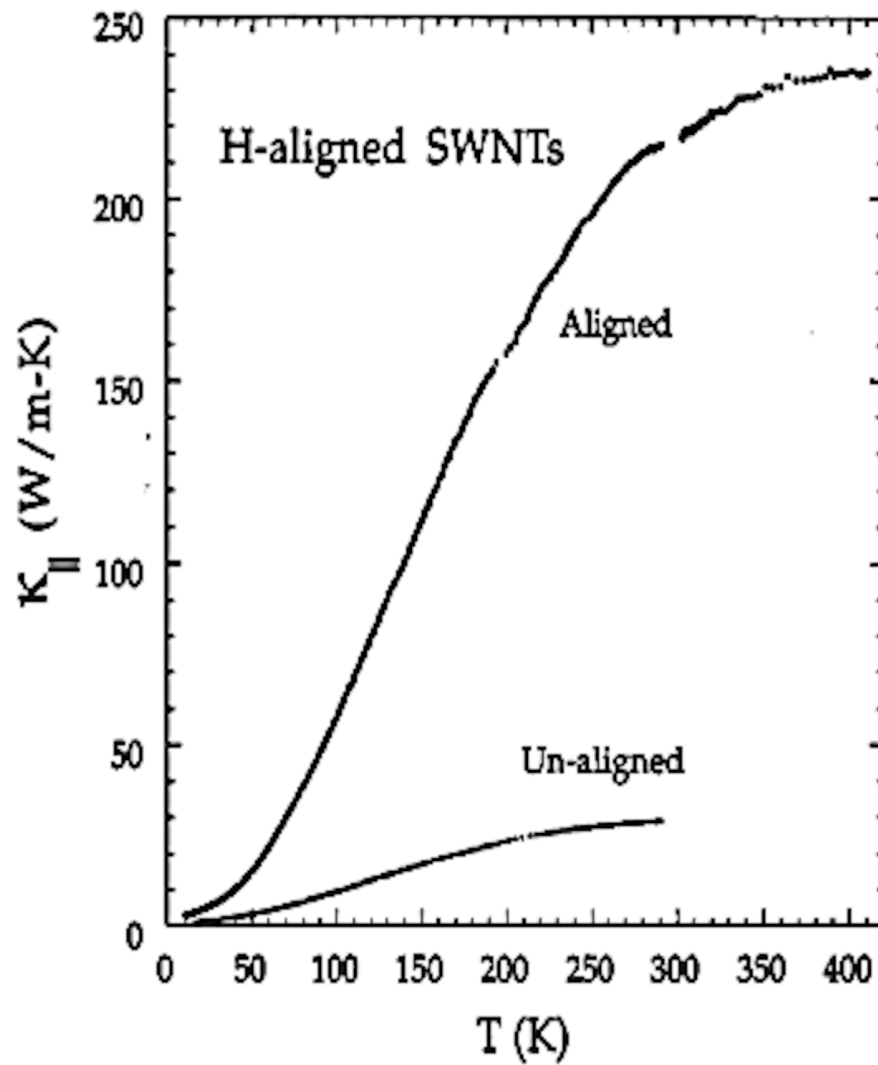


Fig.16



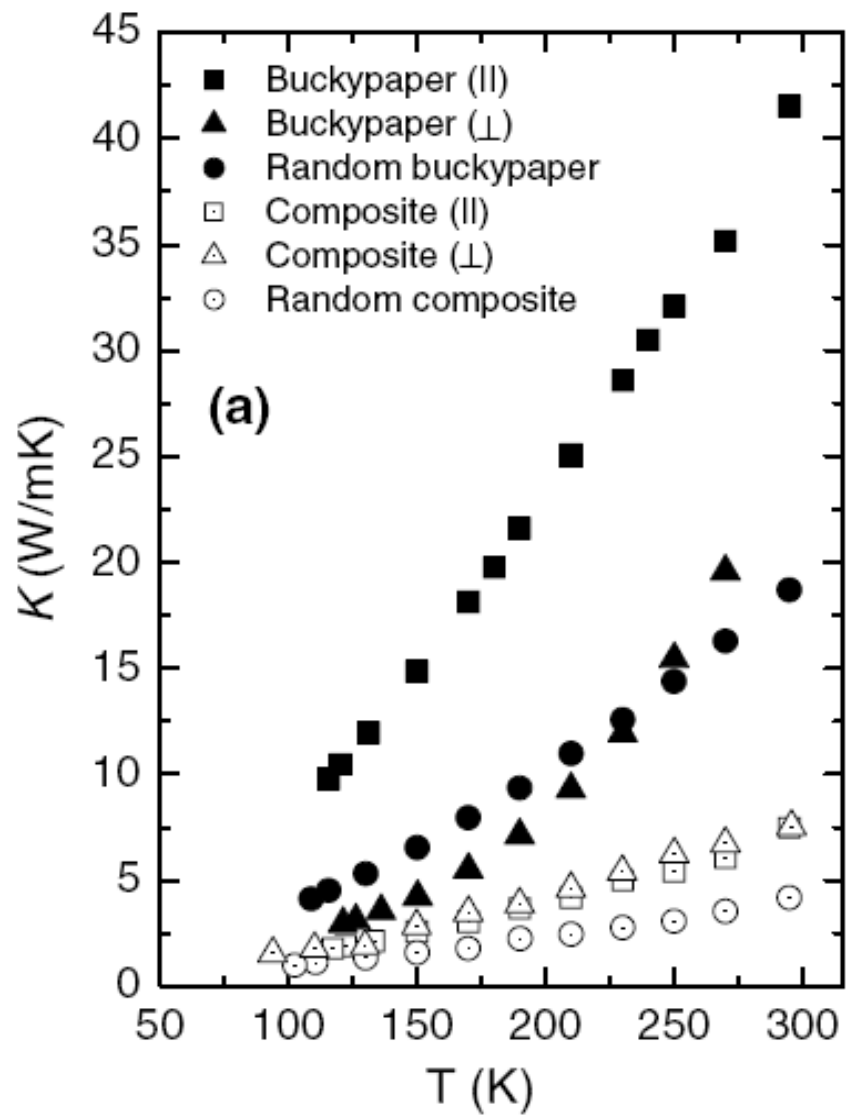


Fig.17

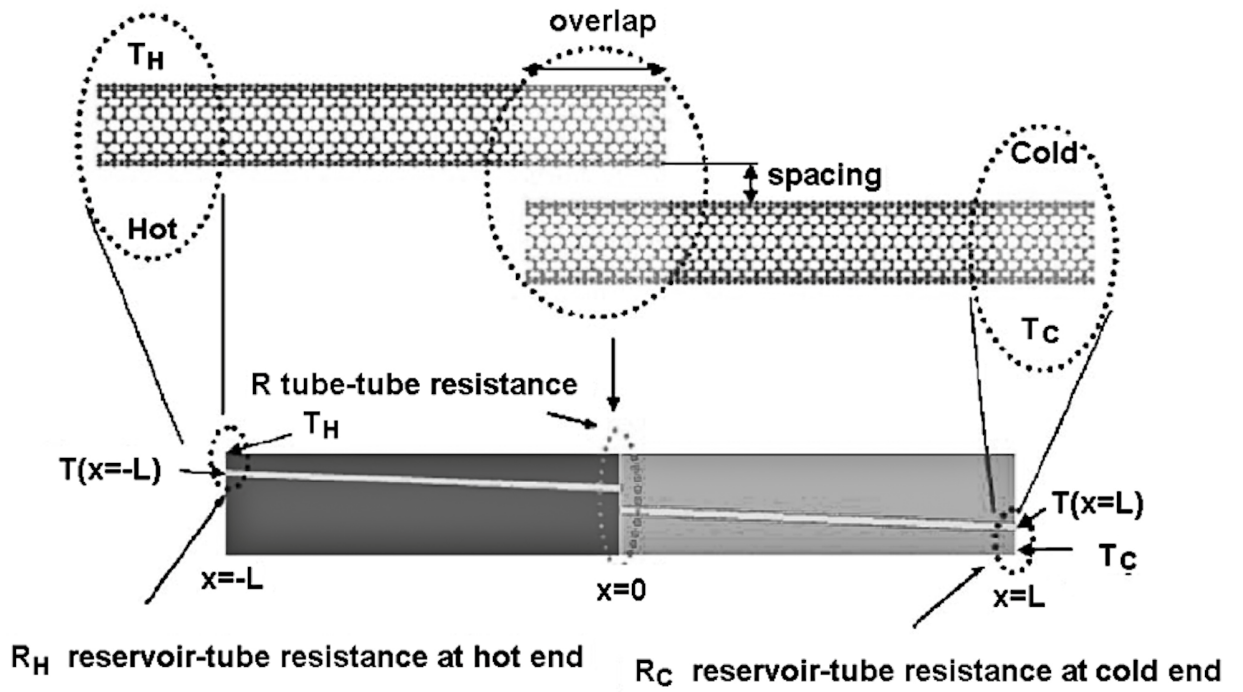


Fig.18

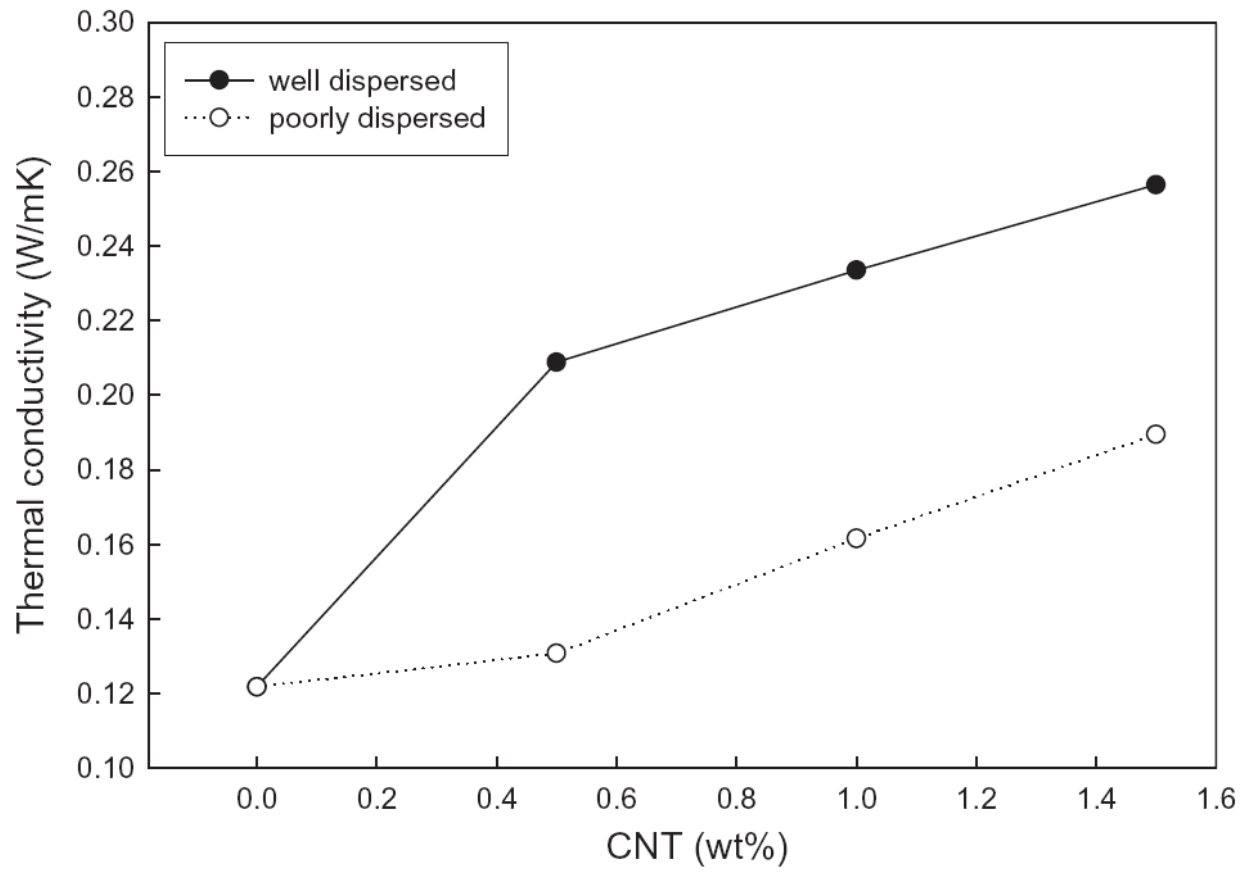


Fig.19

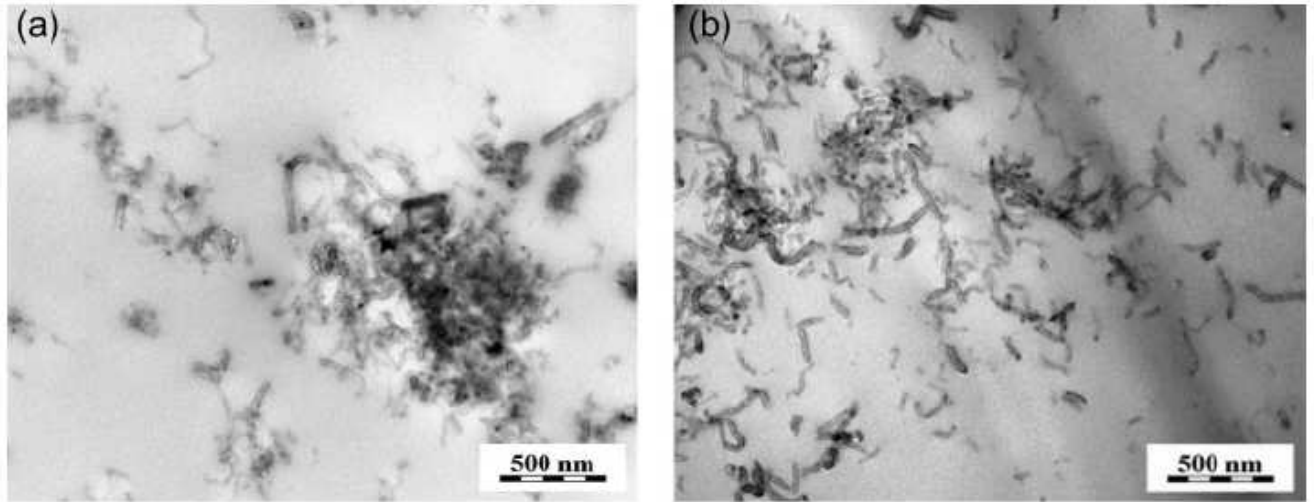


Fig.20

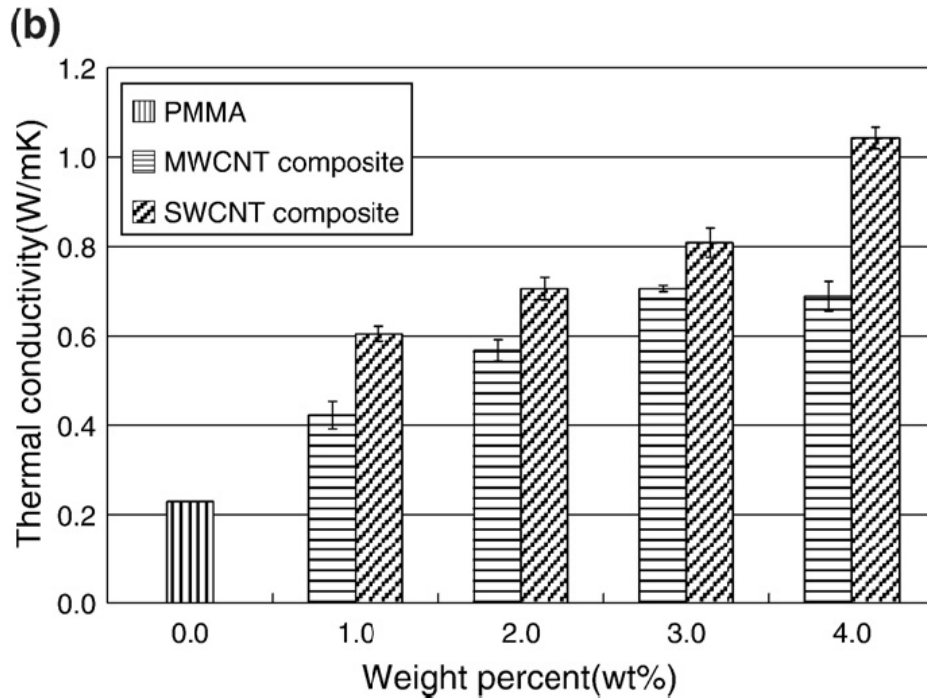
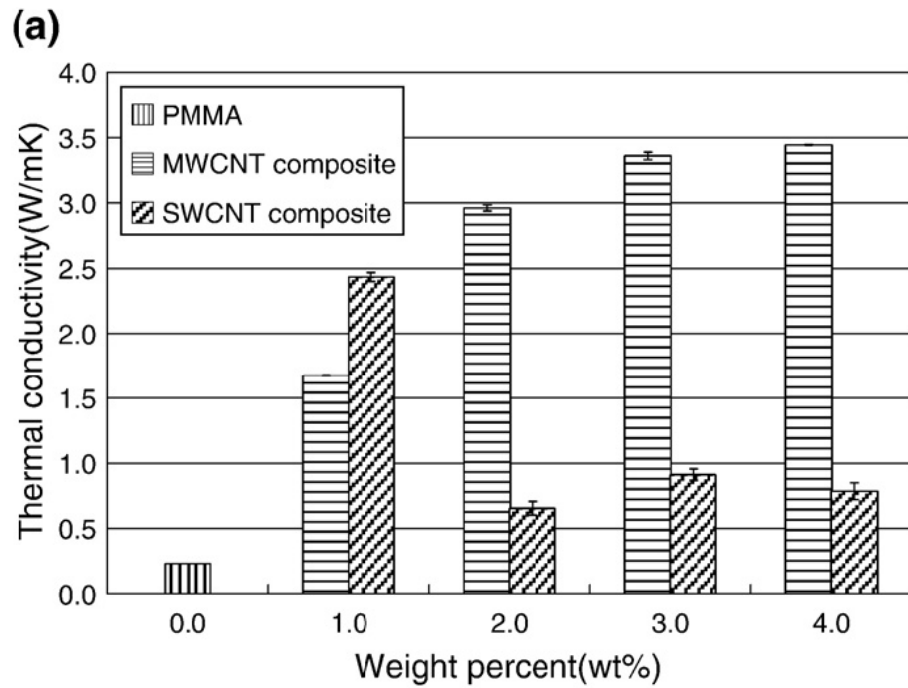


Fig.21

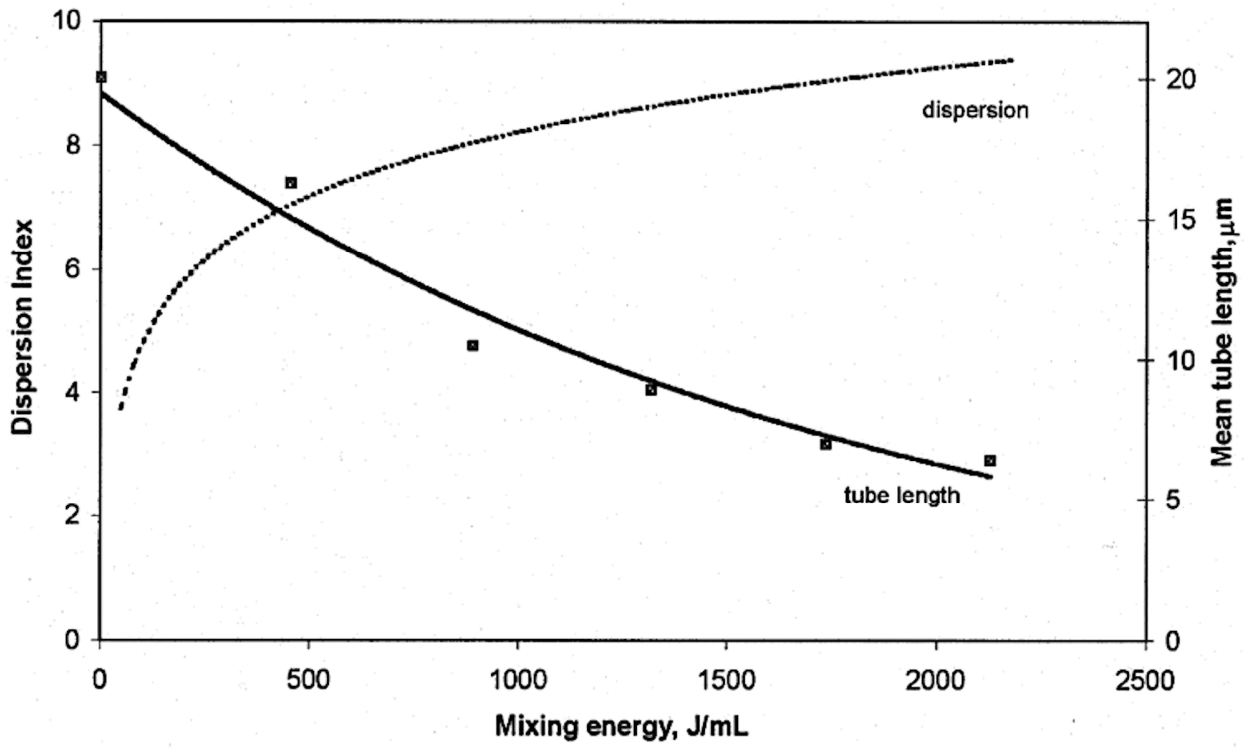


Fig.22

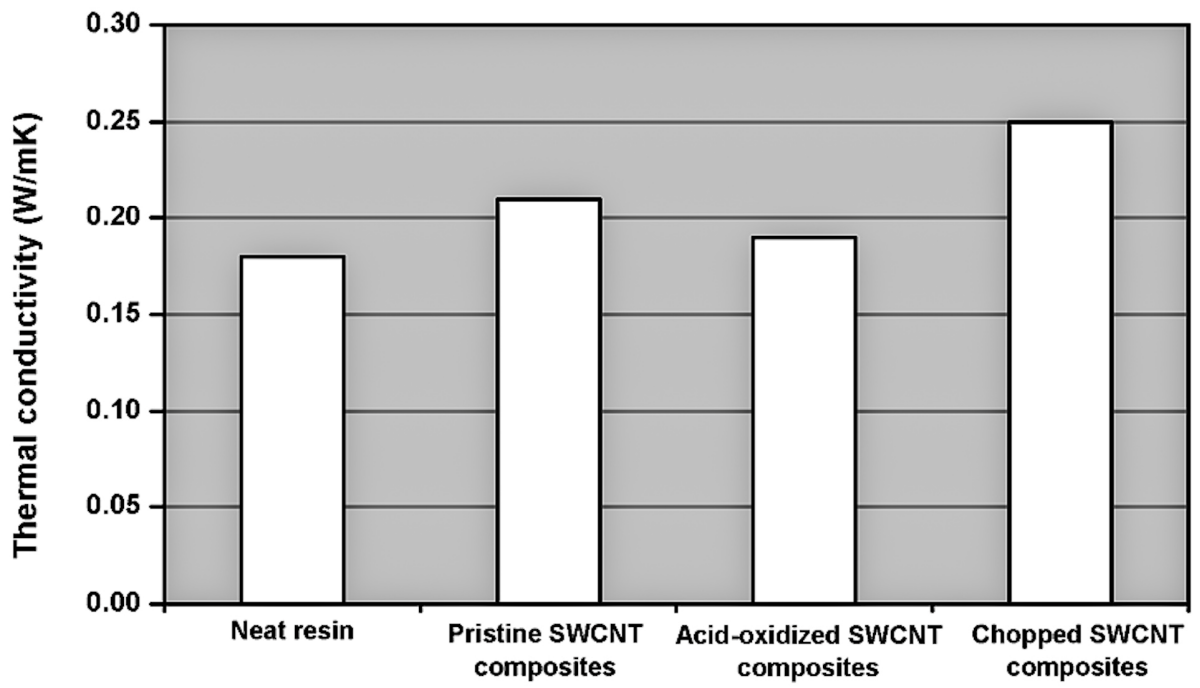


Fig.23

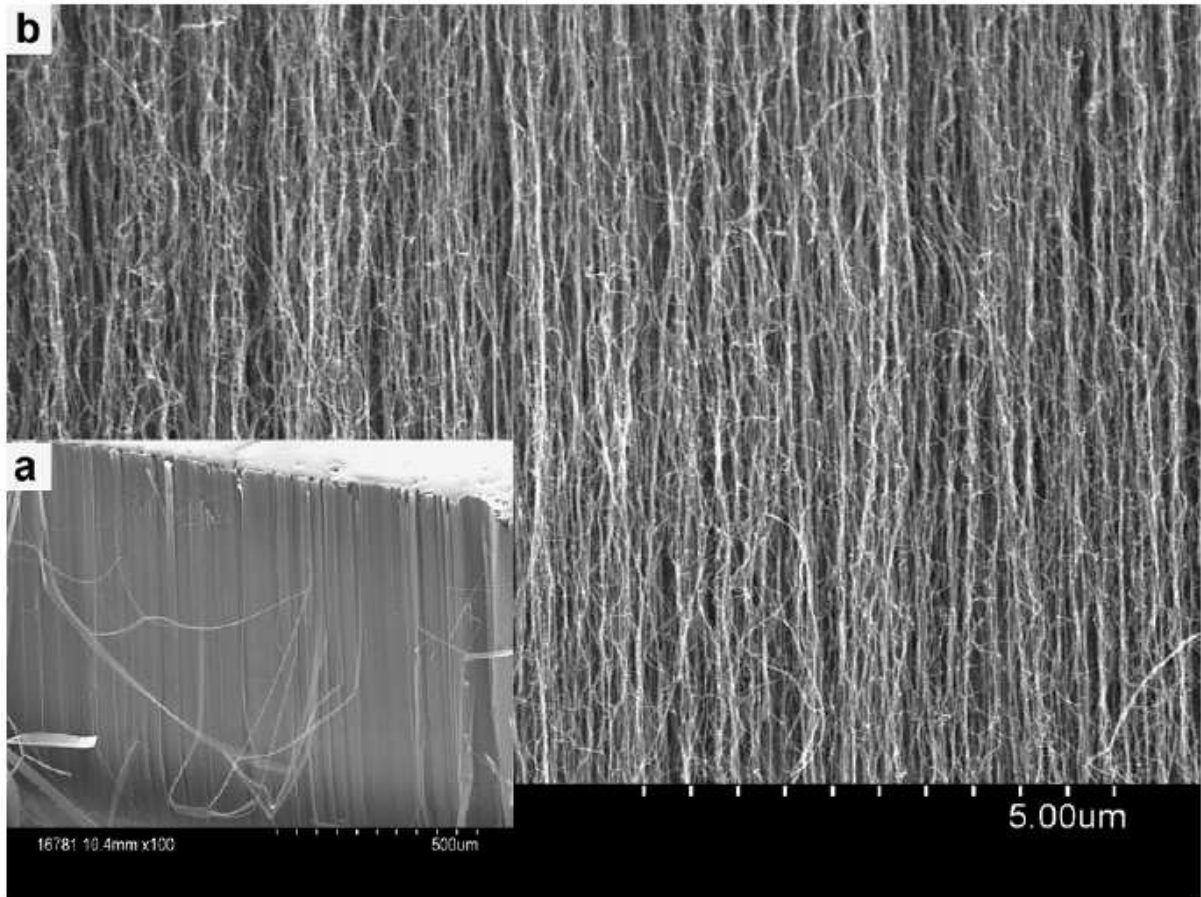


Fig.24



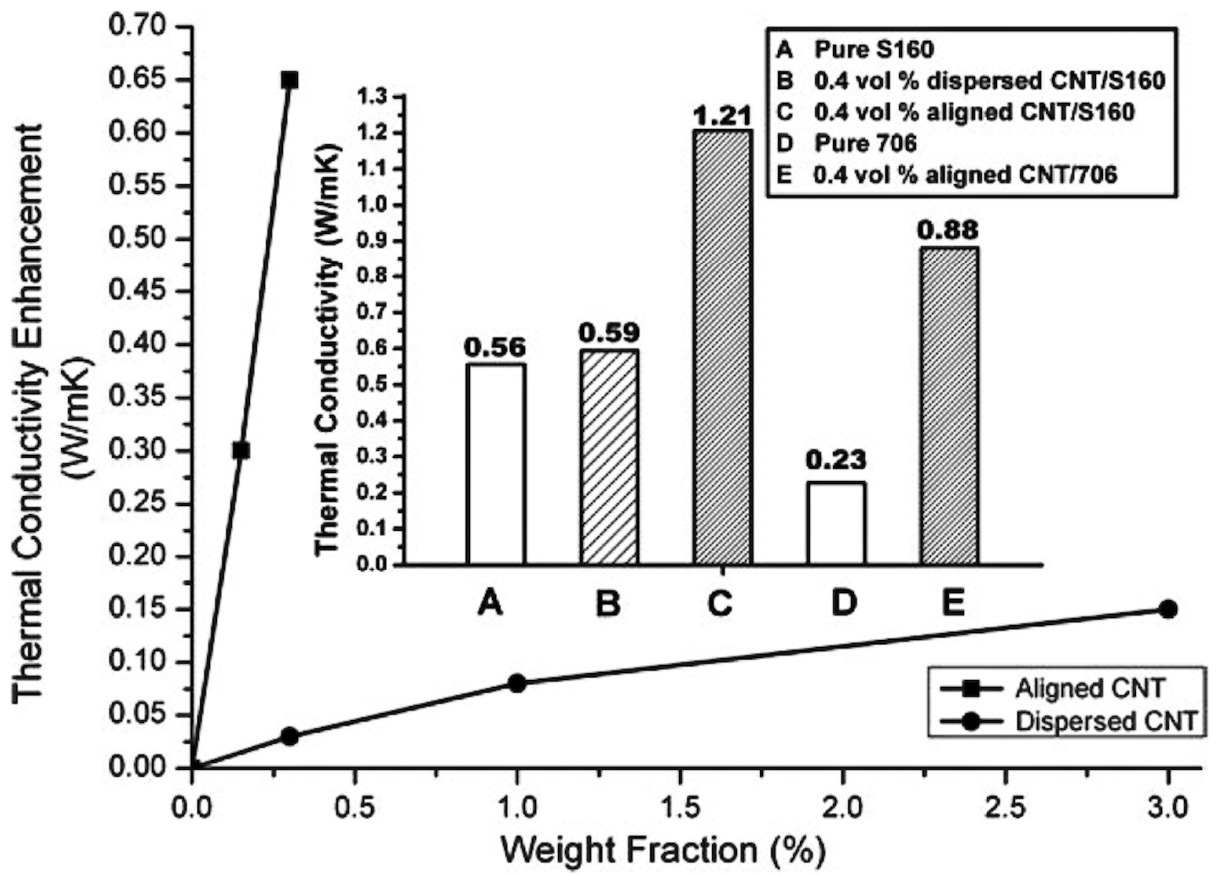


Fig.25

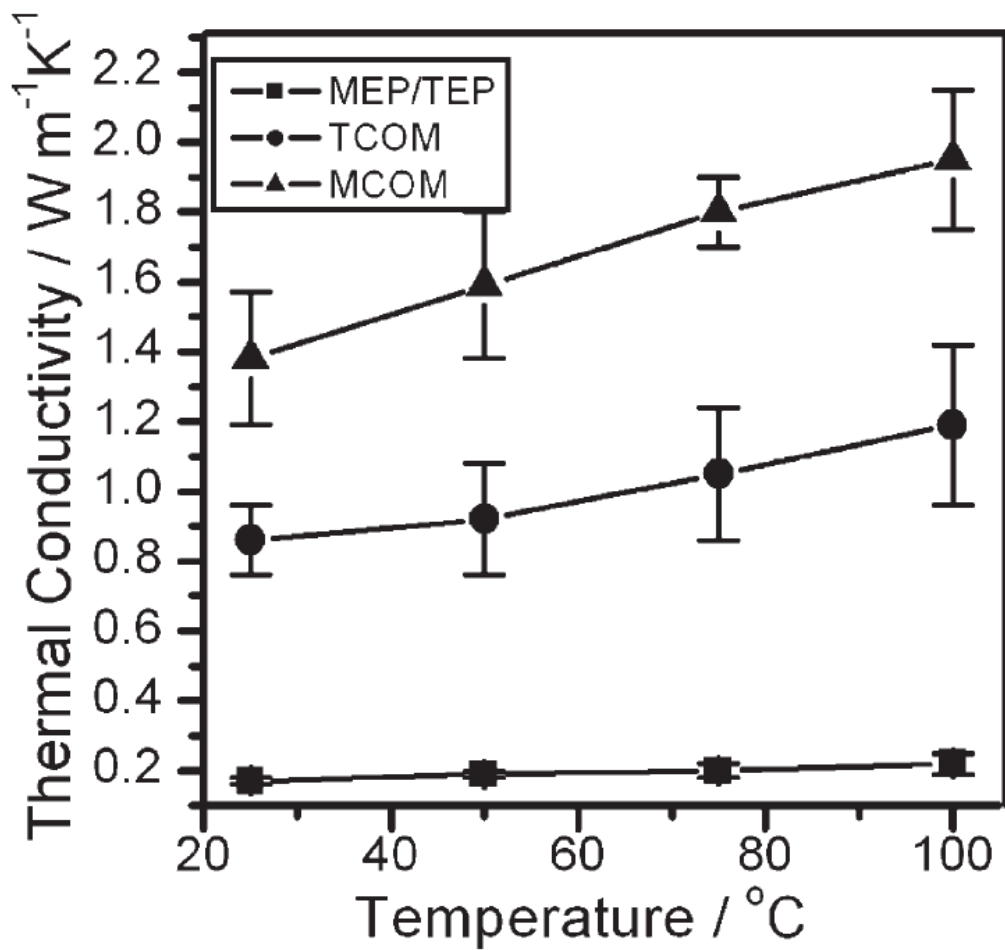


Fig.26

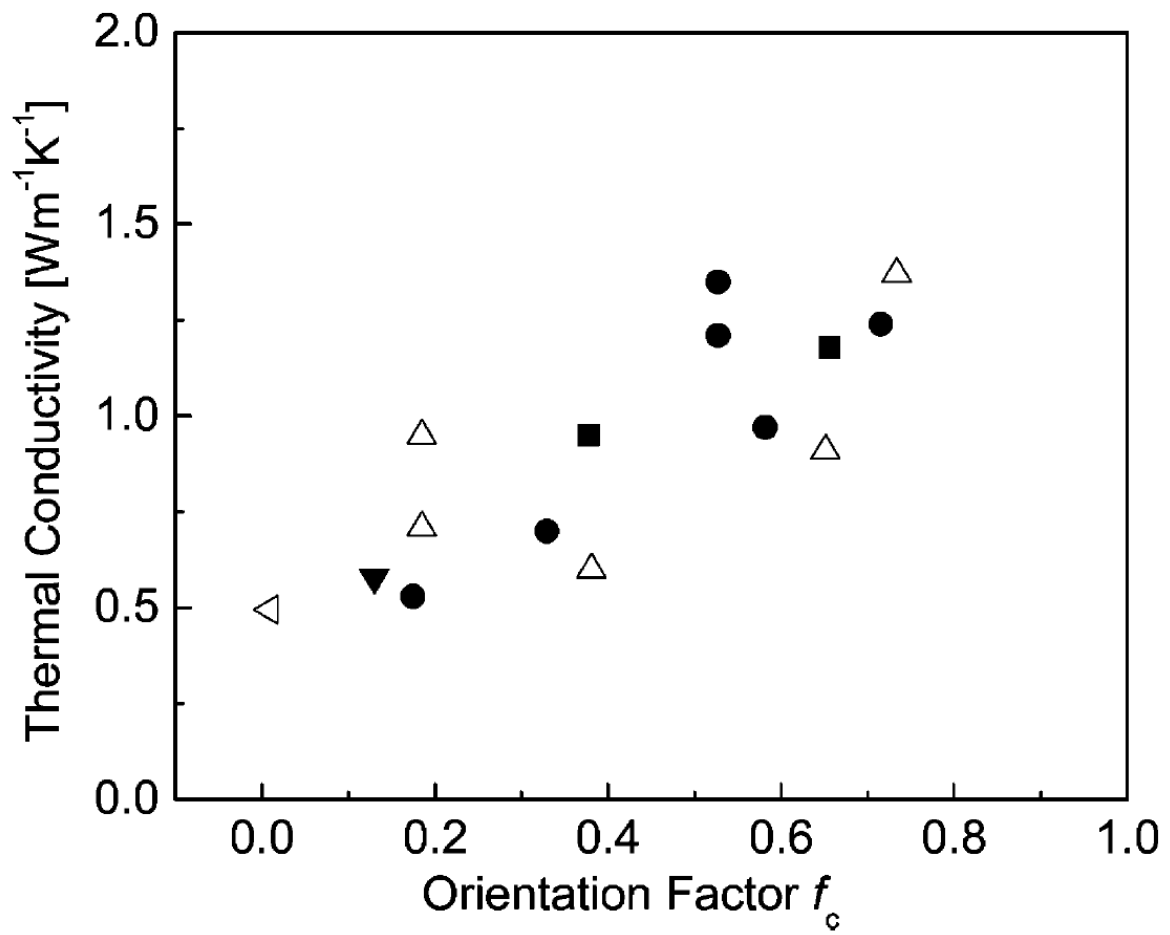


Fig.27